Turun yliopisto
University of Turku

# HEALING RESPONSE TO CORONARY STENTING IN ACUTE CORONARY SYNDROME

Early Anatomical and Functional Healing Assessed by
Optical Coherence Tomography and Flow Reserve

Ville Varho

## University of Turku

Faculty of Medicine

Department of Cardiology and Cardiovascular Medicine

University of Turku Doctoral Programme of Clinical Investigation

Heart Center, Satakunta Central Hospital

Heart Center, Turku University Hospital

## Supervised by

Docent Tuomas Kiviniemi
Heart Center
Turku University Hospital
University of Turku
Turku, Finland

Docent Pasi Karjalainen
Heart Center
Satakunta Central Hospital
Pori, Finland

## Reviewed by

Docent Juha Sinisalo
Helsinki University Hospital
Heart and Lung Center
University of Helsinki
Helsinki, Finland

Docent Tuomas Rissanen
Heart Center
North Karelia Central Hospital
Joensuu, Finland

## Opponent

Professor Timo Mäkikallio
Department of Cardiology
Oulu University Hospital
University of Oulu
Oulu, Finland

To my parents

# ABSTRACT

Ville Varho
**HEALING RESPONSE TO CORONARY STENTING IN ACUTE CORONARY SYNDROME – Early Anatomical and Functional Healing Assessed by Optical Coherence Tomography and Flow Reserve**

University of Turku, Faculty of Medicine, Department of Cardiology and Cardiovascular Medicine, Doctoral Programme of Clinical Investigation
Heart Center, Satakunta Central Hospital
Heart Center, Turku University Hospital

Drug-eluting stents are associated with delayed vascular healing. Anatomical and functional healing of coronary arteries after balloon angioplasty with stenting was investigated in patients presenting with acute coronary syndrome. Bioactive stents, sirolimus-, zotarolimus-, and everolimus-eluting stents were compared in two randomized trials with optical coherence tomography and coronary flow reserve measurement at 2- or 3-month follow-up after stenting. Coronary flow reserve measurements were obtained by invasive thermodilution and transthoracic echocardiography. Variability of optical coherence tomography data was assessed between observers and sampling intervals.

Uncovered stent struts and impaired coronary flow reserve values were detected in all stent groups, and a link between anatomical and functional healing was discovered. Bioactive stents showed earlier and more comprehensive neointimal coverage, which happened at the expense of luminal narrowing. Strut malapposition occurred frequently despite post-dilatation.

Measurement of coronary flow reserve by transthoracic echocardiography was feasible after stenting in the left anterior descending artery of non-diabetic patients, and agreement with the invasive method was good. The results confirm that non-invasive measurement of coronary flow reserve by echocardiography can be considered for follow-up after stenting.

The sampling interval of optical coherence tomography cross-sections had a significant effect on the observed percentage of uncovered and malapposed struts. The shorter sampling interval of 0.6 mm can be used to reduce variability and overestimation of strut level data.

**Keywords:** optical coherence tomography, stent, vascular healing, neointimal coverage, coronary flow reserve

# TIIVISTELMÄ

Ville Varho
**SEPELVALTIMOSTENTTIEN PARANEMISVASTE SEPELVALTIMO-TAUTIKOHTAUKSEN HOIDOSSA – varhainen anatominen ja toiminnallinen paraneminen valokerroskuvauksella ja virtausreservillä tarkasteltuna**

Turun yliopisto, Lääketieteellinen tiedekunta, Kardiologian ja kardiovaskulaari-lääketieteen oppiaine, Turun yliopiston kliininen tohtoriohjelma
Sydänkeskus, Satakunnan keskussairaala
Sydänkeskus, Turun yliopistollinen keskussairaala

Annales Universitatis Turkuensis, Turku, Suomi 2017

Lääkestentteihin liittyy viivästynyttä verisuonen seinämän paranemista. Sepelvaltimoiden anatomista ja toiminnallista paranemista pallolaajennuksen jälkeen selvitettiin akuutin sepelvaltimotautikohtauksen saaneilla potilailla. Bioaktiivisia sekä sirolimuusia, everolimuusia ja tsotarolimuusia vapauttavia stenttejä vertailtiin kahdessa satunnaistetussa tutkimuksessa valokerroskuvantamisella ja virtausreservimittauksella 2 tai 3 kuukauden kuluttua stenttauksesta. Virtausreservimittaukset suoritettiin sekä kajoavalla termodiluutiomenetelmällä että kajoamattomalla kaikututkimuksella rintakehän päältä. Valokerroskuvantamismittausten hajontaa vertailtiin havainnoijien ja otantatiheyksien välillä.

Peittymättömiä stentin osia ja heikentyneitä virtausreserviarvoja havaittiin kaikissa stenttiryhmissä ja anatomisen ja toiminnallisen paranemisen välillä havaittiin yhteys. Bioaktiiviset stentit osoittautuivat peittyneen endoteelilla aikaisemmin ja kattavammin, mikä puolestaan johti suonen kaventumiseen. Huono kontakti suonen seinämään oli yleistä jälkilaajennuksesta riippumatta.

Kaikututkimus mahdollisti virtausreservin mittauksen kajoamattomasti vasemman laskevan haaran stenttauksen jälkitilassa diabetesta sairastamattomilla ja mittausarvot korreloivat hyvin kajoavalla menetelmällä mitattujen arvojen kanssa. Tulokset vahvistavat, että kajoamatonta virtausreservin mittausta kaikututkimuksella voidaan hyödyntää stenttauksen jälkeisessä seurannassa.

Valokerroskuvauksen otantatiheys vaikutti merkitsevästi stenttien havaittuun peittymättömyyden ja malapposition osuuteen. Tiheämmällä 0,6 mm otantavälillä voidaan vähentää hajontaa ja peittymättömyyden yliarviointia.

**Avainsanat:** valokerroskuvaus, stentti, verisuonen paraneminen, endotelisaatio, virtausreservi

# TABLE OF CONTENTS

# ABBREVIATIONS

| | |
|---|---|
| ACS | Acute coronary syndrome |
| ASA | Acetylsalicylic acid |
| AUC | Area under receiver operating characteristic curve |
| BAS B | ioactive stent |
| BMS | Bare metal stent |
| BP-BES | Biodegradable polymer biolimus-eluting stent |
| BP-SES | Biodegradable polymer sirolimus-eluting stent |
| CAD | Coronary artery disease |
| CFR | Coronary flow reserve |
| CI | Confidence interval |
| CoCr-BAS | Cobalt-chromium bioactive stent |
| DAPT | Dual anti-platelet therapy |
| DEB | Drug-eluting balloon |
| DES | Drug-eluting stent |
| DP-ZES | Durable polymer zotarolimus-eluting stent |
| EES | Everolimus-eluting stent |
| FFR | Fractional flow reserve |
| HR | Hazard ratio |
| HSR | Hyperemic stenosis resistance |
| ICC | Intraclass correlation coefficient |
| iFR | Instantaneous wave-free ratio |
| IMR | Index of microcirculatory resistance |
| ISA | Incomplete stent apposition |
| IVUS | Intravascular ultrasound |
| LAD | Left anterior descending artery |
| LLL | Late lumen loss |
| MACE | Major adverse cardiac event |
| MI | Myocardial infarction |
| MLA | Minimal lumen area |
| MLD | Minimal lumen diameter |
| NIH | Neointimal hyperplasia |
| OCT | Optical coherence tomography |
| PCI | Percutaneous coronary intervention |
| PES | Paclitaxel-eluting stent |
| PtCr-EES | Platinum-chromium everolimus-eluting stent |
| RCT | Randomised controlled trial |
| SES | Sirolimus-eluting stent |

| | |
|---|---|
| SOS | Shadow-only strut |
| STEMI | ST-segment elevation myocardial infarction |
| ST | Stent thrombosis |
| TLF | Target lesion failure |
| TLR | Target lesion revascularisation |
| TTE | Transthoracic echocardiography |

# LIST OF ORIGINAL PUBLICATIONS

This thesis is based on the following original articles, which are referred to in the text by their Roman numerals I-IV.

I.    Karjalainen PP*, Varho V*, Nammas W, Mikkelsson J, Pietilä M, Ylitalo A, Airaksinen JK, Sia J, Nyman K, Biancari F, Kiviniemi T. Early neointimal coverage and vasodilator response following biodegradable polymer sirolimus-eluting vs. durable polymer zotarolimus-eluting stents in patients with acute coronary syndrome –HATTRICK-OCT trial. Circ J 2015;79 (2):360-7.

II.   Varho V, Karjalainen PP, Ylitalo A, Airaksinen JK, Mikkelsson J, Sia J, Pietilä M, Kiviniemi TO. Transthoracic echocardiography for non-invasive assessment of coronary vasodilator function after DES implantation. Eur Heart J Cardiovasc Imaging 2014 Sep;15 (9):1029-34.

III.  Varho V, Kiviniemi TO, Nammas W, Sia J, Romppanen H, Pietilä M, Airaksinen JK, Mikkelsson J, Tuomainen P, Perälä A, Karjalainen PP. Early vascular healing after titanium-nitride-oxide-coated stent versus platinum-chromium everolimus-eluting stent implantation in patients with acute coronary syndrome. Int J Cardiovasc Imaging 2016 Jul;32 (7):1031-9.

IV.   Varho V, Nammas W, Kiviniemi TO, Sia J, Romppanen H, Pietilä M, Airaksinen JK, Karjalainen PP. Comparison of two different sampling intervals for optical coherence tomography evaluation of neointimal healing response after coronary stent implantation. Int J Cardiol 2017 Jan 15;227:194-200.

*Authors marked with an asterisk contributed equally to the study.

# 1    INTRODUCTION

Ever since the first percutaneous coronary intervention (PCI) performed by Grüntzig in 1977 (Grüntzig 1978), much of research in cardiology has focused on improving the treatment outcomes of PCI, with drug-eluting stent (DES) currently being the most widely studied product in the entire medical field.

In the early stages of PCI, procedure-related vessel occlusion due to wall dissection, elastic recoil, and vasospasm presented a major limitation to the method. The first coronary stent was implanted in 1987 by Sigwart (Sigwart et al. 1987) in an attempt to circumvent these obstacles. The method was later proven efficient in reducing vessel occlusion. By achieving greater immediate gain of lumen diameter, stenting also resulted in fewer cases of restenosis than angioplasty alone (Fischman et al. 1994). The widespread use of bare metal stents (BMS) led to a reduction in the need for target lesion revascularization (TLR) after PCI (Farshid et al. 1998).

Neointimal hyperplasia caused by the post-PCI vessel healing process and leading to in-stent restenosis remained a limitation to successful treatment (Hoffmann et al. 1996). Sirolimus- and paclitaxel-eluting stents were introduced and successfully employed to avoid TLR (Stone et al. 2004; Morice et al. 2002). Concerns over safety of DES were raised when higher rates of late and very late stent thrombosis (ST) were reported, leading to increased mortality (Lagerqvist et al. 2007; G. W. Stone et al. 2007). Pathological studies revealed, that ST was driven by incomplete neointimal coverage of stent struts and chronic inflammation of the vessel wall (Finn et al. 2007; Joner et al. 2006; Virmani et al. 2004). Discontinued dual anti-platelet therapy (DAPT) correlated strongly with the onset of late ST (Iakovou et al. 2005; Eisenstein et al. 2007), and therefore DAPT was recommended for 12 months after DES implantation despite the scarcity of clinical evidence.

Since then, numerous improvements to stent design have been made, and modern DES with biodegradable polymers, thin struts, and safer drug kinetics using everolimus or zotarolimus offer safety profiles similar to BMS, with lower rates of TLR and ST (Sarno, Lagerqvist, Fröbert, Nilsson, Olivecrona, Omerovic, et al. 2012; Sabate, Cequier, Iñiguez, Serra, Hernandez-Antolin, Mainar, et al. 2012; Sabaté, Brugaletta, Cequier, Iñiguez, Serra, Hernádez-Antolín, et al. 2014; Bønaa, Mannsverk, Wiseth, Aaberge, Myreng, Nygård, et al. 2016). The question of optimal duration of DAPT arose again, as studies on new-generation DES have shown little or no association between ST and DAPT discontinuation after 1-6 months (Valgimigli et al. 2012; Silber et al. 2014).

With the arrival of novel imaging techniques, work in the catheterisation labora-
tory routinely performed under angiographic guidance is increasingly profiting
from adjunct imaging modalities, most universally fractional flow reserve (FFR)
(Pijls et al. 1996). Functional assessment of lesion severity by FFR helps in select-
ing the patients who benefit from stent implantation, and reduces TLR in a manner
that is cost-efficient (Tonino et al. 2009; Layland et al. 2014; Fearon et al. 2010).
Intravascular ultrasound (IVUS) should be used to define lesion characteristics
prior to PCI, to assess stent expansion and apposition post-PCI, and to detect pos-
sible procedure-related complications (Hong, Mintz, Lee, Park, Choi, et al. 2006;
Fujii et al. 2005).

Optical coherence tomography (OCT) is an intravascular imaging modality that
offers a resolution far superior to IVUS, and possesses higher sensitivity in detect-
ing small degrees of neointimal hyperplasia (NIH) and procedure-related compli-
cations after PCI (Suzuki et al. 2008; Kawamori et al. 2010). Despite the lower
tissue penetrance compared to IVUS, OCT is advantageous in the analysis of strut
coverage, as it can visualise endothelial layers of 10 μm in thickness (Tearney et
al. 2012). Therefore, it is a valuable tool for stent follow-up to quantify the degree
of strut coverage. The percentage of uncovered struts is a strong predictor of ST,
and should be used as a surrogate endpoint (Giulio Guagliumi et al. 2012).

These novel imaging modalities allow real time surveillance of procedural success
in PCI, and can be used to investigate vascular healing *in vivo*. However, data on
modern stent devices are lacking and vascular healing patterns in the early time
frame after PCI are largely unknown. The current thesis was solicited by the need
to address this void of clinical evidence.

# 2  REVIEW OF LITERATURE

## 2.1  Devices in percutaneous coronary intervention

### 2.1.1  *Bare metal stents*

Early on in the history of PCI, BMSs quickly proved to be an efficient treatment for the acute vessel occlusion caused by intimal dissection flaps or elastic recoil after angioplasty (Serruys et al. 1994; Fischman et al. 1994). The obtained minimal lumen area (MLA) immediately after stent implantation is significantly larger than that after angioplasty alone, which results in a lower degree of restenosis during follow-up, although this result is offset in part by greater late lumen loss (LLL) due to NIH (Fischman et al. 1994). When comparing different DES and BMS cohorts, LLL by quantitative coronary angiography is a more consistent marker for restenosis propensity than TLR, and is therefore an appropriate surrogate endpoint for restenosis in the research setting, although TLR is more relevant to the clinician (Mauri et al. 2005).

The post-PCI intimal healing process has been described extensively (Komatsu et al. 1998). Thrombus formation near stent struts leads to recruitment of macrophages and spindle cells. Medial dissection triggers an increased inflammatory response (Farb et al. 1999). Through a platelet derived growth factor –mediated mechanism, the tissue composition gradually shifts towards fibrocellular tissue and smooth muscle cells (Ueda et al. 1991; Tanizawa et al. 1996; Farb et al. 1999).The resulting NIH is distributed uniformly across the length of the stent, and accounts for most of the LLL, as opposed to stent recoil or negative remodelling (Hoffmann et al. 1996).

The stainless steel used in early BMS has given way to cobalt-chromium and platinum-chromium alloys, that allow the development of stent platforms with thinner struts, without compromising radial strength or radiopacity, improving deliverability and outcomes (Iqbal et al. 2013). Issues with biocompatibility of the stent alloys have provoked research into coating materials that offer lower thrombogenicity and tissue interaction. Gold coated BMS proved inferior to non-coated BMS in the inhibition of NIH (Kastrati et al. 2000). Silicon carbide coating showed low thrombogenicity due to reduced deposition of platelets, but these properties were not shown to improve clinical or angiographic outcome (Unverdorben et al. 2003). Likewise, heparin-coated stents showed no difference in clinical outcome compared to BMS (Haude et al. 2003; Wöhrle et al. 2001). Titanium-nitride-oxide

coating of stainless steel BMS reduced platelet adhesion and NIH significantly in porcine models (Windecker et al. 2001).

The TiNOX trial was initiated to evaluate the safety and efficacy of titanium-nitride-oxide–coated stents, later termed bioactive stents (BAS), compared with BMS in humans (Windecker et al. 2005). Early results at 6 months were promising with a significant reduction in major adverse cardiac events (MACE) in the BAS group compared to the BMS group (7% vs. 27%, p=0.02) mainly driven by the reduced need for TLR. This result persisted up to 5 years after stent implantation (16% vs. 39%, p=0.03) (Moschovitis et al. 2010). IVUS at 6-month follow-up revealed a significantly smaller NIH volume (18±21 vs. 48±28 mm$^3$, p<0.0001) in keeping with the hypothesis of tissue interaction.

The performance of the first BAS based on a stainless steel platform was confirmed against first-generation DES in trials comparing BAS with paclitaxel-eluting stent (PES), which showed equal rates of MACE (10.9% vs. 13.7%; p=0.40) and a lower incidence of myocardial infarction (MI) in the BAS group (4.5% vs. 10.3%, p=0.025) at one year (Karjalainen et al. 2006). The reduction in the incidence of recurrent MI was accentuated in patients presenting with acute coronary syndrome (ACS): the 2-year rate of MI was 5.1% in the BAS group versus 15.6% in the PES group (p<0.001) (Karjalainen et al. 2009).

New-generation BAS make use of the cobalt-chromium alloy that allows thinner struts. Initial findings suggest a very low rate of MACE: target lesion failure (TLF), defined as a composite of cardiac death, target vessel MI, or ischemia-driven TLR, occurred in 6.3% at 1 year (Karjalainen, Mikkelsson, et al. 2016).

### 2.1.2 *Drug-eluting stents*

The first-generation DES based on stainless steel platforms coated with a thick layer of durable polymer, offering slow release of anti-proliferative drugs, sirolimus and paclitaxel (Stone et al. 2004; Morice et al. 2002). Compared to BMS, they were extremely successful in terms of LLL, which was reflected in decreased need for TLR.

The efficacy of first-generation DES was demonstrated in a large meta-analysis comprising 18,023 patients from 38 trials comparing sirolimus-eluting stents (SES) and PES against BMS; the number needed to treat with SES or PES to prevent TLR were 7 and 8, respectively, compared to BMS. No difference in mortality was observed, although the risk of late ST was significantly greater with PES when

compared to BMS or SES (hazard ratio (HR) 2.11, 1.19-4.23, p=0.017). (Stettler et al. 2007)

The HORIZONS-AMI trial was conducted to elucidate optimal treatment strategies in ST-segment elevation myocardial infarction (STEMI) (Stone et al. 2009). In 3006 patients presenting with STEMI treated with PES or BMS, TLR was significantly reduced in the PES arm (5.8% vs. 8.7%, p=0.006), with equal rates of death (3.5% vs. 3.5%) at 1-year follow-up. The study also acknowledged the limitation of previous trials that routine follow-up angiography increases the diagnosis of in-stent restenosis and the rate of TLR; completing clinical follow-up before scheduled angiography resulted in a lower overall rate of TLR.

DES implantation showed greatest advantage in reducing TLR in high-risk patient groups with long lesions (Applegate et al. 2009). Early DES were associated with a high incidence of incomplete stent apposition (ISA) on IVUS, which in serial follow-ups was primarily attributed to late acquired ISA due to positive remodelling, as opposed to underexpansion of the stent (Cook et al. 2007; Hong, Mintz, Lee, Park, Park, et al. 2006). Arterial remodelling can be readily appreciated in serial IVUS by measuring the cross-sectional area of the external elastic membrane, which is visualised clearly at the echolucent media-adventitia border (Nissen & Yock 2001). Positive remodelling leading to ISA was also observed in patients treated with BMS (Tanabe et al. 2005).

Concerns arose in 2007 over the safety of DES due to the reports on late acquired ISA, which was linked to very late ST (Cook et al. 2007). Studies based on large databases, notably the SCAAR registry, revealed higher rates of late and very late ST after 3–4 years of follow-up, leading to increased mortality rates, which was partly offset by the reduction in in-stent restenosis (Lagerqvist et al. 2007; G. W. Stone et al. 2007; G. G. W. Stone et al. 2007). The difference in the incidence of ST became statistically significant only after the first year: while there were no reported cases of very late ST from 1 to 4 years in patients treated with BMS, five events occurred in patients treated with SES (p=0.025 compared to BMS) and nine events in patients treated with PES (p=0.028) (G. W. Stone et al. 2007). The BAS-KET trial observed similarly increased rates of ST in DES vs. BMS (2.6% vs. 1.3%) associated with discontinuation of clopidogrel between months 7 and 18 (Pfisterer et al. 2006).

Interest in neointimal coverage of DES was aroused by OCT, which for the first time allowed the visualisation of thin neointimal layers covering stent struts. Serial OCT follow-up after PES implantation showed that most of the neointimal coverage develops during the most proliferative first 3 months of the healing response, after which little or no further NIH developed, and no difference was seen in the percentage of uncovered struts (3.77% vs 3.02% at 3 and 9 months, respectively)

(G. Guagliumi et al. 2012). In contrast, the resolution and development of ISA continued up to 9 months (G. Guagliumi et al. 2012).

### 2.1.3    New generation drug-eluting stents

Further iterations of early DES and BMS have spawned new generations of DES, employing more durable and biocompatible metal alloys, thin-strut platforms, biodegradable drug polymers, and safer drugs. Additionally, directional drug delivery to the vessel wall using abluminal drug polymer coating has been suggested to attenuate NIH proliferation without compromising early endothelial coverage of the adluminal strut surface (de la Torre Hernández, Tejedor, Camarero, Duran, Lee, Monedero, et al. 2016). Development in the regulation of drug delivery strives to reconcile inhibition of NIH thickening and facilitation of strut coverage.

Biodegradable polymer everolimus-eluting stents (EES) have been proven efficient in progressive reductions in the incidence of TLR (2.1% vs. 5.0%) at 1-year, definite or probable ST (1.3% vs. 2.8%) at 2-year, and mortality (9% vs. 12%) at 5-year follow-up compared to cobalt-chromium BMS (Sabate, Cequier, Iñiguez, Serra, Hernandez-Antolin, Mainar, et al. 2012; Sabaté, Brugaletta, Cequier, Iñiguez, Serra, Hernádez-Antolín, et al. 2014; Sabaté, Brugaletta, Cequier, Iñiguez, Serra, Jiménez-Quevedo, et al. 2016).

An observational study of the SCAAR registry reported decreased rates of TLR, definite ST, and mortality compared to first-generation DES and BMS (Sarno, Lagerqvist, Fröbert, Nilsson, Olivecrona, Omerovic, et al. 2012). In a large meta-analysis of randomized controlled trials (RCT) comparing BMS, first-generation, and second-generation DES, cobalt-chromium EES were the only DES with a risk of ST lower than BMS (Palmerini et al. 2012). The NORSTENT trial, a RCT comparing 9013 patients treated with second-generation DES vs. BMS, reported decreases in the incidence of ST at 6-year follow-up (0.8% vs. 1.2%, respectively, p=0.0498) as well as TLR (16.5% vs. 19.8%, respectively, p<0.001) (Bønaa et al. 2016). The number needed to treat with DES instead of BMS to prevent one TLR was 30 in 6-year follow-up.

### 2.1.4    Stent polymers

Coating materials of coronary stents are subject to demanding conditions in a dynamic environment. In addition to the required mechanical properties and blood compatibility (i.e. low thrombogenicity), long-term safety is dependent on the absence of rejection and toxicity. (van der Giessen et al. 1996)

Local hypersensitivity reaction and chronic inflammation have been identified as the cause for aneurysmal vessel dilatation and late acquired ISA occurring in patients with very late ST after SES implantation (Virmani et al. 2004). The inflammatory response with eosinophil involvement around DES struts gave reason to suggest that the persisting polymer plays a role in the multifactorial causality related to ST (Joner et al. 2006). The same histopathological findings were present with several polymer coatings, both durable and biodegradable, in the absence of eluted drug (van der Giessen et al. 1996).

The LEADERS trial, a large RCT on 2472 lesions in 1707 patients comparing biodegradable polymer biolimus-eluting stents (BP-BES) with first-generation SES, showed identical rates of ST during the first year, but a significantly lower risk of very late definite ST in the BP-BES group (HR 0.20, 95% confidence interval (CI) 0.06–0.67, p=0.004) (Stefanini et al. 2011). The OCT substudy of 46 patients at 9-month follow-up revealed significantly fewer uncovered struts in the group treated with BP-BES (0.6% vs. 2.1%, p=0.04) (Barlis, Regar, et al. 2010). In contrast, recent data from 3490 patients in the BIO-RESORT trial showed no difference in the incidence of target lesion failure or ST between BP-BES, biodegradable polymer zotarolimus-eluting stents (BP-SES) and durable polymer zotarolimus-eluting stents (DP-ZES) at 12 months (von Birgelen, Kok, van der Heijden, Danse, Schotborgh, Scholte, et al. 2016).

Abluminal drug coating has been used to achieve unilateral drug delivery and earlier neointimal coverage (de la Torre Hernández, Tejedor, Camarero, Duran, Lee, Monedero, et al. 2016). Implantation of 60 platinum-chromium everolimus-eluting stents (PtCr-EES) revealed a low percentage of uncovered struts by OCT (5.5% at 3 months and 3.4% at 6 months), with most of the uncovered struts occurring at sites of malapposition (de la Torre Hernández, Tejedor, Camarero, Duran, Lee, Monedero, et al. 2016).

### 2.1.5 Drug-eluting balloons

Drug-eluting balloons (DEB) have been used effectively to treat in-stent restenosis after DES or BMS implantation, which is reflected in the ESC guidelines as a class IA recommendation (Table 1) (Kolh, Windecker, Alfonso, Collet, Cremer, Falk, et al. 2014). In a large meta-analysis of trials comparing DEB, DES and angioplasty alone, DEB and DES prevented TLR (Lee et al. 2015). DEB also showed a trend towards preventing MI compared to DES and angioplasty alone, but the difference did not reach statistical significance (Lee et al. 2015).

Observational studies have shown the feasibility of DEB for the treatment of *de novo* lesions in small vessels (2.5mm reference diameter), resulting in TLR rates ranging from 1% at 9 months to 3.4% at 6 months (Wöhrle, Zadura, Möbius-Winkler, Leschke, Opitz, Ahmed, et al. 2012; Bondesson, Lagerqvist, James, Olivecrona, Venetsanos & Harnek 2012). Treatment of small vessels with DEB alone was proven non-inferior to PES in a RCT with 2-year follow-up (Naganuma, Latib, Sgueglia, Menozzi, Castriota, Micari, et al. 2015). DEB can also be used in conjunction with DES implantation as a hybrid approach in long lesions (Costopoulos, Latib, Naganuma, Sticchi, Figini, Basavarajaiah, et al. 2013). Treatment with DEB alone brings the advantage of a short DAPT duration of 1 month.

Due to the chronic inflammation and uncovered struts exhibited by DES, it was hypothesised that DEB before BMS implantation might improve the outcome after STEMI, as drug polymer would be absent and drug distribution more homogenous. However, DEB before BMS implantation resulted in a rate of uncovered struts and endothelial dysfunction higher than BMS alone and comparable to DES implantation. Furthermore, DEB failed to decrease the amount of NIH or LLL compared to BMS alone, and both clinical and angiographic results were inferior to DES. (Belkacemi et al. 2012)

**Table 1** Relevant ESC guidelines for PCI.

| Recommendation | Class | Level |
|---|---|---|
| Drug-coated balloons for the treatment of in-stent restenosis (with BMS or DES) | I | A |
| FFR to identify hemodynamically relevant coronary lesions when evidence of ischemia is not available | I | A |
| FFR to guide PCI in patients with multivessel disease | IIa | B |
| IVUS in selected patients to optimize stent implantation | IIa | B |
| IVUS to assess severity and optimize treatment of unprotected left main lesions | IIa | B |
| IVUS or OCT to detect stent-related mechanical problems | IIa | C |
| OCT in selected patients to optimize stent implantation | IIb | C |

(Kolh, Windecker, Alfonso, Collet, Cremer, Falk, et al. 2014)

### 2.1.6   *Bioresorbable vascular scaffolds*

BVS have been designed to prevent vessel closure by scaffolding the vessel wall throughout the acute and subacute phase. After this, as neointimal healing is complete and positive remodelling begins to take place, the device serves no further purpose and deliberate bioresorption occurs, hypothetically eliminating the risk of chronic inflammation and late ST (Iqbal et al. 2014).

The ABSORB trials have given critical information on a novel everolimus-eluting polymer-based BVS designed to support the vessel wall for the first year after implantation, after which complete bioresorption of the device takes place over the following years (Ellis et al. 2015; Serruys et al. 2014). 2008 BVS implanted in a randomised fashion in patients with stable or unstable coronary artery disease (CAD) were non-inferior to EES for TLF, the lesion-specific composite endpoint of cardiac death, target vessel MI, or ischemia-driven TLR (7.8% vs. 6.1% respectively) at 1-year follow-up (Ellis et al. 2015). IVUS showed enlargement of mean lumen, scaffold, plaque and vessel area up to two years, implying positive remodelling. Recent 3-year results in 468 patients revealed increased TLF in the BVS group compared to EES (10% vs. 5%, respectively), higher LLL (0.37mm vs. 0.25mm, respectively), and no improvement in vasodilatory response to nitrates (Serruys, Chevalier, Sotomi, Cequier, Carri??, Piek, et al. 2016). Eight patients with BVS had definite ST and one had probable ST, of which 6 occurred between 1–3 years; incidence of ST was 3% in contrast to none in EES, making the polymer-based BVS highly unappealing (Serruys, Chevalier, Sotomi, Cequier, Carri??, Piek, et al. 2016). Considering the promising 1-year clinical results, it appears that the long resorption time of the scaffold material with 150µm strut thickness plays a key role in the poor vascular healing.

BVS based on a second generation magnesium platform and covered with a sirolimus-eluting poly-L-lactide drug polymer were studied in the BIOSOLVE-II study (Haude, Huseyin Ince, et al. 2016; Haude, Hüseyin Ince, et al. 2016). In contrast to polymeric BVS, the magnesium scaffold was shown to dissolve rapidly through oxidation and absorption of the magnesium ions, with only 5% of the magnesium left at 1 year (Haude, Hüseyin Ince, et al. 2016). The 12-month clinical outcome was excellent, with 3.4% incidence of TLF (95% CI 0.9–8.4) and no ST (Haude, Huseyin Ince, et al. 2016). No progress in LLL was seen from 6 to 12 months, although a decrease in MLA from 4.58 mm$^2$ to 4.19 mm$^2$ was seen in an OCT substudy of 11 patients, (p=0.032) (Haude, Huseyin Ince, et al. 2016). Further improvements in radial strength and strut thickness could make BVS the future PCI treatment of choice, but this requires large RCT data to verify clinical outcomes.

## 2.2      Stent thrombosis

### *2.2.1    Pathogenesis and risk factors*

According to ARC consensus standardised definitions, ST should be identified based on different levels of evidence and timing of the event (Cutlip et al. 2007). Definite ST requires evidence on angiography, thrombectomy, or autopsy and can be occlusive or non-occlusive. This category is highly specific, but may not be sufficient to capture the rare occurrences of ST in the setting of clinical trials. Any unexplained death within 30 days of stenting, or MI of the stented vessel territory at any time point in the absence of a known cause is categorised as probable ST. Any unexplained death >30 days after stenting is a possible ST for the purposes of clinical follow-up. Reporting of both definite and probable ST is recommended in studies on stent safety. (Cutlip et al. 2007)

ST can be termed acute (within the first 24 hours), subacute (1 to 30 days), late (1 to 12 months), or very late (>1 year) (Cutlip et al. 2007). The temporal classification of ST also correlates with the pathophysiology: the majority of ST occur early (acute or subacute) and are invariably related to procedure-related factors or inadequate antiplatelet therapy (Cutlip et al. 2001; Iakovou et al. 2005; Uren et al. 2002; Andrew T.L. Ong et al. 2005). The most consistently documented risk factors of late ST are DAPT interruption, delayed neointimal coverage, and ISA (Andrew T L Ong et al. 2005; Parodi et al. 2013). The factors leading to very late ST are poorly known (Cutlip et al. 2007).

Acute or subacute ST is nearly always the consequence of a procedure-related complication (Cutlip et al. 2001). Patients who suffered an acute or subacute ST after BMS implantation had underexpansion, ISA, plaque prolapse, dissection, or thrombus detectable on post-PCI IVUS in 94% of cases, which was visible on angiography in only 32% of the cases (Uren et al. 2002). Localized medial dissection is a procedure-related adverse event leading to high rates of subacute stent thrombosis (Komatsu et al. 1998). In-stent dissection was present in 98% of patients with ACS immediately after treatment with DES, and edge dissection in 27-37% (De Cock et al. 2014). Eight percent of detected in-stent dissections are visible by OCT at 9 months, and edge dissection persists in 27-30% of lesions (De Cock et al. 2014). Whereas subacute ST was related to underexpansion, late and very late ST are more often associated with ISA and uncovered struts (Parodi et al. 2013). ISA and complex vessel morphology cause disturbances in flow and shear stress, which induces downregulation of native anticoagulants and stagnation of activated platelets (Chatzizisis, Coskun, Jonas, Edelman, Feldman & Stone 2007).

Early DES were characterized by high rates of late acquired ISA, which is a well-recognized substrate for very late ST (Cook et al. 2007). Post-mortem studies have pointed towards local hypersensitivity and chronic inflammation as the cause for positive remodelling and late acquired ISA occurring in patients with very late ST after SES implantation (Virmani et al. 2004). However, prospective IVUS studies have not been able to demonstrate a correlation between the rare occurrences of ISA and late or very late ST (Steinberg et al. 2010).

### 2.2.2   *Antiplatelet therapy*

Early clinical trials on BMS implantation were complicated by alarmingly high rates of early stent occlusion due to acute of subacute ST (23%), which led to the adoption of various anticoagulation strategies involving heparin, acetylsalicylic acid (ASA), dipyridamole, and vitamin K antagonists (Serruys et al. 1991). Sub-sequent RCT data on drug regimens showed that a combination of ticlopidine and ASA prevented ST more efficiently than ASA alone or a combination of ASA and anticoagulation with heparin or vitamin K antagonists (Leon et al. 1998; Schömig et al. 1996; Bertrand et al. 1998; Urban et al. 1998). Clopidogrel in combination with ASA resulted in fewer bleeding complications than the combination of ticlopidine and ASA, which led to the widespread use of DAPT with a 1-month regimen of clopidogrel and ASA (Bertrand et al. 2000). The incidence of ST was thus reduced to a level <1.0%, although it was associated with a 64.4% rate of death or MI, making it a rare but serious complication (Cutlip et al. 2001). The median time to ST after PCI was 1 day (Cutlip et al. 2001).

Later investigation into the effects of clopidogrel on platelet reactivity revealed considerable variability after standard clopidogrel treatment in patients undergoing elective PCI, and high pre-treatment platelet reactivity was identified as the most important factor leading to impaired antithrombotic protection (Gurbel, Bliden, Hiatt & O'Connor 2003). High platelet reactivity defined as >208 $P2Y_{12}$ reaction units in VerifyNow point-of-care assays was observed in 42.7% of patients under DAPT with clopidogrel and ASA. This group of patients was at a significantly higher risk of ST at 1-year follow-up compared to patients without high platelet reactivity (1.3% vs. 0.5%, HR 2.54 [95% CI 1.55–4.16], p=0.0002) despite uninterrupted DAPT. High platelet reactivity was inversely related to bleeding (HR 0.65 [0.43–0.99], p=0.04) (Stone et al. 2013).

Prasugrel and ticagrelol were derived from further iterations on $P2Y_{12}$ inhibitor drug design with better anti-ischemic efficiency. The PLATO study was a large RCT comparing ticagrelol with clopidogrel in 18624 patients with ACS, where ticagrelol reduced the rate of MI, stroke or death from vascular causes at one year

from 11.7% to 9.8%, albeit with an increase in major bleeding unrelated to bypass surgery (Wallentin, Becker, Budaj, Cannon, Emanuelsson, Held, et al. 2009). A similar study on prasugrel yielded comparable results, with a reduction from 12.1% to 9.9% in the composite endpoint, and an increase in major bleeding (Wiviott, Braunwald, McCabe, Montalescot, Ruzyllo, Gottlieb, et al. 2007). Although this effect is mainly produced by faster onset of action and reversible $P2Y_{12}$ binding, recent findings suggest, that ticagrelol also has adenosine-mediated cardioprotective properties (Vilahur, Gutiérrez, Casani, Varela, Capdevila, Pons-Lladó, et al. 2016).

The rate of ST was deemed acceptable, until frequent cases of late and very late ST were reported in patients treated with DES exhibiting incomplete neointimal coverage and chronic inflammation (Finn et al. 2007; Joner et al. 2006; Virmani et al. 2004). Prospective cohort studies from the first-generation DES era showed evidence of a 1.3–1.7% cumulative incidence of definite or probable ST, mainly augmented by late ST at a rate ranging from 0.35% (95% CI 0.17%-0.72%) (Andrew T L Ong et al. 2005) to 0.5–0.8% (Iakovou et al. 2005). Late ST was strongly associated with premature DAPT discontinuation, but occurred also in patients who were clinically stable on long-term aspirin therapy.

Studies on new generation DES have reported ST rates that were lower compared to BMS and first-generation DES, and caused a paradigm shift in ST risk reduction (Palmerini et al. 2012; Stefanini et al. 2011; Baber et al. 2011). In a *post hoc* analysis of the pooled RESOLUTE dataset, DAPT discontinuation during the first month after DP-ZES implantation led to a 3.61% incidence of ST (compared to 0.84% with uninterrupted 12-month DAPT), but no correlation was observed between ST and DAPT discontinuation between 1 and 12 months (Silber et al. 2014). Comparison between a polymer-free biolimus-coated stent and a modern BMS in LEADERS FREE, a RCT on 2432 patients at high bleeding risk on 1-month DAPT, showed similar rates of definite or probable ST in 1-year follow-up (2.0 % vs. 2.2%, respectively) (Urban, Meredith, Abizaid, Pocock, Carrié, Naber, et al. 2015). RCT have shown no difference in the incidence of ST between 6-month and 12-month (Schulz-Schüpke et al. 2015), 6-month and 24-month (Valgimigli et al. 2012), 12-month and 24-month (Lee, Ahn, Park, Kang, Lee, Kim, et al. 2014) or 3-month and 12-month (Feres et al. 2013) DAPT; however prolonged DAPT beyond 1 year up to 30 months significantly reduced the risks of ST and MI, but was associated with an increased risk of bleeding and all-cause mortality (Mauri, Kereiakes, Yeh, Driscoll-Shempp, Cutlip, Steg, et al. 2014). These findings were confirmed in meta-analysis, where DAPT discontinuation caused no increase in the risks of ST or MI, until after the first 12 months, where prolonged DAPT was associated with a reduction in non-stent-related MI and a minor effect on ST (D'Ascenzo, Moretti, Bianco, Bernardi, Taha, Cerrato, et al. 2016). Any possible

effect on mortality may have been offset by the increase in major bleeding. With modern DES, the benefits of DAPT beyond 3 months appear not to surpass the risks in patients at high risk of bleeding.

The PARIS registry is an observational all-comers study of 5018 patients, where adherence to DAPT after PCI with stenting was linked to MACE and ST in 2-year follow-up (Mehran et al. 2013). Recommended, physician-directed DAPT discontinuation was associated with a lower risk of MACE (0.63, 95% CI 0.46–0.86, p=0.004) with no difference in the risk of definite or probable ST (0.92, 95% CI 0.53–1.58, p=0.748) compared to patients under uninterrupted DAPT for 2 years. Most of the ST (80%) occurred during DAPT. Temporary interruption of DAPT due to surgery did not increase the risk of MACE or ST. Permanent cessation of DAPT due to bleeding complication or non-compliance increased the risk of MACE significantly; the effect was highest for the first 7 days, but attenuated over 30 days. Interruption or cessation of DAPT was associated with an increase in the risk of MACE from 5.7% to 8.4% and ST from 0.5% to 1.1% in 2-year follow-up (Mehran et al. 2013). An individualized approach to risk assessment remains crucial to the optimization of DAPT duration after stenting.

## 2.3 Invasive imaging of coronary arteries

### 2.3.1 *Intravascular ultrasound*

#### 2.3.1.1 *Introduction*

IVUS was first successfully employed in 1990 to give additional information on coronary morphology and luminal dimensions (Davidson et al. 1990). In addition to good agreement with digital subtraction angiography, it revealed atherosclerotic plaques that were undetectable in angiography. Compared to histology IVUS accurately identifies plaque characteristics, luminal dimensions and intimal dissections, whereas assessment by angiography frequently underestimates percent area stenosis (Tobis et al. 1991). In reference segments where the vessel wall appeared normal on angiography, atheroma occupied 35% of cross-sectional lumen area on average on IVUS. Despite the independent value of IVUS, it should be considered supplemental to angiography rather than an alternative, as angiography is still the most important imaging method to quickly assess coronary anatomy and to guide therapy (Nissen & Yock 2001).

IVUS is performed by introducing an imaging catheter ranging from 2.6 to 3.5 French past the coronary lesion of interest and performing a motorised pullback to scan the segment. Imaging catheters exist in two types: mechanically rotated systems utilise a single-element ultrasound transducer at the tip of the catheter rotated at 1800 rpm and achieve greater resolution due to frequency of 40-45 MHz (Nissen & Yock 2001). Electronic solid-state systems use a multi-element annular array of 64 transducers around the catheter activated sequentially at 20 MHz, resulting in inferior image quality, but lacking the rotational distortion artefacts of the single-element catheter (McDaniel et al. 2011). The axial resolution of IVUS is dependent on the frequency used, and varies between 100-150 μm (Waksman et al. 2013).

Intravascular imaging has been suggested as a tool providing useful information to guide PCI. IVUS may be used prior to PCI to define lesion characteristics, and in post-PCI assessment to detect stent underexpansion, malapposition, and possible procedure-related complications (Hong, Mintz, Lee, Park, Choi, et al. 2006; Fujii et al. 2005). IVUS-guided new-generation DES implantation reduces the need for target lesion revascularization in long, complex lesions by detecting underexpansion (Hong et al. 2015). Percent atheroma volume measured by IVUS and the increase thereof were both strong predictors of MACE and TLR at 2-year follow-up, and should therefore be useful surrogate endpoints in research of anti-atherosclerotic therapies (Nicholls et al. 2010).

### 2.3.1.2 Assessment of stenosis severity

Area stenosis is defined on IVUS as the difference between the reference luminal area and MLA, expressed as a percentage of the reference area (McDaniel et al. 2011). The external elastic membrane can be visualised easily at the echolucent media-adventitia border, and is therefore used in preference to the echo-silent media as a reference for the assessment of plaque burden (Nissen & Yock 2001). The external elastic membrane, however, is subject to arterial remodelling, thus making plaque burden unreliable for the assessment of stenosis severity (McDaniel et al. 2011).

Briguori et al. performed a study comparing IVUS to FFR in the assessment of the functional severity of intermediate lesions (Briguori et al. 2001). In regression analysis, percent area stenosis (r = −0.58, p <0.001), minimal lumen diameter (MLD) (r = 0.51, p <0.001), and MLA (r = 0.41, p <0.004) showed a significant correlation with FFR. Areas stenosis >70% (sensitivity 100%, specificity 68%), MLD ≤1.8 mm (sensitivity 100%, specificity 66%), and MLA ≤4.0 mm$^2$ (sensitivity 92%, specificity 56%) were established as the best cut-off values to fit with a FFR <0.75. Combining the criteria of both percent area stenosis and MLD made

the IVUS examination more specific (sensitivity 100%, specificity 76%) (Briguori et al. 2001). A more recent study with a similar research setting reported that MLA $\geq 2.4$ mm$^2$ excludes abnormal FFR (<0.80) with great certainty (negative predictive value 96%), but when MLA <2.4mm$^2$, poor specificity limits its usefulness for physiological assessment of stenosis severity (Kang et al. 2011).

Deferral of revascularisation of intermediate lesions gave excellent results when MLA was $\geq 4.0$ mm$^2$ (Abizaid et al. 1999), which was also highly predictive of coronary flow reserve (CFR) $\geq 2.0$ (accuracy 89%) (Abizaid et al. 1998). For the assessment of lesion severity FFR remains the gold standard, and current ESC guidelines recommend IVUS only for optimization of PCI (Table 1).

### 2.3.1.3  Intravascular ultrasound in the left main coronary artery

The assessment of stenosis severity is challenging particularly in left main coronary artery stenoses, where hemodynamically significant stenoses may manifest in a wide range of angiographic findings, even <30% diameter stenosis on quantitative coronary angiography (Hamilos et al. 2009; de la Torre Hernandez et al. 2011). Functionally significant stenoses (FFR<0.75) can be detected accurately using IVUS-derived MLD of 2.8mm (93% sensitivity and 98% specificity) or MLA of 5.9mm$^2$ (93% sensitivity and 95% specificity) (Jasti et al. 2004). MLD and MLA seem to be more reliable parameters than percent stenosis, as the measurement of reference vessel diameter in the left main is afflicted by numerous sources of error (de la Torre Hernandez et al. 2011). Deferral of revascularisation in left main stenosis with MLA $\geq 7.5$mm$^2$ resulted in favourable outcomes (Fassa et al. 2005). Following a larger study using MLA of 6 mm$^2$ as the cut-off (de la Torre Hernandez et al. 2011), the lower cut-off of 6 mm$^2$ was established; however FFR remains the best parameter for functional assessment of left main stenosis severity, and IVUS is recommended only after the indication for revascularisation is established, as it is far superior to FFR in the characterisation of lesion and reference vessel data (Montalescot et al. 2013). The benefit of IVUS in the treatment of left main stenoses is in the guidance of DES implantation, as evidenced by the decreased mortality rate compared to angiography guidance in the MAIN-COM-PARE registry (Park et al. 2009).

### 2.3.1.4  Intravascular ultrasound guidance in stenting

In a meta-analysis of 7 RCT comparing IVUS-guided against angiography-guided BMS implantation in the pre-DES era, the use of IVUS to accurately measure the

lumen calibre and detect ISA requiring post-dilatation resulted in a significantly greater post-PCI MLA. At 6-month follow-up, in-stent restenosis was reduced significantly (22% vs 29%, odds ratio 0.64, 95% CI 0.42 to 0.96, p=0.02), as was TRL (13% vs 18%, odds ratio 0.66, 95% CI 0.48 to 0.91, p = 0.004) with no difference in the incidence of MI or mortality at a follow-up ranging from 6 months to 2.5 years (Parise et al. 2011). In a more recent RCT of DES implantation in complex lesions, improvement was seen in MLA, but not in the 2-year clinical outcome (Chieffo et al. 2013). In agreement with these findings, another study with a similar protocol showed no difference in 18-month clinical outcome between DES implantation with IVUS guidance or standard high-pressure post-dilatation (Jakabčin et al. 2010). It appears that the reduction of LLL achieved by the emergence of DES has eliminated the need for MLA maximization using IVUS guidance (Gerber & Colombo 2008).

Along with increased concern over late and very late ST after DES implantation, studies on large propensity score matched populations have suggested that IVUS guidance reduces the incidence of ST (Roy et al. 2008; Witzenbichler et al. 2014). A substudy from the ADAPT-DES registry reported lower 1-year rates of definite or probable ST associated with IVUS guidance compared with angiography alone (0.6% versus 1.0%, HR 0.40, p =0.003) (Witzenbichler et al. 2014). The composite endpoint of cardiac death, MI, or ST was also significantly reduced (3.1% versus 4.7%; HR 0.70; p=0.002). This reduction was stronger in high-risk patients with ACS or complex lesion morphology such as three-vessel disease, calcification, bifurcation, in-stent restenosis, or left main disease, but was present in all patient subgroups (Witzenbichler et al. 2014). A smaller study with very similar patient characteristics also found a decrease in ST (0.7% vs. 2.0%; P = 0.014) but not in MACE (Roy et al. 2008). IVUS guidance for stent implantation in long lesions (>27 mm), compared to angiography guidance, caused a more robust risk reduction (2.9% vs. 5.8%) in the composite endpoint of TLF at 1 year (Hong et al. 2015). The number needed to treat to prevent one MACE was 34 patients.

A meta-analysis of 3 randomized trials and 12 observational studies from the DES era showed evidence that IVUS guidance reduced the incidence of death, MI and ST (Jang et al. 2014). However, it is still controversial whether improved clinical outcomes can be achieved using routine IVUS guidance, so risk profiles and lesion subsets need to be further characterized to identify patients who benefit from IVUS.

## 2.3.2    *Optical coherence tomography*

### 2.3.2.1  *Introduction*

Analogous to the IVUS, intravascular OCT requires a catheter that both emits beams of light and records the reflections from the vessel wall. As light travels at a much higher speed, it is necessary to use interferometry techniques to quantify the echo time delay and the distance travelled. This is achieved by using a rotating reference arm at a calibrated distance from the detector. In time-domain OCT systems broadband light in the visible spectrum is used, and specified depths are scanned and coupled to the beam reflected from the reference arm. Each axial scan can be performed in 100-200ns, enabling pullback at a speed of 3mm/s. Frequency-domain OCT utilises a swept laser with variable frequencies to scan all depths of the axial scan simultaneously, allowing higher lateral resolution and faster image acquisition. (Bezerra, Costa, et al. 2009)

Blood in the coronary segment of interest must be voided, as red blood cells cause considerable signal attenuation. In time-domain OCT systems this is achieved by closing off the distal vessel with a highly compliant low-pressure balloon, and saline is infused to displace the blood. Newer frequency-domain OCT systems enable non-occlusive imaging of coronary vessels (Chinn et al. 1997); using a variable frequency light source it can acquire 100 frames/s, which allows pullback speeds up to 20 mm/s. Consequently, epicardial vessels 4 to 6 cm in length can be flushed with viscous contrast and scanned in less than 5 seconds (Tearney et al. 2008). The tissue penetration of an OCT beam of 1300 nm wavelength is limited to 1-3 mm, compared to 4-8 mm achieved by IVUS, although ultrasound penetrates poorly in calcified lesions (Bezerra, Costa, et al. 2009).

### 2.3.2.2  *Assessment of stenosis severity*

Despite its accuracy in the measurement of luminal dimensions, OCT has sparked little interest in deriving a marker of stenosis severity in the era of FFR. OCT-derived criteria of lumen narrowing showed good agreement with FFR in intermediate lesions (40-70% diameter stenosis): the best cut-offs to identify FFR<0.80 were MLA <2.05 mm$^2$ (sensitivity 75%, specificity 90%, area under receiver operating characteristic curve (AUC) 0.91) and MLD <1.28 mm (sensitivity 71%, specificity 84%, AUC 0.90) (Pawlowski, Prati, Kulawik, Ficarra, Bil & Gil 2013). The optimal cut-off for MLA differed by 1.11 mm$^2$ depending on reference vessel diameter (</≥3mm) (Pawlowski, Prati, Kulawik, Ficarra, Bil & Gil 2013).

Similar studies have shown comparable results: MLA <1.62 mm$^2$ (sensitivity 70%, specificity 97%, AUC 0.80) and MLD <1.23 mm (sensitivity 70%, specificity 87%, AUC 0.76) for FFR<0.80 (Zafar, Ullah, Dinneen, Matiullah, Hanley, Leahy, et al. 2014); and MLA <1.91 mm$^2$ (sensitivity 93.5%, specificity 77.4%, AUC 0.90) and MLD <1.35 mm (sensitivity 90.3%, specificity 80.6%, AUC 0.92) for FFR<0.75 (Shiono, Kitabata, Kubo, Masuno, Ohta, Ozaki, et al. 2012). Cut-offs varied between studies depending on patient selection and vessel diameter. A high association was seen between FFR<0.75 and >70% area stenosis by OCT (sensitivity 96.8%, specificity 83.9%, AUC 0.94) (Shiono, Kitabata, Kubo, Masuno, Ohta, Ozaki, et al. 2012), but not with FFR<0.80 (AUC 0.63) (Zafar, Ullah, Dinneen, Matiullah, Hanley, Leahy, et al. 2014).

In a comparison between OCT and IVUS to assess functional severity in intermediate lesions the OCT-derived cut-off of MLA 1.95 mm$^2$ identified FFR<0.80 with 82% sensitivity and 63% specificity, which was superior to IVUS (67% sensitivity, 65% specificity, p=0.04) (Gonzalo et al. 2012). Surprisingly, the OCT-derived percentage of area stenosis yielded an inferior diagnostic accuracy. The accuracy of OCT-derived MLA was improved in vessels <3.0 mm$^2$ (Gonzalo, Escaned, Alfonso, Nolte, Rodriguez, Jimenez-Quevedo, et al. 2012; Zafar, Ullah, Dinneen, Matiullah, Hanley, Leahy, et al. 2014), but overall the poor specificity limits its use as an alternative for FFR in functional stenosis assessment (Gonzalo et al. 2012).

### 2.3.2.3 *Assessment of coronary stents*

OCT and IVUS may be used to detect stent-related mechanical problems during PCI (Table 1). One of the great advantages of OCT over IVUS is that, in addition to cross-sectional analysis of NIH and luminal dimensions, it allows strut-level analysis of neointimal coverage of coronary stents, owing to its high axial resolution and capacity to visualise 10-µm layers of tissue (Mehanna et al. 2011). Struts embedded in the vessel wall can easily be detected in OCT cross-sections (Figure 1). A comprehensive study of 622 OCT cross-sections acquired at 1–3 months after DES implantation, matched with histology in a porcine model, showed excellent agreement in measurements of NIH thickness and area; luminal and stent area measurements were higher by OCT due to the cutting artefact of histology sections (Murata et al. 2010). Detection of binary strut coverage had high agreement; NIH thickness measurements matched consistently in the range of 0–20 µm, spread between 20–80 µm, and converged again at thicknesses >80 µm (Murata et al. 2010).

Another histopathological study has also shown that heterogeneous NIH appearance is associated with fibrin deposition and peri-strut inflammation (Kim et al. 2014).
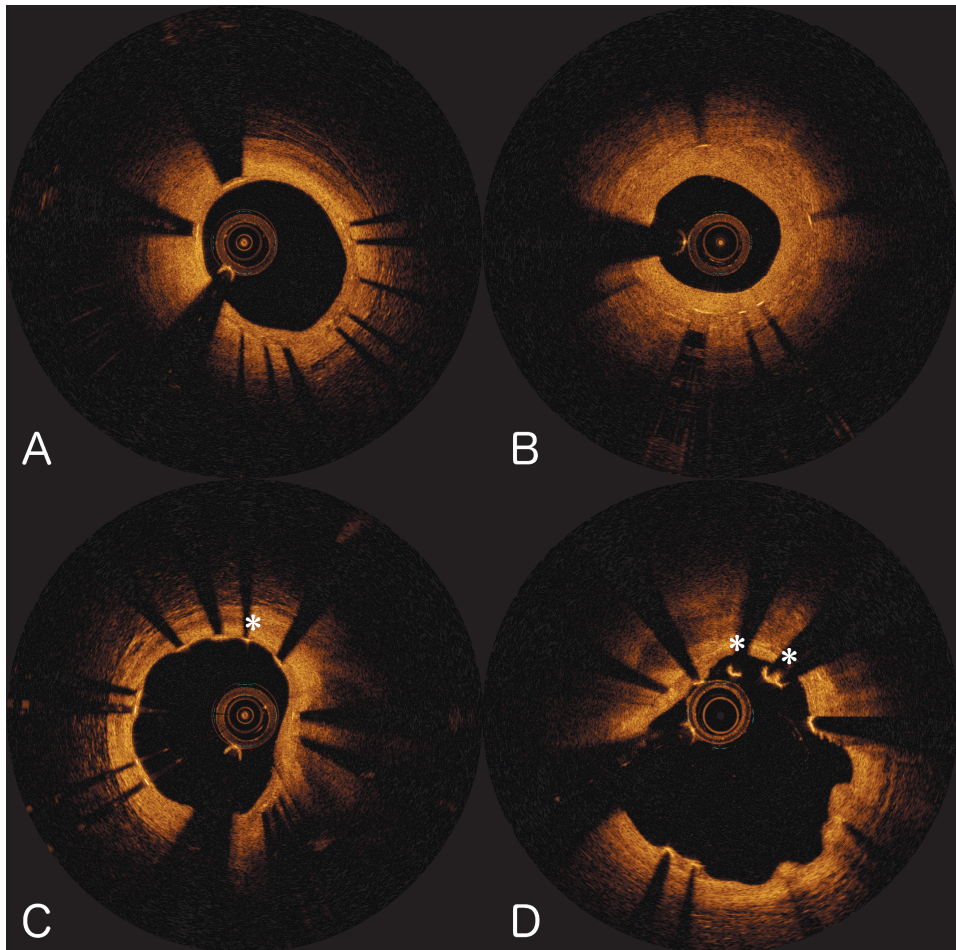


**Figure 1** OCT cross-sections of stents depicting different patterns of vascular healing. A: good anatomical healing with comprehensive neointima; B: thick neointimal hyperplasia; C: poor neointimal coverage with uncovered struts (asterisk); D: incomplete stent apposition with malapposed struts (asterisk).

Strut coverage assessed in 16 patients at a mean follow-up 4.7±2.8 months after stent implantation, performed at 1-mm sampling interval revealed high intra- and inter-observer agreement; mean NIH thickness was 169.6 μm vs. 175.5 μm between observers. In Bland-Altman analysis intra-observer repeatability coefficient was 26.7 μm, with an intraclass correlation (ICC) of 98.6%. Inter-observer repeatability coefficient was 24.1 μm and ICC between observers was high (99.6%). (Barlis, Dimopoulos, et al. 2010)

Modern frequency-domain OCT systems generally acquire 10 cross-sections per 1mm (Gutiérrez-Chico et al. 2012). Due to the overwhelming amount of data and cumbersome manual analysis, it is common practice to sample a prespecified quantity of the cross-sections, and to perform the analysis at 1-mm or, less commonly, 0.6-mm intervals. Whereas cross-sectional analysis of area measurements can be performed at sampling intervals as long as 2.4 mm with low variability, strut-level analysis of binary strut coverage may be subject to high variability even at 1-mm sampling interval (Bezerra, Guagliumi, et al. 2009). Brugaletta et al. determined inter- and intra-observer agreements for binary strut coverage, and showed that the categorisation of struts as covered or uncovered varied significantly between observers depending on the zoom setting used in the analysis (Brugaletta et al. 2013). Significant discrepancy has been discovered between quantitative measurements of NIH by OCT and histology for layers of NIH between 20 and 80 µm in thickness, which is the most commonly reported range of NIH thickness in modern DES (Murata et al. 2010).

## 2.4 Functional measurements in coronary artery disease

### 2.4.1 *Physiology of coronary circulation*

The hemodynamics in a coronary vessel can be simplified using a hydraulic analogy of Ohm's law:

$$Q = \frac{\Delta P}{R}$$

where Q is the blood flow across a segment of a coronary artery, $\Delta p$ is the change in pressure across that segment, and R is the flow resistance across that segment. The resistances of successive stenoses are cumulative and directly proportional to their corresponding pressure gradients, since flow remains constant (Bernoulli's principle for incompressible flows). Thus, $\Delta p$ and R can be measured from stenoses in series. (Gould & Lipscomb 1974)

To measure this pressure gradient more accurately, coronary flow is increased using a vasodilating stimulus that reduces microcirculatory resistance, most commonly adenosine. This is demonstrated in Figure 2, where $P_a$ is the aortic pressure, $P_d$ is the pressure distal to the epicardial stenosis, and $P_v$ is the right atrial pressure. Under resting conditions, most of the flow resistance arises from the microcirculation and the myocardial pressure gradient ($P_d - P_v$) is high. Under hyperemia microcirculatory resistance is minimal and flow increases, the stenosis becomes

flow limiting and $P_d$ drops. Since the hyperemic microcirculatory resistance is independent of epicardial stenosis, FFR can be calculated as $P_d/P_a$, and it is not influenced by baseline flow. This is one of the main advantages of FFR in the assessment of functional severity compared to CFR, which is defined as the ratio between hyperemic to baseline blood flow. CFR does not leave the microcirculation out of the equation, but is rather a measure of reserve in the entire coronary bed (Figure 2).

As the induction of hyperemia may be problematic in some patients and produces a source of error, alternative ways of assessing the functional severity of a stenosis without hyperemia have been developed, most notably the instantaneous wave-free ratio (iFR). iFR is based on the theory that end-diastolic microcirculatory resistance is constant and negligible (Sen et al. 2012). However, studies have shown that iFR correlates poorly with FFR as it is not independent of hyperemia, and can only be used as a screening method in the extremes of the scale (Berry et al. 2013; Escaned et al. 2015). iFR has better diagnostic agreement with CFR, and can therefore give additional information when an abnormal FFR is caused by abnormally high hyperemic flow and CFR (Petraco et al. 2014). The performance of iFR-guided PCI compared to FFR remains to be clarified in DEFINE-FLAIR and iFR-SWEDEHEART.

Hyperemic stenosis resistance (HSR) is an index derived from the pressure gradient and flow that corresponds to R in the previous equation. It is defined as the mean pressure gradient across the stenosis divided by the average peak flow velocity distal to the stenosis during hyperemia. HSR identified reversible perfusion defects in SPECT with 79% sensitivity and 90% specificity using a cut-off value of >0.8 mmHg/cm/sec. This biomarker achieved superior predictive accuracy (87%) compared to CFR (75%, p=0.005) or FFR (75%, p=0.007). (Meuwissen, Siebes, Chamuleau, van Eck-Smit, Koch, de Winter, et al. 2002)

In patients who had intermediate coronary lesions (40-70% diameter stenosis by visual estimation), but no perfusion defects on non-invasive stress testing, the quantification of FFR, CFR, and HSR revealed that MACE at 1-year follow-up was significantly more frequent in patients who had concordant abnormal FFR and CFR results (33.3%), and in patients who had discordant FFR and CFR results (19.7%), compared to those who had concordant normal values (5.4%, p=0.008). HSR abnormality had a higher prognostic value (rate of MACE 7% vs. 54%, p < 0.001) than FFR or CFR alone, and there was a trend towards a higher MACE rate in case of an abnormal HSR when FFR and CFR were discordant (40% vs. 14%, p=0.070). This suggests, that abnormal FFR and CFR values are frequently present in intermediate lesions, and bear independent prognostic value, since they may

occur discordantly. Furthermore, HSR appears to give additional prognostic value when the results are discordant. (Meuwissen et al. 2008)

### 2.4.2 *Coronary flow reserve as a prognostic factor*

The distal left anterior descending artery (LAD) can be visualised by transthoracic echocardiography (TTE) in the apical short-axis view using a high-frequency transducer with low focal zone to circumvent the near-field artefacts (Ross et al. 1990). Colour Doppler flow mapping is used to locate the vessel lumen and the transducer is aligned parallel to the distal LAD flow, which can be then measured accurately with pulsed-wave Doppler at rest and monitored continuously during pharmacologically induced hyperemia (Hozumi, Yoshida, Akasaka, et al. 1998). TTE-derived flow measurements have excellent correlation with simultaneous Doppler guidewire measurement (Hozumi, Yoshida, Akasaka, et al. 1998).

Caiati et al. did pioneering work in 1999 to establish TTE as a method for measuring CFR non-invasively. Using intravenous contrast agent increased the feasibility of pulsed-wave Doppler recording in the LAD from 55% to 98-100%. CFR cut-off value <2.0 had 86% sensitivity and 90% specificity for detecting angiographic LAD stenosis >70%. CFR was compared to intravascular Doppler flow wire as a gold standard and Bland-Altman analysis yielded 95% limits of agreement -0.69−0.72. The non-invasive method had low intra-observer variability, with 95% limits of agreement -0.32−0.32. (C Caiati et al. 1999; Carlo Caiati, Zedda, et al. 1999; Carlo Caiati, Montaldo, et al. 1999)

In a prospective multicenter study of 4313 patients with known or suspected CAD, Cortigiani et al. demonstrated how TTE-derived CFR measurement performed adjunctly with wall motion assessment can give additional prognostic information (Cortigiani et al. 2012). Impaired CFR (≤2.0) was a strong predictor of death or MI at 4-year follow-up (HR 3.31; 95% CI 2.29–4.78; p<0.0001) (Cortigiani et al. 2012), especially in high-risk patients with ischemia at stress echocardiography, left bundle branch block, or diabetes (Cortigiani et al. 2013; Cortigiani et al. 2007).

The DEBATE study enrolled patients with stable CAD treated with angioplasty alone in a single vessel, and suggested that neither anatomical (>35% residual diameter stenosis) nor functional (CFR ≤2.5 using intracoronary Doppler wire) parameters alone measured immediately after PCI can predict restenosis or TLR (Serruys et al. 1997). Patients treated successfully with angioplasty (<35% residual diameter stenosis) had impaired CFR (≤2.5) immediately after the procedure in 50% of the cases, which was caused by elevated baseline coronary flow that was normalised at 6 month follow-up (Piek et al. 2001). In these patients CFR was

lower already before angioplasty, suggesting disturbed autoregulation as the cause of impaired CFR rather that distal microembolisation (Piek et al. 2001). Elevated baseline coronary flow is an important source of error in the assessment of coronary pathophysiology after PCI and MI, as distal microembolisation may cause adenosine-mediated hyperemia of the non-occluded microcirculation (Hori et al. 1986).

Ruscazio et al. demonstrated the ability of impaired CFR to predict epicardial coronary restenosis by studying 124 patients treated for stable CAD with PCI of the LAD with or without stenting. At 1 month, impaired CFR (≤2.5) measured by TTE predicted subsequent restenosis with 67% sensitivity and 87% specificity. Ruscazio et al. speculated that at this time point in the post-PCI healing, the transient microvascular impairment has subsided, and impaired CFR is, rather, a manifestation of epicardial coronary stenosis. (Ruscazio et al. 2012)

### 2.4.3 Fractional flow reserve

In contemporary clinical practice, the most important tool in the functional assessment of coronary circulation is FFR (Montalescot et al. 2013; Hannawi et al. 2014). Pijls et al. first described the catheter-based method of measuring FFR in human coronaries that yielded good agreement with non-invasive tests of reversible ischemia using a cut-off value of <0.75 (Pijls et al. 1996). The FAME study showed that FFR-guided PCI in multivessel disease reduces MACE from 18.3% to 13.2% (p=0.02) compared to angiography-guided PCI (Tonino et al. 2009). This benefit occurs with less stenting in a manner that is cost-effective (Fearon et al. 2010). The superiority of FFR-guided PCI for clinical outcome persisted up to 2 years; but from 2 to 5 years outcome remained comparable between the 2 groups, although a noteworthy proportion of patient was lost to follow-up (van Nunen et al. 2015). The 5-year results of the DEFER study, with a similar protocol of patients with a single intermediate coronary stenosis using <0.75 as cut-off, accordingly demonstrated non-inferiority of deferral up to 5-years, with only 2% drop-outs (Pijls et al. 2007). Equal mortality persisted up to 15 years, with a decrease in the rate of MI from 10.0% to 2.2% associated with deferral (Zimmermann, Ferrara, Johnson, van Nunen, Escaned, Albertsson, et al. 2015).

In contrast, in the all-comers FAME 2 study (patients with stable CAD, diagnosed based on typical angina pectoris or documented ischemia in non-invasive stress test), all patients with at least 1 significant lesion (≥50% diameter stenosis) suitable for PCI were assessed for functional severity by FFR. Patients with FFR ≤0.80 were randomised to receive either PCI and medical therapy or medical therapy alone; functionally insignificant stenoses were excluded. Recruitment was halted

prematurely because of a significantly higher need for urgent revascularisation in the group receiving medical therapy alone compared to patients treated with PCI (16.3% vs. 4.0% at 2-year follow-up, p<0.001). Urgent revascularisation was driven by MI in 28 patients (31%), by unstable angina with ischemic changes on electrocardiography in 18 patients (20%), and by clinical features only in the remaining 44 patients (49%). However, there was no significant difference in the overall rate of death or MI between the study groups. (De Bruyne et al. 2014)

The utility of FFR as a predictor of PCI success has also been demonstrated in studies linking good clinical outcome to the normalisation of FFR immediately after stent implantation (Hanekamp et al. 1999; N. H. J. Pijls et al. 2002) or angioplasty alone (Bech et al. 1999). Post-PCI FFR may remain impaired (<0.80) despite good angiographic appearance in 1 out of 5 patients treated with DES (Hakeem et al. 2015). FFR can also be used for follow-up after stenting to detect restenosis, since impaired FFR is strongly associated with LLL and wall shear stress (Van't Veer et al. 2006).

### 2.4.4 *Vasodilator dysfunction after stenting*

Microvascular obstruction caused by capillary swelling, distal embolisation, and vasoconstriction is commonly observed after MI, which is also reflected on decreased CFR and increased index of microcirculatory resistance (IMR) immediately after PCI (Figure 2)  (Cuculi et al. 2014). The stagnant microcirculation begins to recover within 24 hours, and the improvement of CFR and IMR continues up to 6 months after primary PCI (Cuculi et al. 2014). This in turn may cause impairment of an initially adequate FFR as the coronary bed subtended by the target lesion expands, causing an effect that is indistinguishable from restenosis (Cuculi et al. 2014). This post-PCI increase in microvascular resistance has also been reported in the setting of stable CAD, where peri-procedural microembolisation is the likely cause (Cuisset et al. 2008).
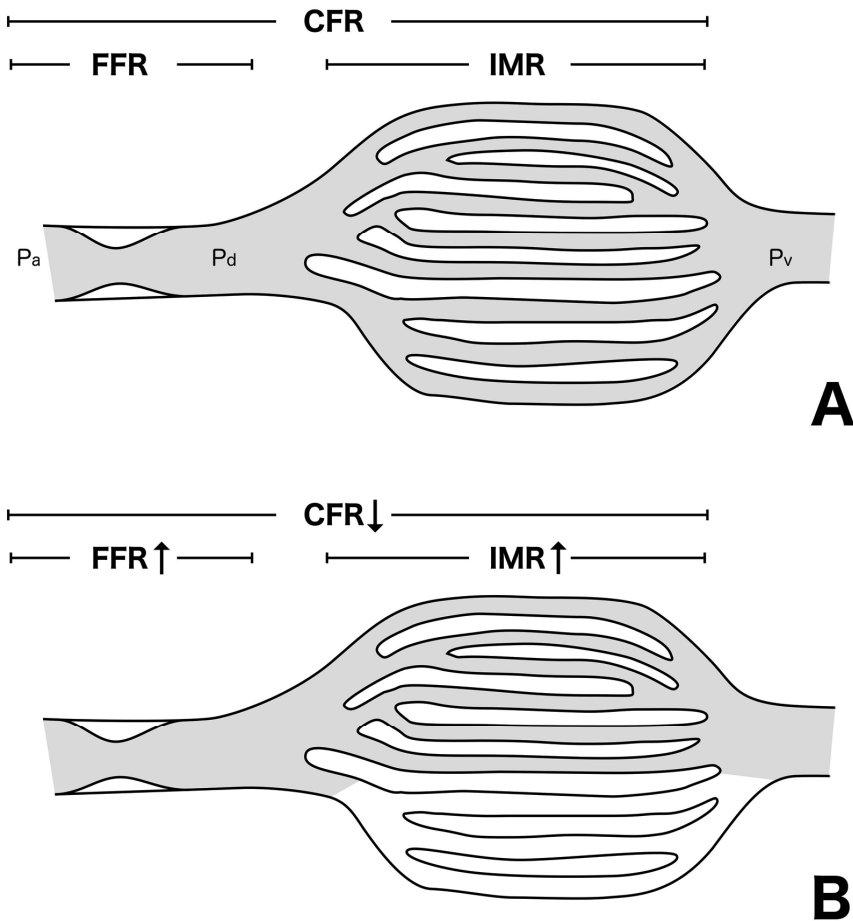
**Figure 2 A**: FFR is used to assess epicardial stenosis, and IMR to assess microcirculation, while CFR evaluates hemodynamic capacity in both. **B**: Microvascular obstruction after myocardial infarction or percutaneous coronary angioplasty causes a decrease in CFR, and an increase in IMR, possibly masking epicardial stenoses. CFR indicates coronary flow reserve; FFR, fractional flow reserve; IMR, index of microcirculatory resistance; $P_a$, aortic pressure; $P_d$, pressure distal to stenosis; $P_v$, right atrial pressure.

Studies on first-generation DES reported impaired endothelial function after DES implantation, as exhibited by paradoxical vasoconstriction in response to intracoronary acetylcholine infusion, rapid atrial pacing, physical exercise, and adenosine as vasodilator stimuli (Togni et al. 2005; Togni et al. 2007; Hofma et al. 2006; Hamilos et al. 2008). Despite normal endothelium-independent vasomotor response to intracoronary nitrates, PES and SES have consistently been shown to cause vasodilator dysfunction proximal and distal to the stented segment, for as long as 1 year after coronary stenting, as compared to BMS (Togni et al. 2005; Togni et al. 2007; Hofma et al. 2006; Hamilos et al. 2008). Second-generation BP-BES showed little or no impairment of endothelial function when compared to SES

(Hamilos et al. 2008). Preserved vasodilator function at 9 months has also been observed with titanium-nitride-oxide–coated BAS compared to EES (Karjalainen et al. 2013), and with BP-SES and DP-ZES compared to first-generation SES (Rusinaru et al. 2015).

Impaired CFR has been shown to predict the occurrence of restenosis after stenting (cut-off <2 for significant and <2.5 intermediate) with high specificity at long-term follow-up after stenting (Pizzuto et al. 2003), although serial measurements can improve sensitivity (Hung & Cherng 2011; Ruscazio et al. 2012). CFR measurement in follow-up after stenting can give additional information to detect target lesion failure.

# 3    AIMS OF THE STUDY

The purpose of the present study was to compare early neointimal coverage of stent struts, and recovery of vasodilator function after treatment with select state-of-the-art stent devices, and to improve upon the methodology of such research. To achieve this goal, the following specific aims were conceived:

1) To compare early vascular healing between BP-SES and DP-ZES in patients presenting with ACS

2) To validate the use of TTE-derived CFR for non-invasive assessment of vasodilator function after PCI with DES implantation

3) To compare early vascular healing between cobalt-chromium bioactive stents (CoCr-BAS) and PtCr-EES in patients presenting with ACS

4) To determine the effect of sampling frequency on OCT-derived indices of vascular healing

# 4    MATERIALS AND METHODS

## 4.1    Study patients

The Healing AT ThRee months after percutaneous coronary Intervention for ACS – HATTRICK-OCT trial (studies I and II) was a prospective multicenter study enrolling 46 patients in 4 study centers (Turku University Hospital, Turku; Satakunta Central Cospital, Pori; Central Ostrobothnia Central Hospital, Kokkola; Central Finland Central Hospital, Jyväskylä). Patients above 18 years with a *de novo* lesion in the LAD ≥50% stenosis on angiography, presenting with ACS were included. ACS comprised STEMI, non-ST-segment elevation myocardial infarction, and unstable angina, as defined by the European Society of Cardiology guidelines (Steg et al. 2012; Roffi et al. 2016). The main exclusion criteria were diabetes, unprotected left main stenosis, ostial lesions, stenting over a side branch >2 mm in diameter, multi-vessel disease, another de novo stenosis of ≥30% in the stented vessel, or bleeding disorder or other contraindication to DAPT.

The study patients underwent PCI of the target lesion and were randomised in a 1:1 ratio to receive either BP-SES (n=23) or DP-ZES (n=23). Computer-generated randomisation was implemented using a closed-envelope system and stratified by study center. Two patients withdrew consent (one in each group) and were lost to follow-up. Investigators involved in data analysis and the study patients were blinded to stent group.

At 3-month follow-up the patients underwent repeat angiography, after which intracoronary OCT and pressure wire measurements were performed on the stented vessel. TTE examination including non-invasive CFR measurement in LAD on adenosine-induced hyperemia was performed on all patients, excluding one of the study centers (Central Finland Central Hospital, Jyväskylä), before invasive measurements. Analysis of acquired images was performed offline blinded to patient characteristics and study group.

The TIDES-OCT trial was a prospective study conducted similarly in 4 study centers (studies III and IV). 40 patients presenting with ACS were enrolled using the same inclusion and exclusion criteria as above, excepting that diabetics and culprit lesions in any coronary branch were permitted. Patients were randomized in a 1:1 ratio to receive either CoCr-BAS (n=19) or PtCr-EES (n=21).

Follow-up was scheduled at 2 months after the index procedure. OCT image acquisition and pressure wire measurements of the stented vessel were attained immediately after follow-up angiography. Two patients in the PtCr-EES group were

excluded from analysis due to follow-up completion past the intended time frame. OCT analysis was performed offline by two observers blinded to stent type and patient characteristics. Observer 1 then repeated the OCT image analysis at a sampling interval of 0.6 mm. This was done in order to evaluate inter-observer variability and for direct comparison of accustomed sampling intervals.

Informed written consent was obtained from all study patients after full explanation of the study protocol. The study protocols were approved by the Ethics Committee of the Hospital District of Southwest Finland before enrolment of patients. The study was initiated and designed by the investigators, and conducted in accordance with the ethical guidelines of the 1964 Declaration of Helsinki, as revised in 2013. No industry representatives were involved in the study design, data collection, analysis, or writing of the manuscripts.

## 4.2 Antiplatelet therapy

Patients already taking ASA before PCI received no additional loading dose of ASA. Patients not previously on ASA received a loading dose of 250 mg orally or 250-500 mg intravenously, and all patients continued ASA at a daily dose of 75-150 mg. Oral clopidogrel was initiated to all patients at a loading dose of 300-600 mg before or immediately after the primary PCI. Low molecular weight heparin or unfractionated heparin was administered intravenously in the standard dosage during the procedure. Glycoprotein IIb/IIIa inhibitor or bivalirudin administration during the procedure, was left to the physician's discretion. Clopidogrel was continued at a daily dose of 75 mg for a minimum of 6 months, after which therapy could be extended to a maximum of 12 months on the physician's recommendation.

## 4.3 Stent devices

### 4.3.1 *Biodegradable polymer sirolimus-eluting stent*

BP-SES (Orsiro, Biotronik AG, Bülach, Switzerland) was devised on a stent platform based on the PRO-Kinetic Energy BMS with a hybrid coating of passive and active layers. The platform is a tubular thin-strut balloon-expandable stent with a helicoid strut design, made of L-605 cobalt-chromium alloy. The stent surface is coated with a layer of silicon carbide (proBIO®) that, as a semiconductor, acts in an effort to reduce the release of allergenic metallic ions. The active coating layer (BIOlute) is a matrix composed of high-molecular-weight poly-L-lactic acid

(PLLA) that completely degenerates into carbon dioxide and water. It covers the whole stent surface with an abluminal thickness of 7.5 µm, and a luminal thickness of 3.5 µm. The matrix is infused with sirolimus at a concentration of 1.4 µg per $mm^2$ of the stent surface area. Complete drug release is achieved in approximately 100 days. The thickness of the coated strut of stents with a nominal diameter of ≤3 mm is 71 µm, and 91 µm for sizes 3.5–4.0 mm.

### 4.3.2   Durable polymer zotarolimus-eluting stent

DP-ZES (Resolute Integrity, Medtronic Cardiovascular, Santa Rosa, CA, USA) was built on the Integrity™ BMS platform, which is a new iteration of the Driver™ BMS design. It is formed of a single cobalt-chromium wire with a thickness of 91 µm wrapped helicoidally to form a continuous sinusoidal pattern. It is coated with the BioLinx™ tripolymer, composed of 3 different polymers: the hydrophobic C10 acts as a drug reservoir for slow and sustained release, the hydrophilic polyvinyl-pyrrolidinone enhances biocompatibility, and C19 contains both hydrophilic and hydrophobic components. The BioLinx matrix contains zotarolimus at a dose of 1.6 µg per $mm^2$ of stent surface area; nearly 85% of the drug is eluted by the end of 60 days, and it is completely eluted at 180 days. The thickness of the coated strut is 97 µm. The stent is CE marked for low risk of ST after discontinuation of DAPT at 1 month.

### 4.3.3   Cobalt-chromium bioactive stent

CoCr-BAS (TiTAN Optimax™, Hexacath, Paris, France) is a third-generation bi-oactive stent employing an L-605 cobalt-chromium alloy platform to achieve greater radial strength and thinner struts compared to the stainless steel platform. The stent is coated with titanium nitride oxide to reduce platelet and fibrin deposition and minimize inflammation. The coated strut thickness is 75 µm.

### 4.3.4   Platinum-chromium everolimus-eluting stent

PtCr-EES (PROMUS Element™ Plus, Boston Scientific, Marlborough, MA, USA) was built on the laser-cut Element platinum-chromium platform, which possesses greater radial strength in spite of thin struts (81 µm). Serial serpentine segments are joined by two connectors in a double helix configuration. The platform is covered with 7 µm of durable polymer in two layers: a poly n-butyl methacrylate primer and a drug matrix composed of a copolymer of polyvinylidene fluoride and

hexafluoropropylen. The drug matrix contains everolimus at a drug density of 1.0 µg/mm$^2$; 80% of the drug is eluted within 30 days, with complete drug elution at 120 days. The thickness of the coated strut is 88 µm. The stent is CE marked for low risk of ST after discontinuation of DAPT at 3 month.

## 4.4 Optical coherence tomography measurements

### 4.4.1 Optical coherence tomography image acquisition

OCT imaging was performed using the C7-XR frequency-domain system (St. Jude Medical Inc., Saint Paul, MN, USA) employing the non-occlusive technique as previously described (Prati et al. 2007). A 0.014-inch guide-wire was positioned into the distal vessel using a 6 F guiding catheter via radial or femoral approach. After intracoronary administration of nitrates, an imaging catheter (Dragonfly, St. Jude Medical Inc.) was advanced distal to the stent, and the vessel was flushed with 4-6 mL/s of iso-osmolar contrast to replace blood flow and permit visualization of the stented segment. The motorized pullback at 20 mm/s was initiated automatically by the contrast flush. During image acquisition, a coronary segment of 54 mm was visualized and images were stored digitally for subsequent offline analysis.

### 4.4.2 Optical coherence tomography data analysis

Offline OCT analysis was performed by two independent observers blinded to patient characteristics and stent group using proprietary software (St. Jude Medical Inc.). All cross-sections from 5 mm proximal to the stent to 5 mm distal to the stent were screened for image quality, dissection, thrombosis and other abnormalities. Cross-sections where >25% of the lumen perimeter was unanalysable due to residual blood, shadow from the guidewire, or other artefact, were discarded from analysis and an adjacent cross-section was used instead. The first distal cross-section with struts encompassing the lumen was established as the 'starting cross-section'. Repeated measurements to derive intra- and inter-observer comparison were all started from the same starting cross-section. Quantitative analysis was performed on cross-sections at 5-frame intervals for the 1-mm interval analysis. The analysis of images from the TIDES-OCT trial was repeated by observer 1 at 3-frame intervals for the 0.6-mm analysis, and by observer 2 at 1-mm intervals.

In cross-sectional analysis, stent area and lumen area were delineated semi-auto-matically, and NIH area was defined as stent area - lumen area. Percent NIH area was calculated as the proportion between NIH area and stent area.

In strut-level analysis each strut was identified by its blooming artefact and shadow and categorised as covered, if a layer of neointima was visible on all reflecting surfaces of the strut, or uncovered if any part of the strut surface was exposed to the lumen. NIH thickness of covered struts was measured from the blooming arte-fact to the endoluminal edge of covering tissue in a straight line perpendicular to the vessel wall towards the center of gravity of the vessel. Struts not embedded in the vessel wall were assessed for apposition by measuring the distance from the endoluminal edge of the blooming to the underlying lumen contour in a straight line away from the center of gravity of the vessel. A malapposition threshold was determined for each stent by summation of strut thickness, polymer thickness, and 18 µm as a correction for half the blooming (Table 2). If this threshold was ex-ceeded, the strut was defined as malapposed and the exceeding distance as the malapposed distance. Struts fully embedded in the vessel wall and identified by their shadow, but lacking a recognisable blooming, were labelled 'shadow only'-struts (SOS) and considered covered and apposed for the purposes of categorical strut level analysis. Struts over side branches were labelled non-apposed side branch struts and excluded from all analyses.

**Table 2** Malapposition thresholds by stent group in micrometers.

| Stent group | Strut | Polymer | Blooming | Total |
|---|---|---|---|---|
| BP-SES ≤3 mm diameter | 60 | 11 | 18 | 90 |
| BP-SES >3 mm diameter | 80 | 11 | 18 | 110 |
| DP-ZES | 91 | 6 | 18 | 115 |
| CoCr-BAS | 75 | | 18 | 100 |
| PtCr-EES | 81 | 7 | 18 | 110 |

BP-SES indicates biodegradable polymer sirolimus-eluting stent; CoCr-BAS, cobalt-chro-mium bioactive stent; DP-ZES, durable polymer zotarolimus-eluting stent; PtCr-EES, plati-num-chromium everolimus-eluting stent.

## 4.5    Functional measurements

### 4.5.1    *Invasive pressure wire and thermodilution*

Patients were instructed to avoid heavy meals, caffeine, alcohol, and tobacco for 12 hours prior to the study. Immediately after follow-up angiography, intracoro-nary pressure wire measurements were obtained as previously described (N. N. H. J. Pijls et al. 2002). After a bolus injection of intracoronary nitroglycerin (0.2 mg),

a pressure-temperature sensor-tipped 0.014-inch guidewire (Certus®, St. Jude Medical Inc.) was introduced into the coronary ostium and, after equalization of pressure wire and guide pressures, advanced across the stented segment. $P_a$ and $P_d$ at baseline were recorded. Thermodilution curves at the ostium and at the distal sensor were obtained using manual 3 ml bolus injections of saline at room temperature, and the measurement was repeated 3 times at baseline. A thermodilution curve was deemed inadequate if >20% variability from the mean transit time was observed, and the measurement was repeated.

Hyperemia was induced by intravenous infusion of adenosine (140 µg/kg/min). The electrocardiogram and blood pressure of the patient were monitored and care was taken to maintain the sensor in position throughout the investigation. Measurement were taken after a minimum of 1 minute of infusion at steady-state maximal hyperemia, confirmed by a drop of the aortic pressure and subjective sensation of adenosine effects.

Hyperemic thermodilution curves were measured 3 times as described above. CFR was calculated as a ratio of baseline to hyperemic mean transit times. Hyperemic $P_a$ and $P_d$ were recorded simultaneously and FFR was calculated as $P_d / P_a$ and IMR as $P_d$ divided by the inverse of the hyperemic mean transit time.

### 4.5.2  *Transthoracic flow measurement*

Echocardiography including coronary flow velocity measurements was performed on patients enrolled in the HATTRICK-OCT study using an Acuson Sequoia C 512 mainframe (Acuson Inc., Mountain View, CA) with a 4.0 MHz transducer. Echocardiographic dimensions, wall motion abnormalities and valvular function were assessed using standard methods.

B-mode and colour Doppler flow mapping were used to identify the distal LAD as previously described (Hyodo et al. 2010; Hozumi, Yoshida, Ogata, et al. 1998). Baseline flow velocity curves were acquired with pulsed-wave Doppler over a minimum of three cardiac cycles. Hyperemia was induced by intravenous adenosine as described above. Pulsed-wave Doppler flow velocity profiles in the distal LAD were monitored throughout the adenosine infusion to confirm that the highest flow velocity steady-state hyperemic response was achieved, at which point hyperemic flow velocity curves were measured over three cardiac cycles. In offline analysis, mean diastolic flow velocities were measured and averages for baseline and hyperemia were determined. CFR was calculated as the ratio of hyperemic to baseline mean diastolic flow velocity. Angle correction of flow measurements was deemed unnecessary, since derived ratios would be unaffected.

## 4.6 Statistical methods

Sample size calculations for both HATTRICK-OCT and TIDES-OCT were made to detect a 5% mean difference with expected SD of 5% in stent-level analysis of the primary endpoint, binary strut coverage, i.e. percent of uncovered struts averaged per stent (power of 80%, two-sided type I error of 0.05). An average of 150 analysed struts per patient was assumed. Therefore, 22 patients per stent group was considered adequate. Categorical variables were reported as counts and percentages, and within-study comparison was performed using Fisher's exact test. Continuous variables were tested against normal distribution using Kolmogorov-Smirnov and Shapiro-Wilk tests. When normal distribution could be assumed, variables were expressed as mean $\pm$ SD and compared using Student's t-test and Pearson correlation coefficient. When significant skewness was observed, variables were expressed as median and interquartile range [IQR], and compared using Mann-Whitney *U* test and Spearman's rank correlation coefficient. Inter-observer variability was assessed using the coefficient of variation and the intraclass correlation coefficient.

Bland-Altman analysis was used to estimate TTE-derived against invasive CFR and the inter-observer variability of strut-level measurements, namely: the percentage of uncovered struts, the mean NIH thickness, the percentage of malapposed struts and the mean malapposition distance. Measurements were compared pairwise using t-test for CFR and Wilcoxon signed-rank sum for strut level measurements with skewed distribution. The coefficient of variation (within which 95% of all differences are included) was calculated as twice the SD of the differences between paired measurements, as described by Bland and Altman (Martin Bland & Altman 1986).

Pooled analysis was performed on strut-level measurements in order to account for clustering of data due to the large number of measurements obtained by OCT. Pooled analysis was performed using random effects model (DerSimonian−Laird), as heterogeneity is expected. Meta-regression was used for comparison between the study groups. All statistical analyses were performed two-sided at the 5% significance level using SPSS statistical software (SPSS v. 16.0.1 or newer, SPSS Inc., Chicago, Ill., USA) and Open Meta-analyst software (http://www.cebm.brown.edu/openmeta)

# 5 RESULTS

## 5.1 Clinical and procedural patient characteristics

The baseline clinical characteristics of the patients are shown in Table 3 and the procedural characteristics in Table 4 stratified with respect to study and stent group. Post-dilation after the index procedure was performed more frequently in BP-SES than DP-ZES (40.9% vs. 78.3%, respectively, p=0.016). Pre-dilatation was performed in 68.4% of patients in the CoCr-BAS group versus 100% in the PtCr-EES group (p=0.020). Due to chance and small sample size, age differed between CoCr-BAS (59.5 ± 9.47) and PtCr-EES (68.2 ± 7.24) (p=0.003), and age adjustment was not deemed feasible. The stent groups were balanced in all other aspects. One patient in CoCr-BAS had in-stent restenosis and one patient in DP-ZES had in-segment restenosis at follow-up angiography, and both underwent TLR.

**Table 3** Baseline clinical characteristics of the study groups

| Variable | HATTRICK-OCT | | | TIDES-OCT | | |
| --- | --- | --- | --- | --- | --- | --- |
| | BP-SES (n=22) | DP-ZES (n=22) | p | CoCr-BAS (n=19) | PtCr-EES (n=19) | p |
| Age (years) | 62.5 ± 9.7 | 62.0 ± 12.1 | 0.87 | 59.5 ± 9.47 | 68.2 ± 7.24 | 0.003 |
| Male sex | 18 (81.1) | 17 (77.3) | 0.72 | 14 (73.7%) | 11 (57.9%) | 0.495 |
| Risk factors | | | | | | |
| Diabetes | | | | 1 (5.3%) | 3 (15.8%) | 0.604 |
| Hypertension | 8 (36.4) | 6 (27.3) | 0.75 | 12 (63.2%) | 16 (84.2%) | 0.269 |
| Hypercholesterolemia | 7 (31.8) | 4 (18.2) | 0.49 | 11 (57.9%) | 16 (84.2%) | 0.151 |
| Current smoking | 5 (22.7) | 8 (36.4) | 0.51 | 7 (36.8%) | 4 (21.1%) | 0.476 |
| Medical history | | | | | | |
| Prior myocardial infarction | 1 (4.5) | 1 (4.5) | 1.00 | 2 (10.5%) | 4 (21.1%) | 0.660 |
| Prior PCI/CABG | 1 (4.5) | 0 | 0.49 | 3 (15.8%) | 5 (26.3%) | 0.693 |
| Medications at discharge | | | | | | |
| ACEI/ARB | 18 (81.8) | 15 (68.2) | 0.49 | 11 (57.9%) | 15 (78.9%) | 0.295 |
| Beta blockers | 21 (95.5) | 22 (100) | 1.00 | 18 (94.7%) | 18 (94.7%) | 1.000 |
| Statins | 22 (100) | 22 (100) | 1.00 | 19 (100%) | 19 (100%) | 1.000 |
| Indication for PCI | | | | | | |
| Unstable angina | 1 (4.5) | 3 (13.6) | 0.61 | 2 (10.5) | 5 (26.3) | 0.127 |
| NSTEMI | 9 (40.9) | 8 (36.4) | 1.00 | 8 (42.1) | 11 (57.9) | |
| STEMI | 12 (54.5) | 11 (50) | 1.00 | 9 (47.4) | 3 (15.8) | |

Continuous variables are presented as mean ± SD, whereas categorical variables are presented as frequency (percentage). BP-SES indicates biodegradable polymer sirolimus-eluting stent; CoCr-BAS indicates cobalt-chromium bioactive stent; DP-ZES, durable polymer zotarolimus-eluting stent; PtCr-EES, platinum-chromium everolimus-eluting stent; PCI, percutaneous coronary intervention; CABG, coronary artery bypass grafting; ACEI, angiotensin converting enzyme inhibitors; ARB, angiotensin II receptor blockers; VKA, vitamin K antagonists; NSTEMI, non-ST-elevation myocardial infarction; STEMI, ST-elevation myocardial infarction. Modified from Karjalainen et al, Circ J 2015;79:360-7 (I) and Varho et al, Int J Cardiovasc Imaging 2016;32:1031-9 (III).

**Table 4** Baseline procedural characteristics of the study groups

| Variable | HATTRICK-OCT | | | TIDES-OCT | | |
|---|---|---|---|---|---|---|
| | BP-SES (n=22) | DP-ZES (n=22) | p | CoCr-BAS (n=19) | PtCr-EES (n=19) | p |
| Stent diameter (mm) | 3.2 ± 0.3 | 3.2 ± 0.3 | 0.71 | 3.33 ± 0.457 | 3.07 ± 0.380 | 0.062 |
| Stent length (mm) | 18.0 ± 3.4 | 17.5 ± 3.2 | 0.65 | 17.4 ± 4.62 | 18.7 ± 4.47 | 0.398 |
| Two overlapping stents | 2 (9.1) | 1 (4.5) | 1.0 | | | |
| Lesion type | | | 0.50 | | | |
| A | 3 (15.8) | 2 (11.1) | | | | |
| B1 | 10 (52.6) | 12 (66.7) | | | | |
| B2 | 6 (31.6) | 3 (16.7) | | | | |
| C | 0 | 1 (5.6) | | | | |
| Vessel | | | | | | 0.348 |
| LAD | | | | 11 (57.9) | 11 (57.9) | |
| LCX | | | | 7 (36.8) | 4 (21.1) | |
| RCA | | | | 1 (5.3) | 4 (21.1) | |
| Pre-procedural TIMI flow grade | 1.7 ± 1.4 | 1.9 ± 1.2 | 0.73 | 1.95 ± 1.31 | 2.26 ± 1.10 | 0.426 |
| Culprit lesion related thrombus | 12 (60.0) | 6 (30.0) | 0.111 | 8 (42.1) | 4 (21.1) | 0.148 |
| Aspiration thrombectomy | 9 (42.9) | 6 (27.3) | 0.347 | 4 (21.1%) | 2 (10.5%) | 0.660 |
| Pre-dilatation | 17 (77.3) | 19 (82.6) | 0.722 | 13 (68.4%) | 19 (100%) | 0.020 |
| Post-dilatation | 9 (40.9) | 18 (78.3) | 0.016 | 11 (57.9%) | 12 (63.2%) | 1.000 |
| Maximal expansion pressure | 13.2 ± 2.6 | 13.1 ± 3.3 | 0.953 | | | |
| Post-procedural TIMI flow grade | 3.0 ± 0.0 | 3.0 ± 0.2 | 0.15 | 3.0 ± 0.0 | 3.0 ± 0.0 | 1.000 |

Continuous variables are presented as mean ± SD, whereas categorical variables are presented as frequency (percentage). BP-SES indicates biodegradable polymer sirolimus-eluting stent; CoCr-BAS, cobalt-chromium bioactive stent; DP-ZES, durable polymer zotarolimus-eluting stent; LAD, left anterior descending artery; LCX, left circumflex artery; PtCr-EES, platinum-chromium everolimus-eluting stent; RCA, right coronary artery; TIMI, Thrombolysis In Myocardial Infarction. Modified from Karjalainen et al, Circ J 2015;79:360-7 (I) and Varho et al, Int J Cardiovasc Imaging 2016;32:1031-9 (III).

## 5.2    **Anatomical healing**

### 5.2.1    *Optical coherence tomography outcomes between stent groups (I and III)*

OCT image acquisition was performed successfully to all patients, and no OCT procedure-related complications were observed in either trial. All OCT measurements are shown in Table 5. Thrombus formation was detected in 2 stents in BP-SES vs. 1 stent in DP-ZES (p=1.000), but not in CoCr-BAS or PtCr-EES.

The percent of uncovered struts was significantly lower in BP-SES compared with DP-ZES in strut-level analysis (3.9% vs. 8.9%, respectively, p<0.001) and in stent-level analysis (3.9 ± 3.2% vs. 8.9 ± 6.9%, respectively, p=0.019). The frequency of malapposed struts was also significantly lower in BP-SES in strut-level analysis (2.1% vs. 5.3%, respectively, p<0.001), but not in stent-level analysis (2.2 ± 3.7% vs. 4.3 ± 9.5%, respectively, p=0.33).

A significantly lower percent of uncovered struts was seen in CoCr-BAS compared with PtCr-EES (1.2% [2.8%] versus 11.3% [17.7%], respectively, p<0.001). The percent of malapposed struts was also lower in CoCr-BAS compared with PtCr-EES in strut-level analysis (0.8% vs. 1.8%, p<0.001) and in stent-level analysis (0 [1.20] vs. 0.68 [3.59], p=0.026).

These strut-level findings were confirmed by pooled analysis, as shown in Figure 3. CoCr-BAS exhibited the lowest rate of uncovered struts (1.0%, 95% CI 0.5–1.5%); the second lowest rate was seen in BP-SES (3.3%, 95% CI 2.3–4.2%); the second highest rate occurred in DP-ZES (8.2%, 95% CI 6.4–9.9%) and the highest rate was seen in PtCr-EES (14.3%, 95% CI 10.9–17.8%). The differences in the incidence of malapposition demonstrated in strut level analysis did not reach statistical significance (Figure 4). It should be appreciated that the follow-up OCT was performed in different time frames between studies I and III.

**Table 5** Optical coherence tomographic measurements of the study groups.

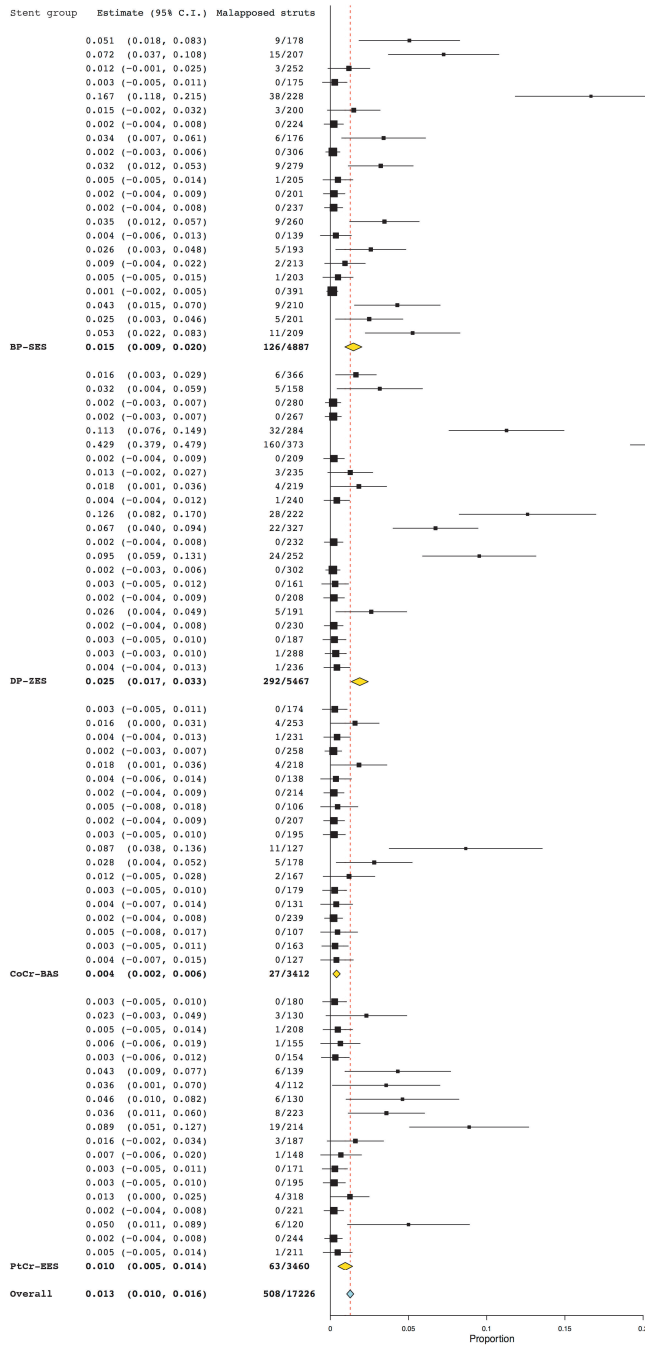| Variable | HATTRICK-OCT | | | TIDES-OCT | | |
|---|---|---|---|---|---|---|
| | BP-SES (n=22) | DP-ZES (n=22) | p | CoCr-BAS (n=19) | PtCr-EES (n=19) | p |
| Follow-up (days) | 93 [23] | 98 [20] | 0.65 | 61.6 ± 9.23 | 63.4 ± 7.34 | 0.501 |
| Cross-sectional analysis | | | | | | |
| Number of cross-sections analysed | 425 | 425 | 1.0 | 302 | 324 | |
| Struts per cross-section | 11.5 ± 0.66 | 12.9 ± 1.2 | <0.001 | 11.4 ± 0.784 | 10.7 ± 1.20 | <0.048 |
| Stent area (mm$^2$) | 6.8 ± 1.6 | 7.5 ± 1.7 | 0.09 | 7.10 ± 1.82 | 6.57 ± 1.92 | 0.382 |
| Lumen area (mm$^2$) | 6.5 [2.2] | 7.1 [2.6] | 0.06 | 5.18 ± 1.50 | 6.33 ± 1.75 | 0.037 |
| NIH area (mm$^2$) | 0.380 [0.410] | 0.460 [0.550] | 0.11 | 1.94 ± 1.01 | 0.427 ± 0.647 | <0.001 |
| % NIH area | 5.7 [5.9] | 5.7 [7.6] | 0.69 | 26.8 ± 13.1 | 5.7 ± 7.7 | <0.001 |
| Strut-level analysis | | | | | | |
| Total number of struts analysed | 4897 | 5467 | 0.13 | 3412 | 3460 | |
| NIH thickness (µm) | 69.1 ± 58.2 | 76.5 ± 82.9 | 0.15 | 203 [108] | 42.2 [41] | <0.001 |
| Uncovered struts | 189 (3.9) | 495 (8.9) | <0.001 | 66 (1.91) | 510 (14.9) | <0.001 |
| Malapposed struts | 101 (2.1) | 292 (5.3) | <0.001 | 27 (0.791) | 63 (1.82) | <0.001 |
| Stent-level analysis | | | | | | |
| % Uncovered struts | 3.9 ± 3.2 | 8.9 ± 6.9 | 0.019 | 1.2 [2.8] | 11.3 [17.7] | <0.001 |
| Stents with >5% uncovered struts | 7 (31.8) | 14 (63.6) | 0.069 | 4 (21.1) | 14 (73.7) | 0.003 |
| % Malapposed struts | 2.2 ± 3.7 | 4.3 ± 9.5 | 0.33 | 0 [1.20] | 0.68 [3.59] | 0.026 |
| Intra-stent thrombus | 2 (9.1) | 1 (4.5) | 1.0 | 0 | 0 | |

Continuous variables are presented as mean ± SD or as median [IQR], whereas categorical variables are presented as frequency (percentage). BP-SES indicates biodegradable polymer sirolimus-eluting stent; CoCr-BAS indicates cobalt-chromium bioactive stent; DP-ZES, durable polymer zotarolimus-eluting stent; NIH, neointimal hyperplasia; PtCr-EES, platinum-chromium everolimus-eluting stent. Modified from Karjalainen et al, Circ J 2015;79:360-7 (I) and Varho et al, Int J Cardiovasc Imaging 2016;32:1031-9 (III).

**Figure 3** Pooled analysis of binary strut coverage. BP-SES indicates biodegradable polymer sirolimus-eluting stent; CoCr-BAS indicates cobalt-chromium bioactive stent; DP-ZES, durable polymer zotarolimus-eluting stent; PtCr-EES, platinum-chromium everolimus-eluting stent. Modified from Varho et al, Int J Cardiovasc Imaging 2016;32:1031-9 (III).

| Stent group | Estimate (95% C.I.) | Malapposed struts |
| --- | --- | --- |
| | 0.051 (0.018, 0.083) | 9/178 |
| | 0.072 (0.037, 0.108) | 15/207 |
| | 0.012 (-0.001, 0.025) | 3/252 |
| | 0.003 (-0.005, 0.011) | 0/175 |
| | 0.167 (0.118, 0.215) | 38/228 |
| | 0.015 (-0.002, 0.032) | 3/200 |
| | 0.002 (-0.004, 0.008) | 0/224 |
| | 0.034 (0.007, 0.061) | 6/176 |
| | 0.002 (-0.003, 0.006) | 0/306 |
| | 0.032 (0.012, 0.053) | 9/279 |
| | 0.005 (-0.005, 0.014) | 1/205 |
| | 0.002 (-0.004, 0.009) | 0/201 |
| | 0.002 (-0.004, 0.008) | 0/237 |
| | 0.035 (0.012, 0.057) | 9/260 |
| | 0.004 (-0.006, 0.013) | 0/139 |
| | 0.026 (0.003, 0.048) | 5/193 |
| | 0.009 (-0.004, 0.022) | 2/213 |
| | 0.005 (-0.005, 0.015) | 1/203 |
| | 0.001 (-0.002, 0.005) | 0/391 |
| | 0.043 (0.015, 0.070) | 9/210 |
| | 0.025 (0.003, 0.046) | 5/201 |
| | 0.053 (0.022, 0.083) | 11/209 |
| **BP-SES** | **0.015 (0.009, 0.020)** | **126/4887** |
| | 0.016 (0.003, 0.029) | 6/366 |
| | 0.032 (0.004, 0.059) | 5/158 |
| | 0.002 (-0.003, 0.007) | 0/280 |
| | 0.002 (-0.003, 0.007) | 0/267 |
| | 0.113 (0.076, 0.149) | 32/284 |
| | 0.429 (0.379, 0.479) | 160/373 |
| | 0.002 (-0.004, 0.009) | 0/209 |
| | 0.013 (-0.002, 0.027) | 3/235 |
| | 0.018 (0.001, 0.036) | 4/219 |
| | 0.004 (-0.004, 0.012) | 1/240 |
| | 0.126 (0.082, 0.170) | 28/222 |
| | 0.067 (0.040, 0.094) | 22/327 |
| | 0.002 (-0.004, 0.008) | 0/232 |
| | 0.095 (0.059, 0.131) | 24/252 |
| | 0.002 (-0.003, 0.006) | 0/302 |
| | 0.003 (-0.005, 0.012) | 0/161 |
| | 0.002 (-0.004, 0.009) | 0/208 |
| | 0.026 (0.004, 0.049) | 5/191 |
| | 0.002 (-0.004, 0.008) | 0/230 |
| | 0.003 (-0.005, 0.010) | 0/187 |
| | 0.003 (-0.003, 0.010) | 1/288 |
| | 0.004 (-0.004, 0.013) | 1/236 |
| **DP-ZES** | **0.025 (0.017, 0.033)** | **292/5467** |
| | 0.003 (-0.005, 0.011) | 0/174 |
| | 0.016 (0.000, 0.031) | 4/253 |
| | 0.004 (-0.004, 0.013) | 1/231 |
| | 0.002 (-0.003, 0.007) | 0/258 |
| | 0.018 (0.001, 0.036) | 4/218 |
| | 0.004 (-0.006, 0.014) | 0/138 |
| | 0.002 (-0.004, 0.009) | 0/214 |
| | 0.005 (-0.008, 0.018) | 0/106 |
| | 0.002 (-0.004, 0.009) | 0/207 |
| | 0.003 (-0.005, 0.010) | 0/195 |
| | 0.087 (0.038, 0.136) | 11/127 |
| | 0.028 (0.004, 0.052) | 5/178 |
| | 0.012 (-0.005, 0.028) | 2/167 |
| | 0.003 (-0.005, 0.010) | 0/179 |
| | 0.004 (-0.007, 0.014) | 0/131 |
| | 0.002 (-0.004, 0.008) | 0/239 |
| | 0.005 (-0.008, 0.017) | 0/107 |
| | 0.003 (-0.005, 0.011) | 0/163 |
| | 0.004 (-0.007, 0.015) | 0/127 |
| **CoCr-BAS** | **0.004 (0.002, 0.006)** | **27/3412** |
| | 0.003 (-0.005, 0.010) | 0/180 |
| | 0.023 (-0.003, 0.049) | 3/130 |
| | 0.005 (-0.005, 0.014) | 1/208 |
| | 0.006 (-0.006, 0.019) | 1/155 |
| | 0.003 (-0.006, 0.012) | 0/154 |
| | 0.043 (0.009, 0.077) | 6/139 |
| | 0.036 (0.001, 0.070) | 4/112 |
| | 0.046 (0.010, 0.082) | 6/130 |
| | 0.036 (0.011, 0.060) | 8/223 |
| | 0.089 (0.051, 0.127) | 19/214 |
| | 0.016 (-0.002, 0.034) | 3/187 |
| | 0.007 (-0.006, 0.020) | 1/148 |
| | 0.003 (-0.005, 0.011) | 0/171 |
| | 0.003 (-0.005, 0.010) | 0/195 |
| | 0.013 (0.000, 0.025) | 4/318 |
| | 0.002 (-0.004, 0.008) | 0/221 |
| | 0.050 (0.011, 0.089) | 6/120 |
| | 0.002 (-0.004, 0.008) | 0/244 |
| | 0.005 (-0.005, 0.014) | 1/211 |
| **PtCr-EES** | **0.010 (0.005, 0.014)** | **63/3460** |
| **Overall** | **0.013 (0.010, 0.016)** | **508/17226** |

**Figure 4** Pooled analysis of binary strut malapposition. BP-SES indicates biodegradable polymer sirolimus-eluting stent; CoCr-BAS indicates cobalt-chromium bioactive stent; DP-ZES, durable polymer zotarolimus-eluting stent; PtCr-EES, platinum-chromium everolimus-eluting stent

### 5.2.2    *Effect of sampling interval on optical coherence tomography outcomes (IV)*

For direct comparison of sampling frequencies (1-mm and 0.6-mm) 6128 struts in 533 cross-sections were analysed in the CoCr-BAS group and 6203 struts in 605 cross-sections in the PtCr-EES group by observer 1 at the 0.6-mm sampling interval. Stent-level analysis of binary strut coverage and apposition are compared stratified by stent group in medians (Table 6) and in means (Table 7). The overall percent uncovered and malapposed struts were significantly lower in 0.6-mm sampling in all analyses ($p<0.05$); the difference in the primarily low rate of uncovered struts in CoCr-BAS remained statistically insignificant.

**Table 6** Median [IQR] percentage of uncovered and malapposed struts in the two sampling intervals stratified by stent group.

| Stent group | 1-mm interval | 0.6-mm interval | *p* value |
|---|---|---|---|
| Percent uncovered struts | | | |
|     CoCr-BAS | 0.77 [2.0] | 0.45 [1.6] | 0.273 |
|     PtCr-EES | 10.6 [9.1] | 9.8 [6.7] | 0.002 |
|     Overall | 3.27 [11.1] | 3.38 [9.76] | 0.001 |
| Percent malapposed struts | | | |
|     CoCr-BAS | 0 [1.45] | 0 [1.09] | 0.031 |
|     PtCr-EES | 0.59 [3.85] | 0.55 [2.77] | 0.151 |
|     Overall | 0.42 [2.04] | 0.12 [1.63] | 0.003 |

Pairwise Wilcoxon signed-rank sum was used to calculate the p-values. CoCr-BAS indicates cobalt-chromium bioactive stent; PtCr-EES, platinum-chromium everolimus-eluting stent. Modified from study IV.

**Table 7** Mean ±SD percentage of uncovered and malapposed struts in the two sampling intervals stratified by stent group.

| Stent group | 1-mm interval | 0.6-mm interval | *p* value |
|---|---|---|---|
| Percent uncovered struts | | | |
|     CoCr-BAS | $1.77 \pm 3.16$ | $1.24 \pm 1.63$ | 0.261 |
|     PtCr-EES | $13.6 \pm 11.0$ | $11.3 \pm 8.97$ | 0.007 |
|     Overall | $7.69 \pm 9.99$ | $6.27 \pm 8.14$ | 0.004 |
| Percent malapposed struts | | | |
|     CoCr-BAS | $1.08 \pm 2.40$ | $0.73 \pm 1.70$ | 0.053 |
|     PtCr-EES | $2.16 \pm 2.68$ | $1.55 \pm 2.02$ | 0.085 |
|     Overall | $1.62 \pm 2.57$ | $1.14 \pm 1.88$ | 0.014 |

Pairwise t-test was used to calculate the p-values. CoCr-BAS indicates cobalt-chromium bioactive stent; PtCr-EES, platinum-chromium everolimus-eluting stent. Modified from study IV.

These findings were confirmed in pooled analysis, where the ratio of percent uncovered struts between 1-mm and 0.6-mm sampling intervals was 1.34 (95% CI

0.947–1.89, p=0.098) for CoCr-BAS, 1.26 (95% CI 1.11–1.43, p<0.001) for PtCr-EES, and 1.27 (95% CI 1.13–1.43, p<0.001) for the cohort overall (Figure 5).
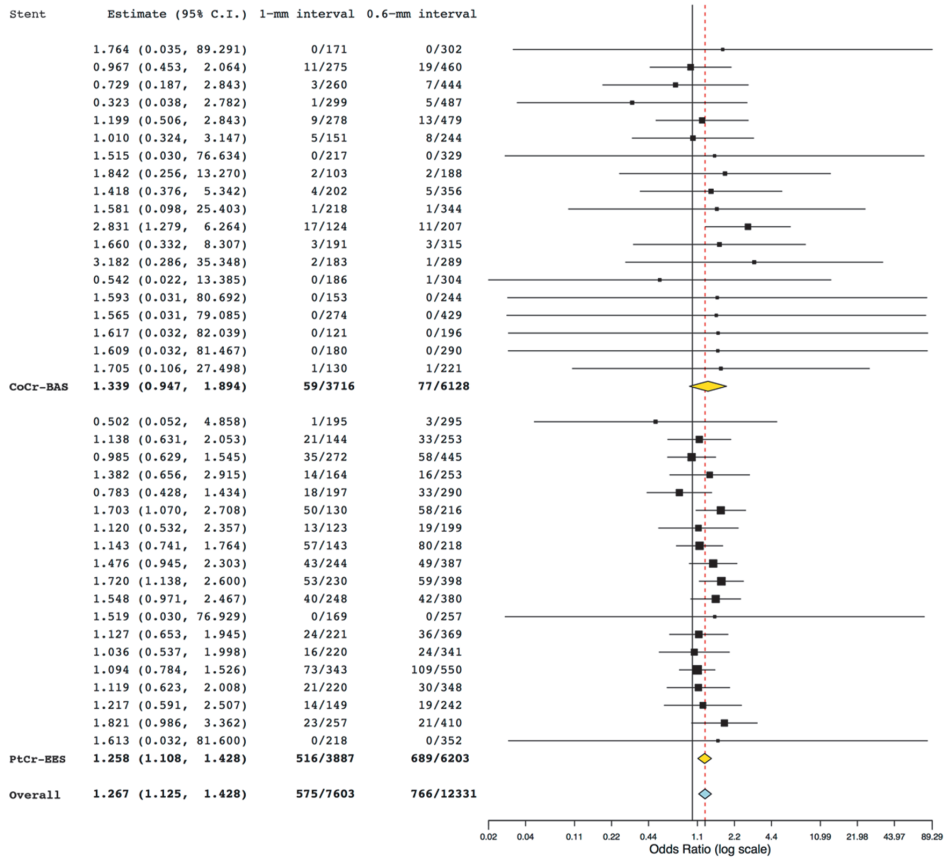


**Figure 5** Pooled comparison of sampling intervals. CoCr-BAS indicates cobalt-chromium bioactive stent; PtCr-EES, platinum-chromium everolimus-eluting stent. Modified from study IV.

In 1-mm sampling, 299 struts without blooming in CoCr-BAS and 236 struts in PtCr-EES were labelled as covered SOS. When SOS were excluded from the analysis, a total of 3417 struts remained in the BAS group, and 3651 struts in the EES group. This led to an increase in the mean percent of uncovered struts from 1.77% to 1.90% in CoCr-BAS (p=0.020), and from 13.6% to 14.6% in PtCr-EES (p=0.001). In 0.6-mm sampling, 540 SOS were detected in CoCr-BAS and 352 in PtCr-EES, and a similar increase in mean percent uncovered struts was seen after exclusion (1.24% to 1.32% in CoCr-BAS, p=0.002; and 11.3 to 11.9% in PtCr-EES, p<0.001).

### 5.2.3    *Inter-observer variability of OCT measurements (IV)*

In cross-sectional analysis all morphometric measurements showed high ICC and acceptable levels of variation between the two observers (Table 8). For strut-level measurements ICC was high for all, except the malapposition distance (Table 8).

**Table 8** Coefficient of variation and intraclass correlation coefficient of the two observers for the morphometric measurements.

| Variable | Observer 1 | | Observer 2 | | CV% | ICC |
|---|---|---|---|---|---|---|
| | Mean | SD | Mean | SD | | |
| Cross-sectional | | | | | | |
| Frames | 18.26 | 5.290 | 16.47 | 4.285 | 7.29 | 0.933 |
| Struts | 200.08 | 57.337 | 180.84 | 49.118 | 7.61 | 0.939 |
| Struts per frame | 11.0344 | 1.15326 | 11.0176 | 1.05975 | 2.94 | 0.931 |
| Lumen area mm$^2$ | 5.8105 | 1.75811 | 5.7528 | 1.71192 | 1.61 | 0.997 |
| Stent area mm$^2$ | 6.8973 | 1.88095 | 6.8351 | 1.86441 | 1.66 | 0.996 |
| NIH area mm$^2$ | 1.2558 | 1.08588 | 1.1819 | 1.13430 | 6.84 | 0.995 |
| NIH area % | 17.52 | 14.25 | 16.27 | 15.02 | 7.45 | 0.994 |
| Strut-level | | | | | | |
| Malapposition µm | 60 | 80 | 81 | 136 | | 0.806 |
| NIH thickness µm | 163 | 136 | 152 | 132 | | 0.997 |
| Uncovered n | 15.13 | 19.137 | 15.16 | 19.095 | | 0.970 |
| Uncovered % | 7.69 | 9.99 | 8.68 | 11.85 | | 0.956 |
| Malapposed n | 3.08 | 4.652 | 2.37 | 3.879 | | 0.932 |
| Malapposed % | 1.64 | 2.56 | 1.42 | 2.29 | | 0.952 |

Continuous variables are presented as mean ± SD. CV indicates coefficient of variance; ICC, intraclass correlation coefficient; NIH, neointimal hyperplasia. Modified from study IV.

Bland-Altman analysis of strut-level measurements showed low inter-observer variability, as expressed by the limits of agreement in Figure 6. No systematic difference was found between the two observers in cross-sectional or strut-level measurements in 2-sided test (p>0.05) except for the NIH thickness with a mean difference of 11 µm (95% CI 7.5–14.5, p<0.001).
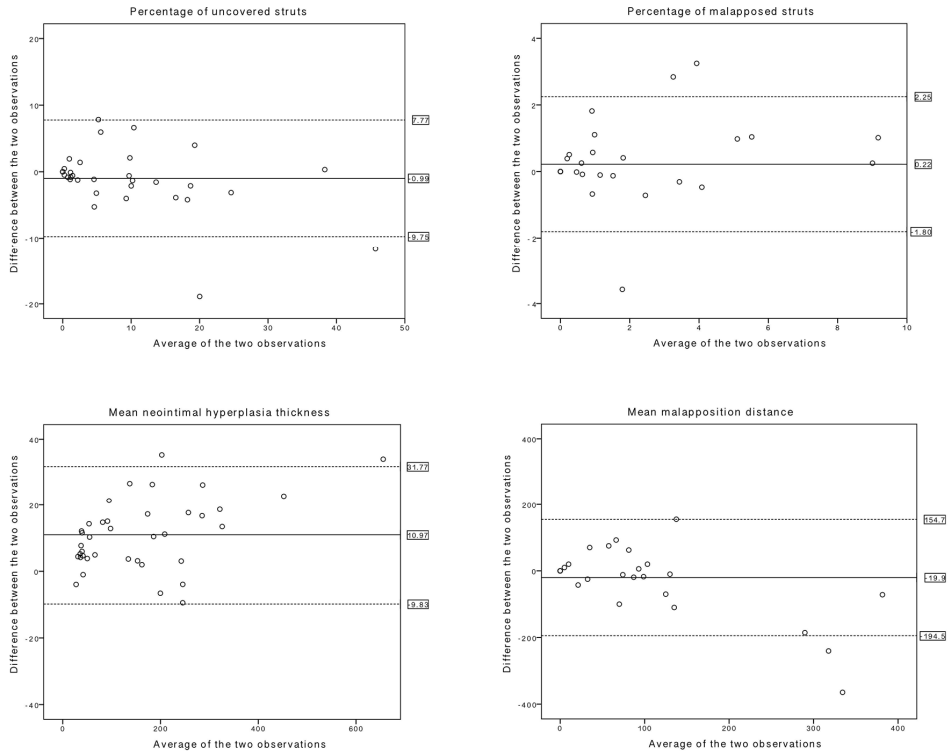
**Figure 6** Bland-Altman plots of strut level measurements between the two observers. Modified from study IV.

## 5.3 Functional healing

### 5.3.1 *Invasive assessment of functional healing (I and III)*

4 patients in BP-SES, 3 patients in DP-ZES, and 2 patients in CoCr-BAS had functional restenosis (FFR ≤0.80) at follow-up, and were excluded from CFR and IMR analysis (Table 9). CFR measurement by thermodilution was unsuccessful in 3 patients in CoCr-BAS due to technical difficulties. No statistically significant differences were observed in mean FFR, CFR, or IMR between stent groups; however, abnormal CFR values were observed frequently in patients treated with BP-SES (44.4%) or PtCr-EES (47.4%), and there was a trend towards a higher proportion of patients with CFR <2.5 in BP-SES compared to DP-ZES (p=0.06). No statistically significant correlation between FFR, CFR, or IMR was found in either study (p>0.05 for all).

**Table 9** Invasive hemodynamic measurements of the study groups.

| Variable | HATTRICK-OCT | | | TIDES-OCT | | |
|---|---|---|---|---|---|---|
| | BP-SES (n=18) | DP-ZES (n=16) | *p* | CoCr-BAS (n=15) | PtCr-EES (n=19) | *p* |
| FFR | 0.87 ± 0.07 | 0.87 ± 0.06 | 0.93 | 0.86 ± 0.13 | 0.90 ± 0.06 | 0.276 |
| CFR | 3.0 ± 1.3 | 3.2 ± 1.0 | 0.56 | 2.56 ± 1.16 | 2.58 ± 1.36 | 0.981 |
| FFR ≤0.80 | 4 (19.0) | 3 (15.8) | 1.00 | 1 (5.3) | 0 | 1.000 |
| CFR <2.5 | 8 (44.4) | 2 (12.5) | 0.06 | | | |
| CFR <2.0 | | | | 4 (28.6) | 9 (47.4) | 0.310 |
| IMR | 19.2 ± 8.1 | 22.7 ± 13.0 | 0.32 | 14.3 ± 5.7 | 23.1± 10.6 | 0.116 |

Continuous variables are presented as mean ± SD, whereas categorical variables are presented as frequency (percentage). BP-SES indicates biodegradable polymer sirolimus-eluting stent; CoCr-BAS indicates cobalt-chromium bioactive stent; DP-ZES, durable polymer zotarolimus-eluting stent; PtCr-EES, platinum-chromium everolimus-eluting stent; FFR, fractional flow reserve; CFR, coronary flow reserve; IMR, index of microcirculatory resistance. Modified from Karjalainen et al, Circ J 2015;79:360-7 (I) and Varho et al, Int J Cardiovasc Imaging 2016;32:1031-9 (III).

Hemodynamic measurements did not correlate significantly with OCT outcomes in either study. However, an inverse relation was observed when data from the two studies was pooled and CFR was plotted against percent uncovered struts (Figure 7). Inverse transformation of CFR resulted in significant correlation between the variables (*r*=0.305, p=0.011). After data pooling significant correlation was also found between CFR and mean NIH area (*r*=0.313, p=0.009).
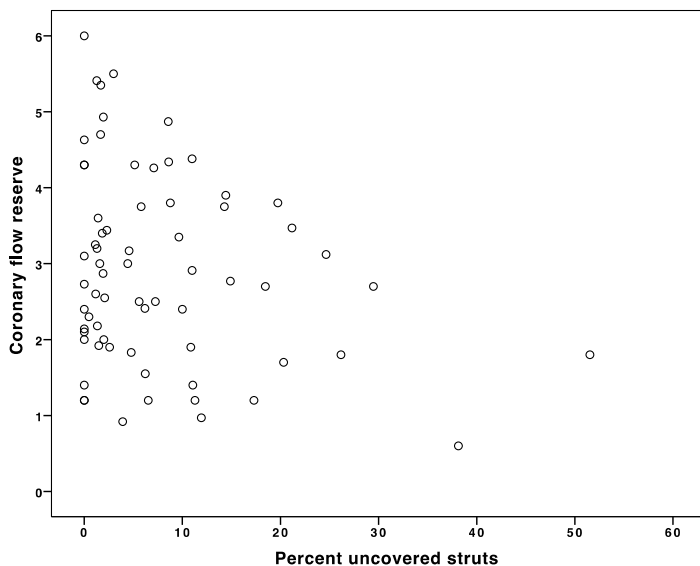


**Figure 7** Coronary flow reserve against percent uncovered struts (n=68).

### 5.3.2 *Validation of transthoracic coronary flow reserve measurement after stenting (II)*

Paired measurements of CFR by TTE and invasive thermodilution were obtained in 25 patients enrolled in HATTRICK-OCT. CFR measurement by TTE was unsuccessful in one patient, where the distal LAD could not be visualised adequately (feasibility 97%). CFR measurement by thermodilution was unsuccessful in five patients due to unreliable (>20% variability) baseline thermodilution curves (feasibility 84%). One patient was excluded from CFR comparison due to functionally significant epicardial stenosis (FFR<0.75). CFR values in the remaining 24 patients demonstrated strong correlation (r=0.71, p<0.001, Figure 8), with mean difference 0.29, (95% CI -0.06–0.59, p=0.054, Table 10). Figure 9 shows the Bland-Altman plot of the two methods with 95% limits of agreement.

**Table 10** Invasive hemodynamic measurements of the study groups

| Variable | Invasive | TTE-derived | Mean difference | *p* |
|---|---|---|---|---|
| Mean CFR | 3.2 ± 1.0 | 2.9 ± 0.72 | 0.29 ± 0.71 | 0.054 |
| CFR <2.5 | 6 (25) | 8 (33) | | 0.001 |

Continuous variables are presented as mean ± SD, whereas categorical variables are presented as frequency (percentage). CFR, coronary flow reserve; TTE, transthoracic echocardiography. Modified from Varho et al, Eur Heart J Cardiovasc Imaging 2014;15:1029-34 (II).

TTE successfully identified moderately impaired CFR (<2.5) (p<0.001) with 100% sensitivity (95% CI 54.05–100.00 %) and 89% specificity (95% CI 65.25–98.30%) as compared to invasive method. The positive and negative predictive values were 75% and 100%, respectively and accuracy was 92%.
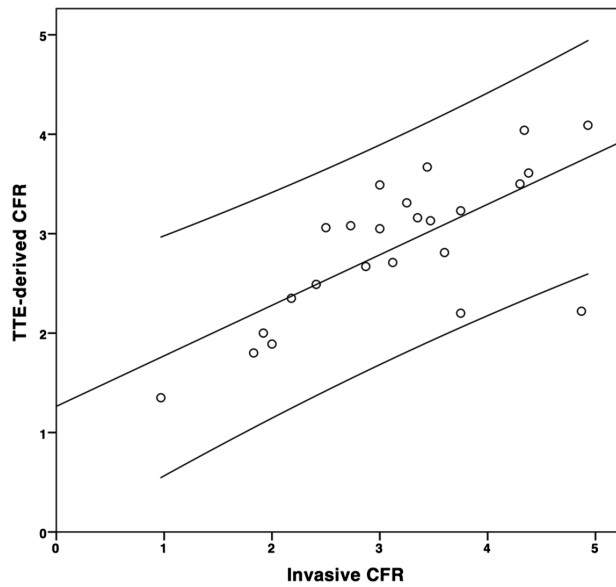
**Figure 8** Correlation between measurements of coronary flow reserve (n=24). CFR indicates coronary flow reserve, TTE, transthoracic echocardiography. Modified from Varho et al, Eur Heart J Cardiovasc Imaging 2014;15:1029-34 (II).
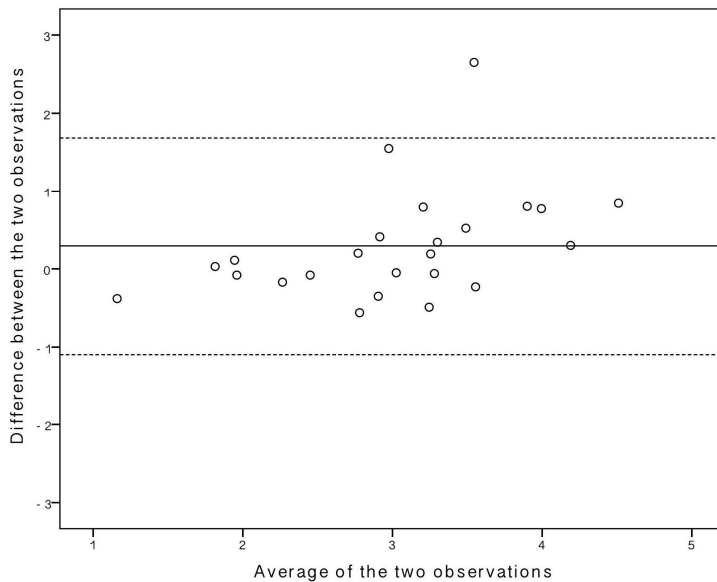


**Figure 9** Bland-Altman plot of coronary flow reserve measured by transthoracic echocardiography or thermodilution (n=24). Modified from Varho et al, Eur Heart J Cardiovasc Imaging 2014;15:1029-34 (II).

# 6 DISCUSSION

## 6.1 Anatomical healing

### 6.1.1 *Optical coherence tomography outcomes between stent groups (I and III)*

The primary endpoint, percent uncovered struts, varied significantly between stent groups, as illustrated by the 95% CI of each stent group with no overlap in Figure 3. Incomplete neointimal coverage at the early follow-up was detected in all stent groups, indicating that healing was not complete at 2–3 months. Similar rates of uncovered struts have been reported with BP-SES (3.9% at 4 months) (Qian et al. 2012), ZES (6.2% at 3 months) (Kim, Kim, Shin, Kim, Ko, Choi, et al. 2013), and PtCr-EES (8.46% at 6 months) (Guagliumi et al. 2013). The exceptionally early time frame of the current study distinguished it from previous research. The 2-month follow-up OCT in study III was appropriately timed for verification of the high rate of strut coverage in CoCr-BAS, which was anticipated due to the absence of drug coating. Early neointimal healing is crucial to patients at high risk of bleeding, who require cessation of DAPT.

A first-in-man report on a BP-SES designed on a cobalt-chromium stent platform with abluminal grooves for the biodegradable drug polymer, implanted for patients with ACS or stable CAD, revealed a comparable percentage of uncovered struts at 4 months (3.8%, vs. 3.9% in study I at 3 months); however, the percentage of malapposed struts was much lower (0.1% vs. 2.1% in our study) (Qian et al. 2012). DP-ZES also exhibited a high rate of malapposed struts (5.3%). The high incidence of malapposition at 3 months is partly explained by the exclusive enrolment of patients with ACS and the high proportions of STEMI and thrombus aspiration in study I, although no significant difference in these risk factors was seen between the stent groups. Notably, malapposition was more frequent in DP-ZES despite a higher rate of post-dilatation, suggesting late acquired ISA due to positive remodelling rather that underexpansion, as supported by the statistically insignificant increase in cross-sectional lumen area. This may have been caused by the dissolution of jailed thrombus, which has been hypothesised as a cause for ISA after stenting in ACS (Hong, Mintz, Lee, Park, Park, et al. 2006; Cook et al. 2007). However, the lack of baseline OCT data precludes drawing such conclusions. Very low rates of uncovered and malapposed struts (0.5% and 0.2%, respectively) have been reported with DP-ZES at 9-month follow up in patients with stable CAD (Wijns et

al. 2015). The cause of this malapposition in patients with ACS remains to be revealed in serial OCT studies.

CoCr-BAS performed best regarding comprehensiveness of neointimal coverage with a mean of 1.0% uncovered struts in pooled analysis at 2 months, which can be largely accredited to the absence of antiproliferative drug and polymer. This early neointimal coverage was achieved at the expense of thicker NIH, as demonstrated by the decreased lumen area and increased NIH area, percent NIH area, and strut-level NIH thickness compared to PtCr-EES, and one case of functionally significant restenosis. Preliminary results of CoCr-BAS in 1-year follow-up showed adequate clinical safety, with low rates of cardiac death (1.3%), non-fatal MI (3.1%), ischemia-driven TLR (3.1%), and the composite endpoint of MACE (6.3%) (Karjalainen, Mikkelsson, et al. 2016).

Reports from BASE-ACS, a prospective RCT powered for comparison of clinical outcomes between a stainless steel platform BAS and a second-generation EES in ACS, both MACE and the stent-oriented composite endpoint of cardiac death, target vessel-related MI or ischaemia-driven TLR occurred at a similar rate between the two stent in 2-year follow-up (Romppanen et al. 2013). Recently, the final report from BASE-ACS confirmed non-inferiority of BAS in 5-year follow-up, with a lower incidence of non-fatal MI compared to EES (5.9% vs. 9.7%, respectively, p = 0.028) (Karjalainen, Nammas, et al. 2016). Successive OCT studies on stainless steel platform BAS have revealed early NIH formation averaging 109.7 µm at 30 days, with only moderate increase in long-term follow-up (274.2 µm at 9 months and 265.8 µm at 4 years) (Annala et al. 2013; Karjalainen et al. 2013; Lehtinen et al. 2012). The current findings with CoCr-BAS (203 µm NIH thickness at 2 months) are in agreement with this pattern of early healing. In light of these assuring data, CoCr-BAS may be considered for the treatment of patients with ACS. The optimal duration of DAPT cannot be deduced from these OCT results alone, as there is no consensus for a universally acceptable rate of binary strut coverage for DAPT discontinuation, and the present study was underpowered to correlate the OCT findings with clinical endpoints.

### 6.1.2    *Effect of sampling interval on OCT outcomes (IV)*

The percentage of uncovered and malapposed struts, as evaluated by OCT at 2 months, differed significantly between the conventional 1-mm sampling interval and the more comprehensive 0.6-mm sampling interval. Such comparison between sampling methods has not been reported previously. Cross-sectional area measurements show very little variability even at 2.4-mm sampling intervals (Bezerra, Guagliumi, et al. 2009); strut-level analysis of binary strut coverage, however,

shows high variability from cross-section to cross-section. Binary strut-level data are highly clustered by nature: the majority of uncovered struts (85%) appear in clusters averaging $21.1 \pm 14.7$ uncovered struts, and the same applies to malapposed struts (78% in clusters of $19.7 \pm 11.8$) (Adriaenssens et al. 2014). This makes the data susceptible to sampling bias. The hierarchical nesting of strut-level data within cross-sections, lesions, and patients should be accounted for in pooled analysis.

Like most diagnostic classifiers, the binary strut-level data is subject to class imbalance, since the percentage of uncovered struts and malapposed struts in stent follow-up tends to be in the order of <10%. When the sample size is increased by one strut, it is more probable that the strut is classified as covered, which increases the chances of identifying the majority class, i.e. the pool of covered struts. The cost of misclassification of the minority class (uncovered struts) is increased in such datasets, where over-sampling of the minority class and under-sampling the majority class have been suggested as methods for improving the performance of the classifier (Chawla & Bowyer 2002). This has certain limitations when measuring percent uncovered struts, where the response of each particular stent is clinically relevant; whereas the response of an individual strut is negligible. According to Finn et al., the strongest predictor of ST is the proportion of uncovered to total struts (Finn et al. 2007).

Automatic algorithms are in trial for rapid analysis of the extensive bulk of data acquired from OCT pullbacks of stented vessels (Ughi et al. 2012; Adriaenssens et al. 2014). This tool would enable the express analysis of all cross-sections effortlessly extending the clinical applications of OCT. Inclusive analysis of all OCT cross-sections would circumvent the dilemma of sampling intervals. However, binary strut coverage thus far remains dependent on human interpretation. When faced with challenging classification of binary strut coverage, higher intra-observer agreement can be achieved by Core Lab analysts, compared with interventional cardiologists with experience in OCT (Brugaletta et al. 2013).

Proportions of uncovered struts derived after exclusion of SOS differed significantly from values obtained when including SOS into the pool of covered struts. The difference, albeit clinically insignificant, was demonstrated consistently across both stent groups and sampling intervals. This observation supports the proposition that SOS should be systematically included in the analysis of binary strut coverage.

The difference in the primary endpoints of percent uncovered struts and percent malapposed struts between 1-mm and 0.6-mm sampling intervals suggests, that the sporadic sampling at the arbitrary 1-mm interval may cause bias in the inclusion

of strut level data resulting in overestimated levels of uncoverage and malapposition. Further investigation relating the findings to histopathological data is warranted to ascertain the optimal sampling interval.

### 6.1.3   *Inter-observer variability of OCT measurements (IV)*

The inter-observer variability assessed at the 1-mm sampling interval was comparable to previous studies (Barlis, Dimopoulos, et al. 2010; Gonzalo & Garcia-Garcia 2009; Heeger et al. 2016). Inter-observer variability of percent uncovered and malapposed struts, the primary OCT endpoints in the current investigation, are seldom reported, and the reproducibility of categorical strut level-data has been questioned: Brugaletta et al. demonstrated that binary strut coverage assessment by OCT is highly dependent on the zoom setting used in the analysis, and suffers from wide inter- and intra-observer variability (Brugaletta et al. 2013). Nevertheless, the current analysis exhibited high agreement with ICC 0.956, in contrast to a recent study reporting binary strut coverage using 0.6-mm sampling with inter-observer ICC at 0.91 (Heeger et al. 2016). Strut-level measurements of NIH thickness were also in concordance, although a small but consistent difference of 11 µm was perceived. The difference is clinically irrelevant and can be attributed to the visual acuity of the OCT images (14 µm) and the blooming thickness (36 µm). Residual blood has been shown *in vitro* to increase the thickness of blooming artefacts (Mancuso et al. 2014); blooming remains a limitation to the detection of thin layers of endothelial coverage on stent struts.

Strut-level measurement of malapposed distance showed weaker agreement. The high variability of the stent-level averages is caused by the rare occurrence of malapposed struts: only 2–3 malapposed struts were detected on average in each stent, and malapposed struts tend to coincide in clusters heterogeneously across the stent (Adriaenssens et al. 2014). This generates high variability from cross-section to cross-section, and makes the results highly dependent on the reading frame of the analysis. Variability could undoubtedly be reduced by shortening the sampling interval and prespecifying a minimum number of cross-sections to include in the analysis. On a further note, it remains controversial whether the malapposed distance has clinical relevance, or only the percentage of malapposed struts; the risk of ST associated with large cross-sectional areas of malapposition appears to attenuate in stents with only a modest degree of ISA (Lindsey & Marso 2010).

## 6.2    Functional healing

### 6.2.1    *Invasive hemodynamic measurements (I and III)*

The incidence of impaired CFR was relatively high in all stent groups, possibly implying that vasodilator function has not fully recovered at 2–3 months after stent implantation. Study I yielded CFR values that were comparable to previous studies on DES follow-up (Hofma et al. 2006; Ruscazio et al. 2012). Mean CFR was lower and impaired CFR was more frequent in CoCr-BAS and PtCr-EES, which is partially attributable to earlier follow-up and diabetic patients in study III. No statistically significant differences in CFR were detected between stent groups in either study, although a tendency to lower CFR was seen in BP-SES. The incidence of culprit lesion thrombus and aspiration was high in BP-SES, and pre-dilation was performed more frequently in PtCr-EES, which are factors predisposing to distal microembolisation and impairment of CFR (Heusch et al. 2009; Hori et al. 1986; Cuisset et al. 2008). Additionally, MI reduces CFR by decreasing the myocardial mass subtended by the occluded artery. Thus a higher rate of impaired CFR can be anticipated in this ACS setting compared to patients with stable CAD.

Previous studies have shown an inverse correlation between CFR and IMR development after PCI (Murai et al. 2016; Cuisset et al. 2008). CFR measurements in either study did not correlate with invasive IMR measurements, which may be due to the small study sample. It is noteworthy, that even in the absence of epicardial stenosis, there was no significant correlation between CFR and IMR, and patients with impaired CFR (<2.5) had IMR levels that were normal and comparable to patients with normal CFR. This verifies that CFR is not contingent on microvascular resistance alone, but rather reflects global atherosclerotic burden, endothelial dysfunction, and microvascular damage, as suggested by previous studies on impaired CFR in the absence of epicardial stenosis (Ascione et al. 2013).

Modest, yet statistically significant correlations were shown between functional and anatomical healing. The direct correlation of mean cross-sectional NIH area and the inverse correlation of percent uncovered struts with CFR at 2-3 months suggest that preserved CFR after stent implantation is linked to complete endothelial coverage of the stent. Several confounding factors need to be acknowledged: lesion length, vessel size, and stent underexpansion influence neointimal growth (Serruys et al. 1999; Hoffmann et al. 1998; Kastrati et al. 1999), and may affect the epicardial physiology, even after exclusion of significant stenoses. The correlation may have been weakened by the various error sources in CFR measurement discussed earlier. However, it is reasonable to infer that delayed neointimal coverage provokes poor functional healing, the causes of which are multifactorial.

### 6.2.2    *Validation of transthoracic coronary flow reserve measurement after stenting (II)*

The present study showed a good agreement between TTE-derived CFR and invasive thermodilution, despite a trend towards higher values with the invasive method. TTE was proven to be reliable in the lower end of the scale and performed with high sensitivity and specificity in identifying impaired CFR values using thermodilution as the gold standard. Conjectures about the effect of impaired endothelial function on adverse outcomes such as TLR or ST cannot be made since the study is underpowered to link findings to clinical endpoints. Nevertheless, measurement of CFR by TTE displayed excellent feasibility, and should be considered for assessment of vasodilator function as a low-cost, non-invasive, accessory test during echocardiographic follow-up.

Owing to simultaneous invasive measurement of FFR, CFR, and IMR, patients with functionally significant restenosis were successfully excluded from the analysis. This allowed evaluation of vasodilator dysfunction in the healing period after DES implantation without the confounding factor of epicardial stenosis, and improved the efficiency of the experimental design with relatively few patients. Thermodilution overestimated CFR in select cases, as shown by the difference between the methods in Figure 6. This may be explained by epicardial vasodilation leading to an increase in flow but not velocity, or coronary steal during hyperaemia, where flow to proximal side branches is increased.

## 6.3    Clinical implications and future research

The results from studies I and III show that early vascular healing is not complete 2 months after the implantation of CoCr-BAS or PtCr-EES, or 3 months after the implantation of BP-SES or DP-ZES. Premature discontinuation of DAPT cannot be recommended at these time points. All stent devices displayed reassuring outcomes, suggesting safe use in the setting of ACS. Treatment with CoCr-BAS allowed early and comprehensive neointimal healing. Whether this facilitates shorter duration of DAPT remains to be verified in prospective studies powered for comparison of clinical endpoints. Serial OCT studies are warranted to uncover mechanisms of malapposition and delayed neointimal coverage.

The sound agreement between CFR values derived from invasive thermodilution and non-invasive TTE in study II validate the use of TTE-derived CFR measurement in patients with ACS treated with DES. Current ESC guidelines recommend CFR measurement by TTE using adenosine-induced hyperemia to assess epicardial stenosis or microvascular disease non-invasively (Montalescot et al. 2013). As

vasodilator dysfunction is common after DES implantation, particularly in the setting of ACS, it is convenient to have a tool for prognostic stratification in follow-up after PCI. The described method enables CFR measurement during TTE evaluation in a manner that is non-invasive and repeatable at different time points.

The critical results from study IV on OCT methodology suggests that the reliability of OCT data may be compromised by inadequate sampling and struts lacking a blooming effect, and that standardization is needed. Currently, assessment of strut coverage is dependent on analyst interpretation. Automated algorithms are needed to analyse the large amount of data and turn it into a tool for the clinician.

## 6.4    Study limitations

Studies I and III were limited in sample size, as they were designed for comparison of OCT- and pressure wire-derived surrogate endpoints of vascular healing. The studies were underpowered for direct comparison of clinical endpoints, hence conclusion regarding post-PCI clinical outcome should be drawn cautiously. Detailed hypotheses on the aetiology of ISA and impaired CFR cannot be made due to the lack of baseline OCT and CFR data. OCT data analysis was not performed in an independent core lab, potentially weakening the statistical power of OCT comparison.

The omission of contrast agent for the measurement of CFR by TTE may have limited the feasibility and repeatability of the method in study II. The study was performed on a highly select population of non-diabetic patients with single-vessel disease in the LAD presenting with ACS. The results are therefore not readily generalizable to wider populations.

Study IV was performed on patients treated with two different stents displaying distinct healing patterns. This may have reduced the statistical power of the study despite data stratification. Even though the change of sampling interval had similar effects in both stent groups, extrapolations to different healing patterns and time frames should be made cautiously.

# 7    CONCLUSIONS

The main findings of the present investigation were:

1. Neointimal coverage by OCT was incomplete in BP-SES and DP-ZES at 3 months after treatment for ACS; the percentage of uncovered struts was lower in BP-SES. Malapposition occurred frequently irrespective of post-dilatation. Vasodilator dysfunction was present in both groups.

2. CFR measurement by TTE is feasible after DES implantation and shows good agreement with invasive thermodilution.

3. CoCr-BAS demonstrated rapid and comprehensive neointimal coverage at 2 months after treatment for ACS compared with PtCr-EES. Vasodilator dysfunction was present in both groups.

4. The sampling interval has significant effect on OCT-derived binary strut coverage and apposition, and the 0.6-mm interval can be used to reduce variation.

# ACKNOWLEDGEMENTS

And finally, I want to express my deepest gratitude to my family, my parents Tarja and Kari, my brother Jan, and my sister Minna, for giving me everything; their love and caring, their support and understanding.

Pori, January 2017

Ville Varho

# REFERENCES

Abizaid A, Mintz GS, Pichard AD, Kent KM, Satler LF, Walsh CL, et al., 1998. Clinical, intravascular ultrasound, and quantitative angiographic determinants of the coronary flow reserve before and after percutaneous transluminal coronary angioplasty. *Am. J. Cardiol.*, 82(4), pp.423–8.

Abizaid AS, Mintz GS, Mehran R, Abizaid A, Lansky AJ, Pichard AD, et al., 1999. Long-term follow-up after percutaneous transluminal coronary angioplasty was not performed based on intravascular ultrasound findings: importance of lumen dimensions. *Circulation*, 100(3), pp.256–61.

Adriaenssens T, Ughi GJ, Dubois C, Onsea K, De Cock D, Bennett J, et al., 2014. Automated detection and quantification of clusters of malapposed and uncovered intracoronary stent struts assessed with optical coherence tomography. *Int. J. Cardiovasc. Imaging*, 30(5), pp.839–848.

Annala A-P, Lehtinen T, Kiviniemi TO, Ylitalo A, Nammas W & Karjalainen PP, 2013. Vascular healing early after titanium-nitride-oxide-coated stent implantation assessed by optical coherence tomography. *J. Invasive Cardiol.*, 25(4), pp.186–9.

Applegate RJ, Sacrinty MT, Kutcher MA, Santos RM, Gandhi SK & Little WC, 2009. Effect of Length and Diameter of Drug-Eluting Stents Versus Bare-Metal Stents on Late Outcomes / CLINICAL PERSPECTIVE. *Circ. Cardiovasc. Interv.*, 2(1), pp.35–42.

Ascione L, Carlomagno G, Sordelli C, Iengo R, Monda V, Severino S, et al., 2013. Dipyridamole coronary flow reserve stratifies prognosis in acute coronary syndrome patients without left anterior descending disease. *Eur. Hear. J. - Cardiovasc. Imaging*, 14(9), pp.858–864.

Baber U, Mehran R, Sharma SK, Brar S, Yu J, Suh J-W, et al., 2011. Impact of the Everolimus-Eluting Stent on Stent Thrombosis. *J. Am. Coll. Cardiol.*, 58(15), pp.1569–1577.

Barlis P, Regar E, Serruys PW, Dimopoulos K, van der Giessen WJ, van Geuns R-JM, et al., 2010. An optical coherence tomography study of a biodegradable vs. durable polymer-coated limus-eluting stent: a LEADERS trial sub-study. *Eur. Heart J.*, 31(2), pp.165–176.

Barlis P, Dimopoulos K, Tanigawa J, Dzielicka E, Ferrante G, Del Furia F, et al., 2010. Quantitative analysis of intracoronary optical coherence tomography measurements of stent strut apposition and tissue coverage. *Int. J. Cardiol.*, 141(2), pp.151–6.

Bech GJW, Pijls NHJ, De Bruyne B, Peels KH, Michels HR, Bonnier HJRM, et al., 1999. Usefulness of Fractional Flow Reserve to Predict Clinical Outcome After Balloon Angioplasty. *Circulation*, 99(7).

Belkacemi A, Agostoni P, Nathoe HM, Voskuil M, Shao C, Van Belle E, et al., 2012. First Results of the DEB-AMI (Drug Eluting Balloon in Acute ST-Segment Elevation Myocardial Infarction) Trial: A Multicenter Randomized Comparison of Drug-Eluting Balloon Plus Bare-Metal Stent Versus Bare-Metal Stent Versus Drug-Eluting Stent in Primary P. *J. Am. Coll. Cardiol.*, 59(25), pp.2327–2337.

Berry C, van 't Veer M, Witt N, Kala P, Bocek O, Pyxaras SA, et al., 2013. VERIFY (VERification of Instantaneous Wave-Free Ratio and Fractional Flow Reserve for the Assessment of Coronary Artery Stenosis Severity in EverydaY Practice): a multicenter study in consecutive patients. *J. Am. Coll. Cardiol.*, 61(13), pp.1421–7.

Bertrand ME, Rupprecht H-J, Urban P, Gershlick AH & Investigators for the C, 2000. Double-Blind Study of the Safety of Clopidogrel With and Without a Loading Dose in Combination With Aspirin Compared With Ticlopidine in Combination With Aspirin After Coronary Stenting. *Circulation*, 102(6).

Bertrand ME, Legrand V, Boland J, Fleck E, Bonnier J, Emmanuelson H, et al., 1998. Randomized Multicenter Comparison of Conventional Anticoagulation Versus Antiplatelet Therapy in Unplanned and Elective Coronary Stenting. *Circulation*, 98(16).

Bezerra HG, Guagliumi G, Kyono H, Tahara S, Rosenthal N, Musumeci G, et al., 2009. Abstract 4754: Determining the Optimal Cross-sectional Analysis Interval for OCT Assessment of Coronary Stenting. *Circulation*, 120(Suppl_18), p.S1000-.

Bezerra HG, Costa MA, Guagliumi G, Rollins AM & Simon DI, 2009. Intracoronary Optical Coherence Tomography: A Comprehensive Review: Clinical and Research Applications.

*JACC Cardiovasc. Interv.*, 2(11), pp.1035–1046.

von Birgelen C, Kok MM, van der Heijden LC, Danse PW, Schotborgh CE, Scholte M, et al., 2016. Very thin strut biodegradable polymer everolimus-eluting and sirolimus-eluting stents versus durable polymer zotarolimus-eluting stents in allcomers with coronary artery disease (BIO-RESORT): a three-arm, randomised, non-inferiority trial. *Lancet*, 388(10060), pp.2607–2617.

Bønaa KH, Mannsverk J, Wiseth R, Aaberge L, Myreng Y, Nygård O, et al., 2016. Drug-Eluting or Bare-Metal Stents for Coronary Artery Disease. *N. Engl. J. Med.*, 375(13), p.NEJMoa1607991.

Bondesson P, Lagerqvist B, James SK, Olivecrona GK, Venetsanos D & Harnek J, 2012. Comparison of two drug-eluting balloons: A report from the SCAAR registry. , 8(4), pp.444–449.

Briguori C, Anzuini A, Airoldi F, Gimelli G, Nishida T, Gould KL, et al., 2001. Intravascular ultrasound criteria for the assessment of the functional significance of intermediate coronary artery stenoses and comparison with fractional flow reserve. *Am. J. Cardiol.*, 87(2), pp.136–41.

Brugaletta S, Garcia-Garcia HM, Gomez-Lara J, Radu MD, Pawar R, Khachabi J, et al., 2013. Reproducibility of qualitative assessment of stent struts coverage by optical coherence tomography. *Int. J. Cardiovasc. Imaging*, 29(1), pp.5–11.

De Bruyne B, Fearon WF, Pijls NHJ, Barbato E, Tonino P, Piroth Z, et al., 2014. Fractional Flow Reserve–Guided PCI for Stable Coronary Artery Disease. *N. Engl. J. Med.*, 371(13), pp.1208–1217.

Caiati C, Zedda N, Montaldo C, Montisci R & Iliceto S, 1999. Contrast-enhanced transthoracic second harmonic echo doppler with adenosine: A noninvasive, rapid and effective method for coronary flow reserve assessment. *J. Am. Coll. Cardiol.*, 34(1), pp.122–130.

Caiati C, Montaldo C, Zedda N, Bina A & Iliceto S, 1999. New noninvasive method for coronary flow reserve assessment: contrast-enhanced transthoracic second harmonic echo Doppler. *Circulation*, 99(6), pp.771–8.

Caiati C, Montaldo C, Zedda N, Montisci R, Ruscazio M, Lai G, et al., 1999. Validation of a new noninvasive method (contrast-enhanced

transthoracic second harmonic echo Doppler) for the evaluation of coronary flow reserve: Comparison with intracoronary Doppler flow wire. *J. Am. Coll. Cardiol.*, 34(4), pp.1193–1200.

Chatzizisis YS, Coskun AU, Jonas M, Edelman ER, Feldman CL & Stone PH, 2007. Role of Endothelial Shear Stress in the Natural History of Coronary Atherosclerosis and Vascular Remodeling: Molecular, Cellular, and Vascular Behavior. *J. Am. Coll. Cardiol.*, 49(25), pp.2379–2393.

Chawla N & Bowyer K, 2002. SMOTE: Synthetic Minority Over-sampling Technique Nitesh. *J. Artif. Intell. Res.*, 16(1), pp.321–357.

Chieffo A, Latib A, Caussin C, Presbitero P, Galli S, al. et, et al., 2013. A prospective, randomized trial of intravascular-ultrasound guided compared to angiography guided stent implantation in complex coronary lesions: the AVIO trial. *Am. Heart J.*, 165(1), pp.65–72.

Chinn SR, Swanson EA & Fujimoto JG, 1997. Optical coherence tomography using a frequency-tunable optical source. *Opt. Lett.*, 22(5), pp.340–2.

De Cock D, Bennett J, Ughi GJ, Dubois C, Sinnaeve P, Kan S, et al., 2014. Healing course of acute vessel wall injury after drug-eluting stent implantation assessed by optical coherence tomography. *Eur. Heart J. Cardiovasc. Imaging*, 15(7), pp.800–9.

Cook S, Wenaweser P, Togni M, Billinger M, Morger C, Seiler C, et al., 2007. Incomplete Stent Apposition and Very Late Stent Thrombosis After Drug-Eluting Stent Implantation. *Circulation*, 115(18), pp.2426–2434.

Cortigiani L, Rigo F, Gherardi S, Sicari R, Galderisi M, Bovenzi F, et al., 2007. Additional prognostic value of coronary flow reserve in diabetic and nondiabetic patients with negative dipyridamole stress echocardiography by wall motion criteria. *J. Am. Coll. Cardiol.*, 50(14), pp.1354–61.

Cortigiani L, Rigo F, Gherardi S, Bovenzi F, Molinaro S, Picano E, et al., 2012. Coronary flow reserve during dipyridamole stress echocardiography predicts mortality. *JACC. Cardiovasc. Imaging*, 5(11), pp.1079–1085.

Cortigiani L, Rigo F, Gherardi S, Bovenzi F, Molinaro S, Picano E, et al., 2013. Prognostic implication of Doppler echocardiographic derived coronary flow reserve in patients with

left bundle branch block. *Eur. Heart J.*, 34(5), pp.364–373.

Costopoulos C, Latib A, Naganuma T, Sticchi A, Figini F, Basavarajaiah S, et al., 2013. The role of drug-eluting balloons alone or in combination with drug-eluting stents in the treatment of de novo diffuse coronary disease. *JACC Cardiovasc. Interv.*, 6(11), pp.1153–1159.

Cuculi F, De Maria GL, Meier P, Dall'Armellina E, de Caterina AR, Channon KM, et al., 2014. Impact of Microvascular Obstruction on the Assessment of Coronary Flow Reserve, Index of Microcirculatory Resistance, and Fractional Flow Reserve After ST-Segment Elevation Myocardial Infarction. *J. Am. Coll. Cardiol.*, 64(18), pp.1894–904.

Cuisset T, Hamilos M, Melikian N, Wyffels E, Sarma J, Sarno G, et al., 2008. Direct Stenting for Stable Angina Pectoris Is Associated With Reduced Periprocedural Microcirculatory Injury Compared With Stenting After Pre-Dilation. *J. Am. Coll. Cardiol.*, 51(11), pp.1060–1065.

Cutlip DDE, Windecker S, Mehran R, Boam A, Cohen DJ, van Es G-A, et al., 2007. Clinical end points in coronary stent trials a case for standardized definitions. *Circulation*, 115(17), pp.2344–51.

Cutlip DE, Baim DS, Ho KKL, Popma JJ, Lansky AJ, Cohen DJ, et al., 2001. Stent Thrombosis in the Modern Era : A Pooled Analysis of Multicenter Coronary Stent Clinical Trials. *Circulation*, 103(15), pp.1967–1971.

D'Ascenzo F, Moretti C, Bianco M, Bernardi A, Taha S, Cerrato E, et al., 2016. Meta-Analysis of the Duration of Dual Antiplatelet Therapy in Patients Treated With Second-Generation Drug-Eluting Stents. *Am. J. Cardiol.*, 117(11), pp.1714–23.

Davidson CJ, Sheikh KH, Harrison JK, Himmelstein SI, Leithe ME, Kisslo KB, et al., 1990. Intravascular ultrasonography versus digital subtraction angiography: A human in vivo comparison of vessel size and morphology. *J. Am. Coll. Cardiol.*, 16(3), pp.633–636.

Eisenstein EL, Anstrom KJ, Kong DF, Shaw LK, Tuttle RH, Mark DB, et al., 2007. Clopidogrel Use and Long-term Clinical Outcomes After Drug-Eluting Stent Implantation. , 297(2), p.159.

Ellis SG, Kereiakes DJ, Metzger DC, Caputo RP, Rizik DG, Teirstein PS, et al., 2015. Everolimus-Eluting Bioresorbable Scaffolds for Coronary Artery Disease - appendix. *N. Engl. J. Med.*, 373(20), pp.1905–15.

Escaned J, Echavarría-Pinto M, Garcia-Garcia HM, van de Hoef TP, de Vries T, Kaul P, et al., 2015. Prospective Assessment of the Diagnostic Accuracy of Instantaneous Wave-Free Ratio to Assess Coronary Stenosis Relevance: Results of ADVISE II International, Multicenter Study (ADenosine Vasodilator Independent Stenosis Evaluation II). *JACC Cardiovasc. Interv.*, 8(6), pp.824–833.

Farb A, Sangiorgi G, Carter AJ, Walley VM, Edwards WD, Schwartz RS, et al., 1999. Pathology of acute and chronic coronary stenting in humans. *Circulation*, 99(1), pp.44–52.

Farshid A, Allan RM, Giles RW, McCredie RM, Pitney MR & Walsh WF, 1998. Impact of an aggressive coronary stenting strategy on the incidence of target lesion revascularization. *Am. J. Cardiol.*, 82(12), pp.1441–1444.

Fassa A-A, Wagatsuma K, Higano ST, Mathew V, Barsness GW, Lennon RJ, et al., 2005. Intravascular ultrasound-guided treatment for angiographically indeterminate left main coronary artery disease. *J. Am. Coll. Cardiol.*, 45(2), pp.204–211.

Fearon WF, Bornschein B, Tonino PAL, Gothe RM, Bruyne B De, Pijls NHJ, et al., 2010. Economic Evaluation of Fractional Flow Reserve-Guided Percutaneous Coronary Intervention in Patients With Multivessel Disease. *Circulation*, 122(24), pp.2545–2550.

Feres F, Costa RA, Abizaid A, Leon MB, Marin-Neto JA, O F, et al., 2013. Three vs Twelve Months of Dual Antiplatelet Therapy After Zotarolimus-Eluting Stents. , 310(23), pp.998–1008.

Finn A V, Joner M, Nakazawa G, Kolodgie F, Newell J, John MC, et al., 2007. Pathological Correlates of Late Drug-Eluting Stent Thrombosis: Strut Coverage as a Marker of Endothelialization. *Circulation*, 115(18), pp.2435–2441.

Fischman DL, Leon MB, Baim DS, Schatz RA, Savage MP, Penn I, et al., 1994. A Randomized Comparison of Coronary-Stent Placement and Balloon Angioplasty in the Treatment of Coronary Artery Disease. *N. Engl. J. Med.*, 331(8), pp.496–501.

Fujii K, Carlier SG, Mintz GS, Yang Y, Moussa I, Weisz G, et al., 2005. Stent underexpansion and residual reference segment stenosis are related to stent thrombosis after sirolimus-eluting stent

implantation: an intravascular ultrasound study. *J. Am. Coll. Cardiol.*, 45(7), pp.995–8.

Gerber R & Colombo A, 2008. Does IVUS guidance of coronary interventions affect outcome? a prime example of the failure of randomized clinical trials. *Catheter. Cardiovasc. Interv.*, 71(5), pp.646–654.

van der Giessen WJ, Lincoff AM, Schwartz RS, van Beusekom HMM, Serruys PW, Holmes DR, et al., 1996. Marked Inflammatory Sequelae to Implantation of Biodegradable and Nonbiodegradable Polymers in Porcine Coronary Arteries. *Circulation*, 94(7).

Gonzalo N, Escaned J, Alfonso F, Nolte C, Rodriguez V, Jimenez-Quevedo P, et al., 2012. Morphometric Assessment of Coronary Stenosis Relevance With Optical Coherence Tomography: A Comparison With Fractional Flow Reserve and Intravascular Ultrasound. *J. Am. Coll. Cardiol.*, 59(12), pp.1080–1089.

Gonzalo N & Garcia-Garcia H, 2009. Reproducibility of quantitative optical coherence tomography for stent analysis.

Gould KL & Lipscomb K, 1974. Effects of coronary stenoses on coronary flow reserve and resistance. *Am. J. Cardiol.*, 34(1), pp.48–55.

Grüntzig A, 1978. Transluminal dilatation of coronary artery stenosis. *Lancet*, 1(C), p.263.

Guagliumi G, Sirbu V, Musumeci G, Gerber R, Biondi-Zoccai G, Ikejima H, et al., 2012. Examination of the In Vivo Mechanisms of Late Drug-Eluting Stent Thrombosis. *JACC Cardiovasc. Interv.*, 5(1), pp.12–20.

Guagliumi G, Capodanno D, Ikejima H, Bezerra HG, Sirbu V, Musumeci G, et al., 2013. Impact of different stent alloys on human vascular response to everolimus-eluting stent: an optical coherence tomography study: the OCTEVEREST. *Catheter. Cardiovasc. Interv.*, 81(3), pp.510–8.

Guagliumi G, Bezerra HG, Sirbu V, Ikejima H, Musumeci G, Biondi-Zoccai G, et al., 2012. Serial Assessment of Coronary Artery Response to Paclitaxel-Eluting Stents Using Optical Coherence Tomography. *Circ. Cardiovasc. Interv.*, 5(1), pp.30–38.

Gurbel PA, Bliden KP, Hiatt BL & O'Connor CM, 2003. Clopidogrel for coronary stenting: Response variability, drug resistance, and the effect of pretreatment platelet reactivity. *Circulation*, 107(23), pp.2908–2913.

Gutiérrez-Chico JL, Alegría-Barrero E, Teijeiro-Mestre R, Chan PH, Tsujioka H, de Silva R, et al., 2012. Optical coherence tomography: from research to practice. *Eur. Heart J. Cardiovasc. Imaging*, 13(5), pp.370–84.

Hakeem A, Agarwal SK, Kasula S, Hacioglu Y, Ahmed Z & Uretsky B, 2015. Value of routine post-PCI FFR in the identification and management of angiographically optimized stented lesions. *J. Am. Coll. Cardiol.*, 65(10), p.A1860.

Hamilos M, Muller O, Cuisset T, Ntalianis A, Chlouverakis G, Sarno G, et al., 2009. Long-term clinical outcome after fractional flow reserve-guided treatment in patients with angiographically equivocal left main coronary artery stenosis. *Circulation*, 120(15), pp.1505–12.

Hamilos MI, Ostojic M, Beleslin B, Sagic D, Mangovski L, Stojkovic S, et al., 2008. Differential effects of drug-eluting stents on local endothelium-dependent coronary vasomotion. *J. Am. Coll. Cardiol.*, 51(22), pp.2123–2129.

Hanekamp CEE, Koolen JJ, Pijls NHJ, Michels HR & Bonnier HJRM, 1999. Comparison of Quantitative Coronary Angiography, Intravascular Ultrasound, and Coronary Pressure Measurement to Assess Optimum Stent Deployment. *Circulation*, 99(8).

Hannawi B, Lam WW, Wang S & Younis GA, 2014. Current Use of Fractional Flow Reserve: A Nationwide Survey. *Texas Hear. Inst. J.*, 41(6), pp.579–584.

Haude M, Konorza TFM, Kalnins U, Erglis A, Saunamäki K, Glogar HD, et al., 2003. Heparin-coated stent placement for the treatment of stenoses in small coronary arteries of symptomatic patients. *Circulation*, 107(9), pp.1265–1270.

Haude M, Ince H, Abizaid A, Toelg R, Lemos PA, von Birgelen C, Christiansen EH, et al., 2016. Safety and performance of the second-generation drug-eluting absorbable metal scaffold in patients with de-novo coronary artery lesions (BIOSOLVE-II): 6 month results of a prospective, multicentre, non-randomised, first-in-man trial. *Lancet*, 387(10013), pp.31–39.

Haude M, Ince H, Abizaid A, Toelg R, Lemos PA, von Birgelen C, Christiansen EH, et al., 2016. Sustained safety and performance of the second-generation drug-eluting absorbable metal scaffold in patients with de novo coronary lesions: 12-month clinical results and angiographic findings of the BIOSOLVE-II first-in-man trial. *Eur. Heart J.*

Heeger CH, Busjahn A, Hildebrand L, Fenski M, Lesche F, Meincke F, et al., 2016. Delayed coverage of drug-eluting stents after interventional revascularisation of chronic total occlusions assessed by optical coherence tomography: The ALSTER-OCT-CTO registry. , 11(9), pp.1004–1012.

Heusch G, Kleinbongard P, Böse D, Levkau B, Haude M, Schulz R, et al., 2009. Coronary microembolization: from bedside to bench and back to bedside. *Circulation*, 120(18), pp.1822–36.

Hoffmann R, Mintz GS, Mehran R, Pichard AD, Kent KM, Satler LF, et al., 1998. Intravascular Ultrasound Predictors of Angiographic Restenosis in Lesions Treated With Palmaz-Schatz Stents. *J. Am. Coll. Cardiol.*, 31(1), pp.43–49.

Hoffmann R, Mintz GS, Dussaillant GR, Popma JJ, Pichard AD, Satler LF, et al., 1996. Patterns and Mechanisms of In-Stent Restenosis: A Serial Intravascular Ultrasound Study. *Circulation*, 94(6), pp.1247–1254.

Hofma SH, van der Giessen WJ, van Dalen BM, Lemos PA, McFadden EP, Sianos G, et al., 2006. Indication of long-term endothelial dysfunction after sirolimus-eluting stent implantation. *Eur. Heart J.*, 27(2), pp.166–70.

Hong M-K, Mintz GS, Lee CW, Park D-W, Choi B-R, Park K-H, et al., 2006. Intravascular ultrasound predictors of angiographic restenosis after sirolimus-eluting stent implantation. *Eur. Heart J.*, 27(11), pp.1305–10.

Hong M-K, Mintz GS, Lee CW, Park D-W, Park K-M, Lee B-K, et al., 2006. Late stent malapposition after drug-eluting stent implantation: an intravascular ultrasound analysis with long-term follow-up. *Circulation*, 113(3), pp.414–9.

Hong S-J, Kim B-K, Shin D-H, Nam C-M, Kim J-S, Ko Y-G, et al., 2015. Effect of Intravascular Ultrasound-Guided vs Angiography-Guided Everolimus-Eluting Stent Implantation: The IVUS-XPL Randomized Clinical Trial. , 314(20), pp.2155–63.

Hori M, Inoue M, Kitakaze M, Koretsune Y, Iwai K, Tamai J, et al., 1986. Role of adenosine in hyperemic response of coronary blood flow in microembolization. *Am. J. Physiol.*, 250(3 Pt 2), pp.H509-18.

Hozumi T, Yoshida K, Akasaka T, Asami Y, Ogata Y, Takagi T, et al., 1998. Noninvasive Assessment of Coronary Flow Velocity and Coronary Flow Velocity Reserve in the Left Anterior Descending Coronary Artery by Doppler Echocardiography. *J. Am. Coll. Cardiol.*, 32(5), pp.1251–1259.

Hozumi T, Yoshida K, Ogata Y, Akasaka T, Asami Y, Takagi T, et al., 1998. Noninvasive Assessment of Significant Left Anterior Descending Coronary Artery Stenosis by Coronary Flow Velocity Reserve With Transthoracic Color Doppler Echocardiography. *Circulation*, 97(16), pp.1557–1562.

Hung M-JM & Cherng WW-J, 2011. Clinical Applications of Transthoracic Doppler Echocardiographic Coronary Flow Reserve Measurements in the Left Anterior Descending Coronary Artery. *J. Med. Ultrasound*, 19(4), pp.115–121.

Hyodo E, Hirata K, Hirose M, Sakanoue Y, Nishida Y, Arai K, et al., 2010. Detection of Restenosis After Percutaneous Coronary Intervention in Three Major Coronary Arteries by Transthoracic Doppler Echocardiography. *J. Am. Soc. Echocardiogr.*, 23(5), pp.553–559.

Iakovou I, Schmidt T, Bonizzoni E, Ge L, Sangiorgi GM, Stankovic G, et al., 2005. Incidence, Predictors, and Outcome of Thrombosis After Successful Implantation of Drug-Eluting Stents. *JAMA J. Am. Med. Assoc.*, 293(17), pp.2126–2130.

Iqbal J, Onuma Y, Ormiston J, Abizaid A, Waksman R & Serruys P, 2014. Bioresorbable scaffolds: Rationale, current status, challenges, and future. *Eur. Heart J.*, 35(12), pp.765–776.

Iqbal J, Gunn J & Serruys PW, 2013. Coronary stents: historical development, current status and future directions. *Br. Med. Bull.*, 106(1), pp.193–211.

Jakabčin J, Špaček R, Bystroň M, Kvašňák M, Jager J, Veselka J, et al., 2010. Long-term health outcome and mortality evaluation after invasive coronary treatment using drug eluting stents with or without the IVUS guidance. Randomized control trial. HOME DES IVUS. *Catheter. Cardiovasc. Interv.*, 75(4), pp.578–583.

Jang J-S, Song Y-J, Kang W, Jin H-Y, Seo J-S, Yang T-H, et al., 2014. Intravascular Ultrasound-Guided Implantation of Drug-Eluting Stents to Improve Outcome: A Meta-Analysis. *JACC Cardiovasc. Interv.*, 7(3), pp.233–243.

Jasti V, Ivan E, Yalamanchili V, Wongpraparut N & Leesar MA, 2004. Correlations Between Fractional Flow Reserve and Intravascular

Ultrasound in Patients With an Ambiguous Left Main Coronary Artery Stenosis. *Circulation*, 110(18).

Joner M, Finn A V, Farb A, Mont EK, Kolodgie FD, Ladich E, et al., 2006. Pathology of drug-eluting stents in humans: delayed healing and late thrombotic risk. *J. Am. Coll. Cardiol.*, 48(1), pp.193–202.

Kang S-J, Lee J-Y, Ahn J-M, Mintz GS, Kim W-J, Park D-W, et al., 2011. Validation of intravascular ultrasound-derived parameters with fractional flow reserve for assessment of coronary stenosis severity. *Circ. Cardiovasc. Interv.*, 4(1), pp.65–71.

Karjalainen P, Kiviniemi TO, Lehtinen T, Nammas W, Ylitalo A, Saraste A, et al., 2013. Neointimal coverage and vasodilator response to titanium-nitride-oxide-coated bioactive stents and everolimus-eluting stents in patients with acute coronary syndrome: insights from the BASE-ACS trial. *Int. J. Cardiovasc. Imaging*, 29(8), pp.1693–703.

Karjalainen PP, Mikkelsson J, Paana T & Nammas W, 2016. Clinical outcome of titanium-nitride-oxide-coated cobalt-chromium stents in patients with de novo coronary lesions: 12-month results of the OPTIMAX first-in-man study. *Catheter. Cardiovasc. Interv.*, 87(4), pp.E122–E127.

Karjalainen PP, Nammas W, Ylitalo A, de Bruyne B, Lalmand J, de Belder A, et al., 2016. Long-term clinical outcome of titanium-nitride-oxide-coated stents versus everolimus-eluting stents in acute coronary syndrome: Final report of the BASE ACS trial. *Int. J. Cardiol.*, 222, pp.275–280.

Karjalainen PP, Ylitalo A, Niemelä M, Kervinen K, Mäkikallio T, Pietilä M, et al., 2009. Two-year follow-up after percutaneous coronary intervention with titanium-nitride-oxide-coated stents versus paclitaxel-eluting stents in acute myocardial infarction. *Ann. Med.*, 41(8), pp.599–607.

Karjalainen PP, Ylitalo A & Airaksinen JKE, 2006. Titanium and nitride oxide-coated stents and paclitaxel-eluting stents for coronary revascularization in an unselected population. *J. Invasive Cardiol.*, 18(10), pp.462–8.

Kastrati A, Schömig A, Dirschinger J, Mehilli J, von Welser N, Pache J, et al., 2000. Increased risk of restenosis after placement of gold-coated stents: results of a randomized trial comparing gold-coated with uncoated steel stents in patients with coronary artery disease. *Circulation*, 101(21), pp.2478–83.

Kastrati A, Elezi S, Dirschinger J, Hadamitzky M, Neumann FJ & Schömig A, 1999. Influence of lesion length on restenosis after coronary stent placement. *Am. J. Cardiol.*, 83(12), pp.1617–22.

Kawamori H, Shite J, Shinke T, Otake H, Sawada T, Kato H, et al., 2010. The ability of optical coherence tomography to monitor percutaneous coronary intervention: detailed comparison with intravascular ultrasound. *J. Invasive Cardiol.*, 22(11), pp.541–5.

Kim J-S, Afari ME, Ha J, Tellez A, Milewski K, Conditt G, et al., 2014. Neointimal patterns obtained by optical coherence tomography correlate with specific histological components and neointimal proliferation in a swine model of restenosis. *Eur. Heart J. Cardiovasc. Imaging*, 15(3), pp.292–8.

Kim S, Kim J-S, Shin D-H, Kim B-K, Ko Y-G, Choi D, et al., 2013. Comparison of early strut coverage between zotarolimus- and everolimus-eluting stents using optical coherence tomography. *Am. J. Cardiol.*, 111(1), pp.1–5.

Kolh P, Windecker S, Alfonso F, Collet J-P, Cremer J, Zamorano JL, et al., 2014. 2014 ESC/EACTS Guidelines on myocardial revascularization: The Task Force on Myocardial Revascularization of the European Society of Cardiology (ESC) and the European Association for Cardio-Thoracic Surgery (EACTS) * Developed with the special contributio. *Eur. J. Cardio-Thoracic Surg.*, 46(4), pp.517–592.

Komatsu R, Ueda M, Naruko T, Kojima A & Becker AE, 1998. Neointimal Tissue Response at Sites of Coronary Stenting in Humans : Macroscopic, Histological, and Immunohistochemical Analyses. *Circulation*, 98(3), pp.224–233.

de la Torre Hernandez JM, Hernández Hernandez F, Alfonso F, Rumoroso JR, Lopez-Palop R, Sadaba M, et al., 2011. Prospective Application of Pre-Defined Intravascular Ultrasound Criteria for Assessment of Intermediate Left Main Coronary Artery Lesions: Results From the Multicenter LITRO Study. *J. Am. Coll. Cardiol.*, 58(4), pp.351–358.

de la Torre Hernández JM, Tejedor P, Camarero TG, Duran JM, Lee D-H, Monedero J, et al., 2016. Early healing assessment with optical coherence tomography of everolimus-eluting stents with bioabsorbable polymer (synergy$^{TM}$) at 3 and 6 months after implantation. *Catheter. Cardiovasc. Interv.*, 88(3), pp.E67-73.

Lagerqvist B, James SK, Stenestrand U, Lindbäck J, Nilsson T & Wallentin L, 2007. Long-Term Outcomes with Drug-Eluting Stents versus Bare-Metal Stents in Sweden. *N. Engl. J. Med.*, 356(10), pp.1009–1019.

Layland J, Oldroyd KG, Curzen N, Sood A, Balachandran K, Das R, et al., 2014. Fractional flow reserve vs. angiography in guiding management to optimize outcomes in non-ST-segment elevation myocardial infarction: the British Heart Foundation FAMOUS-NSTEMI randomized trial. *Eur. Heart J.*, p.ehu338-.

Lee CW, Ahn J-M, Park D-W, Kang S-J, Lee S-W, Kim Y-H, et al., 2014. Optimal duration of dual antiplatelet therapy after drug-eluting stent implantation: a randomized, controlled trial. *Circulation*, 129(3), pp.304–12.

Lee JM, Park J, Kang J, Jeon K-H, Jung J, Lee SE, et al., 2015. Comparison Among Drug-Eluting Balloon, Drug-Eluting Stent, and Plain Balloon Angioplasty for the Treatment of In-Stent Restenosis. *JACC Cardiovasc. Interv.*, 8(3), pp.382–394.

Lehtinen T, Airaksinen KEJ, Ylitalo A & Karjalainen PP, 2012. Stent strut coverage of titanium-nitride-oxide coated stent compared to paclitaxel-eluting stent in acute myocardial infarction: TITAX-OCT study. *Int. J. Cardiovasc. Imaging*, 28(8), pp.1859–66.

Leon MB, Baim DS, Popma JJ, Gordon PC, Cutlip DE, Ho KKL, et al., 1998. A Clinical Trial Comparing Three Antithrombotic-Drug Regimens after Coronary-Artery Stenting. *N. Engl. J. Med.*, 339(23), pp.1665–1671.

Lindsey JB & Marso SP, 2010. Incomplete stent apposition: Should we appose or oppose? *JACC Cardiovasc. Interv.*, 3(5), pp.495–497.

Mancuso JJ, Halaney DL, Elahi S, Ho D, Wang T, Ouyang Y, et al., 2014. Intravascular optical coherence tomography light scattering artifacts: merry-go-rounding, blooming, and ghost struts. *J. Biomed. Opt.*, 19(12), p.126017.

Martin Bland J & Altman D, 1986. Statistical methods for assessing agreement between two methods of clinical measurement. *Lancet*, 327(8476), pp.307–310.

Mauri L, Orav EJ, Candia SC, Cutlip DE & Kuntz RE, 2005. Robustness of late lumen loss in discriminating drug-eluting stents across variable observational and randomized trials. *Circulation*, 112(18), pp.2833–2839.

Mauri L, Kereiakes DJ, Yeh RW, Driscoll-Shempp P, Cutlip DE, Steg PG, et al., 2014. Twelve or 30 Months of Dual Antiplatelet Therapy after Drug-Eluting Stents. *N. Engl. J. Med.*, 371(23), pp.2155–2166.

McDaniel MC, Eshtehardi P, Sawaya FJ, Douglas JS & Samady H, 2011. Contemporary Clinical Applications of Coronary Intravascular Ultrasound. *JACC Cardiovasc. Interv.*, 4(11), pp.1155–1167.

Mehanna EA, Attizzani GF, Kyono H, Hake M & Bezerra HG, 2011. Assessment of coronary stent by optical coherence tomography, methodology and definitions. *Int. J. Cardiovasc. Imaging*, 27(2), pp.259–69.

Mehran R, Baber U, Steg PG, Ariti C, Weisz G, Witzenbichler B, et al., 2013. Cessation of dual antiplatelet treatment and cardiac events after percutaneous coronary intervention (PARIS): 2 year results from a prospective observational study. *Lancet*, 382(9906), pp.1714–1722.

Meuwissen M, Siebes M, Chamuleau SAJ, van Eck-Smit BLF, Koch KT, de Winter RJ, et al., 2002. Hyperemic Stenosis Resistance Index for Evaluation of Functional Coronary Lesion Severity. *Circulation*, 106(4), pp.441–446.

Meuwissen M, Chamuleau SAJ, Siebes M, de Winter RJ, Koch KT, Dijksman LM, et al., 2008. The prognostic value of combined intracoronary pressure and blood flow velocity measurements after deferral of percutaneous coronary intervention. *Catheter. Cardiovasc. Interv.*, 71(3), pp.291–7.

Montalescot G, Sechtem U, Achenbach S, Andreotti F, Arden C, Yildirir A, et al., 2013. 2013 ESC guidelines on the management of stable coronary artery disease: the Task Force on the management of stable coronary artery disease of the European Society of Cardiology. *Eur. Heart J.*, 34(38), pp.2949–3003.

Morice M-C, Serruys PW, Sousa JE, Fajadet J, Ban Hayashi E, Perin M, et al., 2002. A Randomized Comparison of a Sirolimus-Eluting Stent with a Standard Stent for Coronary Revascularization. *N. Engl. J. Med.*, 346(23), pp.1773–1780.

Moschovitis A, Simon R, Seidenstücker A, Klauss V, Baylacher M, Lüscher TF, et al., 2010. Randomised comparison of titanium-nitride-oxide coated stents with bare metal stents: five year follow-up of the TiNOX trial. , 6(1), pp.63–8.

Murai T, Lee T, Kanaji Y, Matsuda J, Usui E, Araki M, et al., 2016. The influence of elective percutaneous coronary intervention on microvascular resistance: a serial assessment

using the index of microcirculatory resistance. *Am. J. Physiol. - Hear. Circ. Physiol.*, 311(3).

Murata A, Wallace-Bradley D, Tellez A, Alviar C, Aboodi M, Sheehy A, et al., 2010. Accuracy of Optical Coherence Tomography in the Evaluation of Neointimal Coverage After Stent Implantation. *JACC Cardiovasc. Imaging*, 3(1), pp.76–84.

Naganuma T, Latib A, Sgueglia GA, Menozzi A, Castriota F, Micari A, et al., 2015. A 2-year follow-up of a randomized multicenter study comparing a paclitaxel drug-eluting balloon with a paclitaxel-eluting stent in small coronary vessels the BELLO study. *Int. J. Cardiol.*, 184(1), pp.17–21.

Nicholls SJ, Hsu A, Wolski K, Hu B, Bayturan O, Lavoie A, et al., 2010. Intravascular Ultrasound-Derived Measures of Coronary Atherosclerotic Plaque Burden and Clinical Outcome. *J. Am. Coll. Cardiol.*, 55(21), pp.2399–2407.

Nissen SE & Yock P, 2001. Intravascular Ultrasound : Novel Pathophysiological Insights and Current Clinical Applications. *Circulation*, 103(4), pp.604–616.

van Nunen LX, Zimmermann FM, Tonino PAL, Barbato E, Baumbach A, Engstrøm T, et al., 2015. Fractional flow reserve versus angiography for guidance of PCI in patients with multivessel coronary artery disease (FAME): 5-year follow-up of a randomised controlled trial. *Lancet*, 386(10006), pp.1853–1860.

Ong ATL, McFadden EP, Regar E, de Jaegere PPT, van Domburg RT & Serruys PW, 2005. Late angiographic stent thrombosis (LAST) events with drug-eluting stents. *J. Am. Coll. Cardiol.*, 45(12), pp.2088–92.

Ong ATL, Hoye A, Aoki J, van Mieghem CAG, Rodriguez Granillo GA, Sonnenschein K, et al., 2005. Thirty-day incidence and six-month clinical outcome of thrombotic stent occlusion after bare-metal, sirolimus, or paclitaxel stent implantation. *J. Am. Coll. Cardiol.*, 45(6), pp.947–953.

Palmerini T, Biondi-Zoccai G, Riva DDD, Stettler C, Sangiorgi D, D'Ascenzo F, et al., 2012. Stent thrombosis with drug-eluting and bare-metal stents: evidence from a comprehensive network meta-analysis. *Lancet*, 379(9824), pp.1393–1402.

Parise H, Maehara A, Stone GW, Leon MB, Mintz GS, Buettner HJ, et al., 2011. Meta-analysis of randomized studies comparing intravascular ultrasound versus angiographic guidance of percutaneous coronary intervention in pre-drug-eluting stent era. *Am. J. Cardiol.*, 107(3), pp.374–82.

Park S-J, Kim Y-H, Park D-W, Lee S-W, Kim W-J, Suh J, et al., 2009. Impact of intravascular ultrasound guidance on long-term mortality in stenting for unprotected left main coronary artery stenosis. *Circ. Cardiovasc. Interv.*, 2(3), pp.167–77.

Parodi G, La Manna A, Di Vito L, Valgimigli M, Fineschi M, Bellandi B, et al., 2013. Stent-related defects in patients presenting with stent thrombosis: differences at optical coherence tomography between subacute and late/very late thrombosis in the Mechanism Of Stent Thrombosis (MOST) study. , 9(8), pp.936–944.

Pawlowski T, Prati F, Kulawik T, Ficarra E, Bil J & Gil R, 2013. Optical coherence tomography criteria for defining functional severity of intermediate lesions: a comparative study with FFR. *Int. J. Cardiovasc. Imaging*, 29(8), pp.1685–91.

Petraco R, van de Hoef TP, Nijjer S, Sen S, van Lavieren MA, Foale RA, et al., 2014. Baseline Instantaneous Wave-Free Ratio as a Pressure-Only Estimation of Underlying Coronary Flow Reserve: Results of the JUSTIFY-CFR Study (Joined Coronary Pressure and Flow Analysis to Determine Diagnostic Characteristics of Basal and Hyperemic Indices o. *Circ. Cardiovasc. Interv.*, 7(4), pp.492–502.

Pfisterer M, Brunner-La Rocca HP, Buser PT, Rickenbacher P, Hunziker P, Mueller C, et al., 2006. Late Clinical Events After Clopidogrel Discontinuation May Limit the Benefit of Drug-Eluting Stents. *J. Am. Coll. Cardiol.*, 48(12), pp.2584–2591.

Piek JJ, Boersma E, Voskuil M, di Mario C, Schroeder E, Vrints C, et al., 2001. The immediate and long-term effect of optimal balloon angioplasty on the absolute coronary blood flow velocity reserve. A subanalysis of the DEBATE study. *Eur. Heart J.*, 22(18), pp.1725–1732.

Pijls NHJ, Klauss V, Siebert U, Powers E, Takazawa K, Fearon WF, et al., 2002. Coronary Pressure Measurement After Stenting Predicts Adverse Events at Follow-Up. *Circulation*, 105(25).

Pijls NHJ, Schaardenburgh P van, Manoharan G, Boersma E, Bech J-W, Veer M van't, et al., 2007. Percutaneous Coronary Intervention of Functionally Nonsignificant Stenosis: 5-Year

Follow-Up of the DEFER Study. *J. Am. Coll. Cardiol.*, 49(21), pp.2105–2111.

Pijls NHJN, de Bruyne B, Peels K, Van der V, Bonnier HJRM, Bartunek J, et al., 1996. Measurement of fractional flow reserve to assess the functional severity of coronary-artery stenoses. *N. Engl. J. Med.*, 334(26), pp.1703–1708.

Pijls NNHJ, Bruyne B De, Smith L, De Bruyne B, Aarnoudse W, Barbato E, et al., 2002. Coronary thermodilution to assess flow reserve validation in humans. *Circulation*, 105(21), pp.2482–2486.

Pizzuto F, Voci P, Mariano E, Puddu PE, Chiavari PA & Romeo F, 2003. Noninvasive coronary flow reserve assessed by transthoracic coronary Doppler ultrasound in patients with left anterior descending coronary artery stents. *Am. J. Cardiol.*, 91(5), pp.522–526.

Prati F, Cera M, Ramazzotti V, Imola F, Giudice R & Albertucci M, 2007. Safety and feasibility of a new non-occlusive technique for facilitated intracoronary optical coherence tomography (OCT) acquisition in various clinical and anatomical scenarios. , 3(3), pp.365–70.

Qian J, Xu B, Lansky AJ, Yang Y, Qiao S, Wu Y, et al., 2012. First report of a novel abluminal groove filled biodegradable polymer rapamycin-eluting stent in de novo coronary artery disease: results of the first in man FIREHAWK trial. *Chin. Med. J. (Engl).*, 125(6), pp.970–6.

Roffi M, Patrono C, Collet J-P, Mueller C, Valgimigli M, Andreotti F, et al., 2016. 2015 ESC Guidelines for the management of acute coronary syndromes in patients presenting without persistent ST-segment elevation. *Eur. Heart J.*, 37(3), pp.267–315.

Romppanen H, Nammas W, Kervinen K, Airaksinen JKE, Pietilä M, Rivero-Crespo F, et al., 2013. Stent-oriented versus patient-oriented outcome in patients undergoing early percutaneous coronary intervention for acute coronary syndrome: 2-year report from the BASE-ACS trial. *Ann. Med.*, 45(7), pp.488–493.

Ross JJ, Mintz GS & Chandrasekaran K, 1990. Transthoracic two-dimensional high frequency (7.5 MHz) ultrasonic visualization of the distal left anterior descending coronary artery. *J. Am. Coll. Cardiol.*, 15(2), pp.373–377.

Roy P, Steinberg DH, Sushinsky SJ, Okabe T, Pinto Slottow TL, Kaneshige K, et al., 2008. The potential clinical utility of intravascular ultrasound guidance in patients undergoing percutaneous coronary intervention with drug-eluting stents. *Eur. Heart J.*, 29(15), pp.1851–7.

Ruscazio M, Montisci R, Bezante G, Caiati C, Balbi M, Tona F, et al., 2012. Early Noninvasive Evaluation of Coronary Flow Reserve after Angioplasty in the Left Anterior Descending Coronary Artery Identifies Patients at High Risk of Restenosis at Follow-Up. *J. Am. Soc. Echocardiogr.*, 25(8), pp.902–910.

Rusinaru D, Vrolix M, Verheye S, Chowdhary S, Schoors D, Di Mario C, et al., 2015. Bioabsorbable polymer-coated sirolimus-eluting stent implantation preserves coronary vasomotion: A DESSOLVE II trial sub-study. *Catheter. Cardiovasc. Interv.*, 86(7), pp.1141–50.

Sabate M, Cequier A, Iñiguez A, Serra A, Hernandez-Antolin R, Mainar V, et al., 2012. Everolimus-eluting stent versus bare-metal stent in ST-segment elevation myocardial infarction (EXAMINATION): 1 year results of a randomised controlled trial. *Lancet*, 380(9852), pp.1482–1490.

Sabaté M, Brugaletta S, Cequier A, Iñiguez A, Serra A, al. et, et al., 2016. Clinical outcomes in patients with ST-segment elevation myocardial infarction treated with everolimus-eluting stents versus bare-metal stents (EXAMINATION): 5-year results of a randomised trial. *Lancet*, 387(10016), pp.357–366.

Sabaté M, Brugaletta S, Cequier A, Iñiguez A, Serra A, Hernádez-Antolín R, et al., 2014. The EXAMINATION Trial (Everolimus-Eluting Stents Versus Bare-Metal Stents in ST-Segment Elevation Myocardial Infarction): 2-Year Results From a Multicenter Randomized Controlled Trial. *JACC. Cardiovasc. Interv.*, 7(1), pp.64–71.

Sarno G, Lagerqvist B, Fröbert O, Nilsson J, Olivecrona G, Omerovic E, et al., 2012. Lower risk of stent thrombosis and restenosis with unrestricted use of "new-generation" drug-eluting stents: a report from the nationwide Swedish Coronary Angiography and Angioplasty Registry (SCAAR). *Eur. Heart J.*, 33(5), pp.606–13.

Schömig A, Neumann F-J, Kastrati A, Schühlen H, Blasini R, Hadamitzky M, et al., 1996. A Randomized Comparison of Antiplatelet and Anticoagulant Therapy after the Placement of Coronary-Artery Stents. *N. Engl. J. Med.*, 334(17), pp.1084–1089.

Schulz-Schüpke S, Byrne RA, ten Berg JM, Neumann F-J, Han Y, Adriaenssens T, et al., 2015. ISAR-SAFE: a randomized, double-blind, placebo-controlled trial of 6 versus 12 months of clopidogrel therapy after drug-eluting stenting. *Eur. Heart J.*

Sen S, Escaned J, Malik IS, Mikhail GW, Foale RA, Mila R, et al., 2012. Development and validation of a new adenosine-independent index of stenosis severity from coronary wave-intensity analysis: results of the ADVISE (ADenosine Vasodilator Independent Stenosis Evaluation) study. *J. Am. Coll. Cardiol.*, 59(15), pp.1392–402.

Serruys PW, de Jaegere P, Kiemeneij F, Macaya C, Rutsch W, Heyndrickx G, et al., 1994. A Comparison of Balloon-Expandable-Stent Implantation with Balloon Angioplasty in Patients with Coronary Artery Disease. *N. Engl. J. Med.*, 331(8), pp.489–495.

Serruys PW, Strauss BH, Beatt KJ, Bertrand ME, Puel J, Rickards AF, et al., 1991. Angiographic Follow-up after Placement of a Self-Expanding Coronary-Artery Stent. *N. Engl. J. Med.*, 324(1), pp.13–17.

Serruys PW, Chevalier B, Sotomi Y, Cequier A, Carri?? D, Piek JJ, et al., 2016. Comparison of an everolimus-eluting bioresorbable scaffold with an everolimus-eluting metallic stent for the treatment of coronary artery stenosis (ABSORB II): a 3 year, randomised, controlled, single-blind, multicentre clinical trial. *Lancet*, 388(10059), pp.2479–2491.

Serruys PW, Onuma Y, Garcia-Garcia HM, Muramatsu T, Van Geuns RJ, De Bruyne B, et al., 2014. Dynamics of vessel wall changes following the implantation of the Absorb everolimus-eluting bioresorbable vascular scaffold: A multi-imaging modality study at 6, 12, 24 and 36 months. , 9(11), pp.1271–1284.

Serruys PW, Kay IP, Disco C, Deshpande N V & de Feyter PJ, 1999. Periprocedural quantitative coronary angiography after Palmaz-Schatz stent implantation predicts the restenosis rate at six months: Results of a meta-analysis of the belgian netherlands stent study (BENESTENT) I, BENESTENT II pilot, BENESTENT II and MUSIC. *J. Am. Coll. Cardiol.*, 34(4), pp.1067–1074.

Serruys PW, di Mario C, Piek J, Schroeder E, Vrints C, Probst P, et al., 1997. Prognostic value of intracoronary flow velocity and diameter stenosis in assessing the short- and long-term outcomes of coronary balloon angioplasty: the DEBATE Study (Doppler Endpoints Balloon Angioplasty Trial Europe). *Circulation*, 96(10), pp.3369–77.

Shiono Y, Kitabata H, Kubo T, Masuno T, Ohta S, Ozaki Y, et al., 2012. Optical coherence tomography-derived anatomical criteria for functionally significant coronary stenosis assessed by fractional flow reserve. *Circ J*, 76(9), pp.2218–2225.

Sigwart U, Puel J, Mirkovitch V, Joffre F & Kappenberger L, 1987. Intravascular Stents to Prevent Occlusion and Re-Stenosis after Transluminal Angioplasty. *N. Engl. J. Med.*, 316(12), pp.701–706.

Silber S, Kirtane AJ, Belardi JA, Liu M, Brar S, Rothman M, et al., 2014. Lack of association between dual antiplatelet therapy use and stent thrombosis between 1 and 12 months following resolute zotarolimus-eluting stent implantation. *Eur. Heart J.*, 35(29), pp.1949–1956.

Stefanini GG, Kalesan B, Serruys PW, Heg D, Buszman P, Linke A, et al., 2011. Long-term clinical outcomes of biodegradable polymer biolimus-eluting stents versus durable polymer sirolimus-eluting stents in patients with coronary artery disease (LEADERS): 4 year follow-up of a randomised non-inferiority trial. *Lancet*, 378(9807), pp.1940–1948.

Steg PG, James SK, Atar D, Badano LP, Blömstrom-Lundqvist C, Borger MA, et al., 2012. ESC Guidelines for the management of acute myocardial infarction in patients presenting with ST-segment elevation. *Eur. Heart J.*, 33(20), pp.2569–619.

Steinberg DH, Mintz GS, Mandinov L, Yu A, Ellis SG, Grube E, et al., 2010. Long-Term Impact of Routinely Detected Early and Late Incomplete Stent Apposition: An Integrated Intravascular Ultrasound Analysis of the TAXUS IV, V, and VI and TAXUS ATLAS Workhorse, Long Lesion, and Direct Stent Studies. *JACC Cardiovasc. Interv.*, 3(5), pp.486–494.

Stettler C, Wandel S, Allemann S, Kastrati A, Morice MC, Grover A, et al., 2007. Outcomes associated with drug-eluting and bare-metal stents: a collaborative network meta-analysis. *Lancet*, 370(9591), pp.937–948.

Stone GGW, Ellis SGS, Colombo A, Dawkins KD, Grube E, Cutlip DE, et al., 2007. Offsetting impact of thrombosis and restenosis on the occurrence of death and myocardial infarction after paclitaxel-eluting and bare metal stent implantation. *Circulation*, 115(22), pp.2842–7.

Stone GW, Ellis SG, Cox DA, Hermiller J, O'Shaughnessy C, Mann JT, et al., 2004. A

polymer-based, paclitaxel-eluting stent in patients with coronary artery disease. *N. Engl. J. Med.*, 350(3), pp.221–31.

Stone GW, Lansky AJ, Pocock SJ, Gersh BJ, Dangas G, Wong SC, et al., 2009. Paclitaxel-Eluting Stents versus Bare-Metal Stents in Acute Myocardial Infarction. *N. Engl. J. Med.*, 360(19), pp.1946–1959.

Stone GW, Witzenbichler B, Weisz G, Rinaldi MJ, Neumann F-J, Metzger DC, et al., 2013. Platelet reactivity and clinical outcomes after coronary artery implantation of drug-eluting stents (ADAPT-DES): a prospective multicentre registry study. *Lancet*, 382(9892), pp.614–623.

Stone GW, Moses JW, Ellis SG, Schofer J, Dawkins KD, Morice M-C, et al., 2007. Safety and efficacy of sirolimus- and paclitaxel-eluting coronary stents. *N. Engl. J. Med.*, 356(10), pp.998–1008.

Suzuki Y, Ikeno F, Koizumi T, Tio F, Yeung AC, Yock PG, et al., 2008. In Vivo Comparison Between Optical Coherence Tomography and Intravascular Ultrasound for Detecting Small Degrees of In-Stent Neointima After Stent Implantation. *JACC Cardiovasc. Interv.*, 1(2), pp.168–173.

Tanabe K, Serruys PW, Degertekin M, Grube E, Guagliumi G, Urbaszek W, et al., 2005. Incomplete stent apposition after implantation of paclitaxel-eluting stents or bare metal stents: insights from the randomized TAXUS II trial. *Circulation*, 111(7), pp.900–5.

Tanizawa S, Ueda M, van der Loos CM, van der Wal AC & Becker AE, 1996. Expression of platelet derived growth factor B chain and beta receptor in human coronary arteries after percutaneous transluminal coronary angioplasty: an immunohistochemical study. *Heart*, 75(6), pp.549–56.

Tearney GJ, Regar E, Akasaka T, Adriaenssens T, Barlis P, Weisz G, et al., 2012. Consensus Standards for Acquisition, Measurement, and Reporting of Intravascular Optical Coherence Tomography Studies: A Report From the International Working Group for Intravascular Optical Coherence Tomography Standardization and Validation. *J. Am. Coll. Cardiol.*, 59(12), pp.1058–1072.

Tearney GJ, Waxman S, Shishkov M, Vakoc BJ, Suter MJ, Freilich MI, et al., 2008. Three-dimensional coronary artery microscopy by intracoronary optical frequency domain imaging. *JACC. Cardiovasc. Imaging*, 1(6), pp.752–61.

Tobis JM, Mallery J, Mahon D, Lehmann K, Zalesky P, Griffith J, et al., 1991. Intravascular ultrasound imaging of human coronary arteries in vivo. Analysis of tissue characterizations with comparison to in vitro histological specimens. *Circulation*, 83(3).

Togni M, Räber L, Cocchia R, Wenaweser P, Cook S, Windecker S, et al., 2007. Local vascular dysfunction after coronary paclitaxel-eluting stent implantation. *Int. J. Cardiol.*, 120(2), pp.212–220.

Togni M, Windecker S, Cocchia R, Wenaweser P, Cook S, Billinger M, et al., 2005. Sirolimus-eluting stents associated with paradoxic coronary vasoconstriction. *J. Am. Coll. Cardiol.*, 46(2), pp.231–236.

Tonino PAL, De Bruyne B, Pijls NHJ, Siebert U, Ikeno F, van `t Veer M, et al., 2009. Fractional Flow Reserve versus Angiography for Guiding Percutaneous Coronary Intervention. *N. Engl. J. Med.*, 360(3), pp.213–224.

Ueda M, Becker AE, Tsukada T, Numano F & Fujimoto T, 1991. Fibrocellular tissue response after percutaneous transluminal coronary angioplasty. An immunocytochemical analysis of the cellular composition. *Circulation*, 83(4), pp.1327–32.

Ughi GJ, Adriaenssens T, Onsea K, Kayaert P, Dubois C, Sinnaeve P, et al., 2012. Automatic segmentation of in-vivo intra-coronary optical coherence tomography images to assess stent strut apposition and coverage. *Int. J. Cardiovasc. Imaging*, 28(2), pp.229–241.

Unverdorben M, Sippel B, Degenhardt R, Sattler K, Fries R, Abt B, et al., 2003. Comparison of a silicon carbide-coated stent versus a noncoated stent in human beings: the Tenax versus Nir Stent Study's long-term outcome. *Am. Heart J.*, 145(4), p.e17.

Urban P, Meredith IT, Abizaid A, Pocock SJ, Carrié D, Naber C, et al., 2015. Polymer-free Drug-Coated Coronary Stents in Patients at High Bleeding Risk. *N. Engl. J. Med.*, 373(21), pp.2038–47.

Urban P, Macaya C, Rupprecht H-J, Kiemeneij F, Emanuelsson H, Fontanelli A, et al., 1998. Randomized Evaluation of Anticoagulation Versus Antiplatelet Therapy After Coronary Stent Implantation in High-Risk Patients. *Circulation*, 98(20).

Uren NG, Schwarzacher SP, Metz JA, Lee DP, Honda Y, Yeung AC, et al., 2002. Predictors and outcomes of stent thrombosis. An

intravascular ultrasound registry. *Eur. Heart J.*, 23(2), pp.1891–1893.

Valgimigli M, Campo G, Monti M, Vranckx P, Percoco G, Tumscitz C, et al., 2012. Short-versus long-term duration of dual-antiplatelet therapy after coronary stenting: a randomized multicenter trial. *Circulation*, 125(16), pp.2015–26.

Van't Veer M, Pijls NHJ, Aarnoudse W, Koolen JJ & Van De Vosse FN, 2006. Evaluation of the haemodynamic characteristics of drug-eluting stents at implantation and at follow-up. *Eur. Heart J.*, 27(15), pp.1811–1817.

Vilahur G, Gutiérrez M, Casani L, Varela L, Capdevila A, Pons-Lladó G, et al., 2016. Protective Effects of Ticagrelor on Myocardial Injury After InfarctionClinical Perspective. *Circulation*, 134(22).

Virmani R, Guagliumi G, Farb A, Musumeci G, Grieco N, Motta T, et al., 2004. Localized Hypersensitivity and Late Coronary Thrombosis Secondary to a Sirolimus-Eluting Stent: Should We Be Cautious? *Circulation*, 109(6), pp.701–705.

Waksman R, Kitabata H, Prati F, Albertucci M & Mintz GS, 2013. Intravascular Ultrasound Versus Optical Coherence Tomography Guidance. *J. Am. Coll. Cardiol.*, 62(17), pp.S32–S40.

Wallentin L, Becker RC, Budaj A, Cannon CP, Emanuelsson H, Held C, et al., 2009. Ticagrelor versus Clopidogrel in Patients with Acute Coronary Syndromes. *N. Engl. J. Med.*, 361(11), pp.1045–1057.

Wijns W, Vrolix M, Verheye S, Schoors D, Slagboom T, Gosselink M, et al., 2015. Randomised study of a bioabsorbable polymer-coated sirolimus-eluting stent: results of the DESSOLVE II trial. , 10(12), pp.1383–1390.

Windecker S, Simon R, Lins M, Klauss V, Eberli FR, Roffi M, et al., 2005. Randomized comparison of a titanium-nitride-oxide-coated stent with a stainless steel stent for coronary revascularization: the TiNOX trial. *Circulation*, 111(20), pp.2617–22.

Windecker S, Mayer I, De Pasquale G, Maier W, Dirsch O, De Groot P, et al., 2001. Stent coating with titanium-nitride-oxide for reduction of neointimal hyperplasia. *Circulation*, 104(8), pp.928–33.

Witzenbichler B, Maehara A, Weisz G, Neumann F-J, Rinaldi MJ, Metzger DC, et al., 2014. Relationship Between Intravascular Ultrasound Guidance and Clinical Outcomes After Drug-Eluting Stents: The Assessment of Dual Antiplatelet Therapy With Drug-Eluting Stents (ADAPT-DES) Study. *Circulation*, 129(4), pp.463–470.

Wiviott SD, Braunwald E, McCabe CH, Montalescot G, Ruzyllo W, Gottlieb S, et al., 2007. Prasugrel versus Clopidogrel in Patients with Acute Coronary Syndromes. *N. Engl. J. Med.*, 357(20), pp.2001–2015.

Wöhrle J, Al-Khayer E, Grötzinger U, Schindler C, Kochs M, Hombach V, et al., 2001. Comparison of the heparin coated vs the uncoated Jostent® - No influence on restenosis or clinical outcome. *Eur. Heart J.*, 22(19), pp.1808–1816.

Wöhrle J, Zadura M, Möbius-Winkler S, Leschke M, Opitz C, Ahmed W, et al., 2012. SeQuent Please World Wide Registry: Clinical results of SeQuent Please paclitaxel-coated balloon angioplasty in a large-scale, prospective registry study. *J. Am. Coll. Cardiol.*, 60(18), pp.1733–1738.

Zafar H, Ullah I, Dinneen K, Matiullah S, Hanley A, Leahy MJ, et al., 2014. Evaluation of hemodynamically severe coronary stenosis as determined by fractional flow reserve with frequency domain optical coherence tomography measured anatomical parameters. *J. Cardiol.*, 64(1), pp.19–24.

Zimmermann FM, Ferrara A, Johnson NP, van Nunen LX, Escaned J, Albertsson P, et al., 2015. Deferral vs. performance of percutaneous coronary intervention of functionally non-significant coronary stenosis: 15-year follow-up of the DEFER trial. *Eur. Heart J.*, 36(45), pp.3182–3188.